Final Technical Report:

Virtual Pipeline System Testbed to Optimize the U.S. Natural Gas Transmission Pipeline System

Award Number DE-FC26-01NT41322

Prepared for
The U.S. Department of Energy
Strategic Center for Natural Gas

Prepared by
Kirby S. Chapman, Ph.D.
Prakash Krishniswami, Ph.D.
Virg Wallentine, Ph.D.

Mohammed Abbaspour, Ph.D.
Revathi Ranganathan
Ravi Addanki
Jeet Sengupta
Liubo Chen

The National Gas Machinery Laboratory
Kansas State University
245 Levee Drive
Manhattan, Kansas 66502

June, 2005

Disclaimer

Abstract

The goal of this project is to develop a Virtual Pipeline System Testbed (VPST) for natural gas transmission. This study uses a fully implicit finite difference method to analyze transient, non-isothermal compressible gas flow through a gas pipeline system. The inertia term of the momentum equation is included in the analysis. The testbed simulate compressor stations, the pipe that connects these compressor stations, the supply sources, and the end-user demand markets. The compressor station is described by identifying the make, model, and number of engines, gas turbines, and compressors. System operators and engineers can analyze the impact of system changes on the dynamic deliverability of gas and on the environment.

Executive Summary

The natural gas transmission pipeline infrastructure delivers about 22 tcf of natural gas per year, and is made up of over 300,000 miles of pipe driven by 8,000 engines and 1,000 gas turbines with 40 million horsepower of compression capacity. This system has been developed over the last 60 years, and is controlled at a very low level of sophistication.

The goal of this project is to develop a Virtual Pipeline System Testbed (VPST) for natural gas transmission. This study uses a fully implicit finite difference method to analyze transient, non-isothermal compressible gas flow through a gas pipeline system. The inertia term of the momentum equation is included in the analysis. The numerical results show that:

- **Optimization**
  Operational optimization using rigorous mathematical techniques is a viable tool for enhancing the efficiency of pipeline operations. Currently available commercial packages do not provide the capability for fully automated optimization of operational parameters; but rather provide computational support for human decision making. Thus, the solutions are generally not truly optimal, and require considerable user involvement. This work advances the current state of pipeline simulations by using detailed equipment modeling and rigorous mathematical optimization that will automatically generate truly optimal solutions with practically no user involvement.

- **Solution Method**
  The fully implicit method has advantages, such as the guaranteed stability for large time step, which is very useful for simulating long-term transients in natural gas pipelines. The inertia term plays an important role in the gas flow analysis and cannot be neglected in the calculation. The effect of treating the gas in a non-isothermal manner is necessary for pipeline flow calculation accuracies, and is extremely necessary for rapid transient processes. By using a computer simulation, the dynamic response of the compressor can be determined by changing boundary condition with respect to time. The current simulation lays a foundation on which to build a more detailed compressor station model with equipment such as scrubbers, coolers, etc. The penetrations of sudden property changes along long length pipes are very small. The model was validated by comparing simulated results with those of others. The solution method was used to solve a large scale problem that included ten compressor stations, each with five compression units.

- **Implementation**
  The implementation of the simulation methods included the development of a graphical user interface called the Pipeline Editor. This editor is a feature-rich graphical user interface designed to provide pipeline designers with a graphical view of a pipeline systems and simulation data. The Pipeline Editor can be used to graphically build the pipeline system, manipulate an already built graph, simulate the model using parallel or sequential simulators, and display the results of such simulation graphically. The editor is an easy to use application that can be started from any computer using an Internet browser. Once started the Pipeline Editor connects to the Optimizer and the Sequential and Parallel Simulators.

TABLE OF CONTENTS

1.0 INTRODUCTION

The natural gas transmission pipeline infrastructure in the U.S. represents one of the largest and most complex mechanical systems in the world. This system delivers about 0.623 tcm (22 tcf) of natural gas per year, and is made up of over 4.828×10^5 km (300,000 miles) of pipe driven by 8,000 engines and 1,000 gas turbines with 2.983×10^5 MW (40 million horsepower) of compression capacity. The system produces over 1.86×10^9 MW-hrs (250 billion hp-hrs) of compression power every year. This system has been developed over the last 60 years, and is controlled at a very low level of sophistication.

A mathematical model to simulate pipeline system operation, as well as the impact of design changes and equipment enhancements, is urgently needed for this huge system. Several investigators have tried to simulate and optimize gas pipeline networks and equipment for steady state and transient mode with varying degrees of success. The literature review which was presented in the first report shows that historically, most of the efforts have been focused on steady-state flow conditions and only recently have researchers identified the need for transient flow simulations. One of the significant conclusions of the literature review is that very little has been done to advance the state-of-the-art of the simulation of compressor station components. For example, most references model the compressor station as a black box where the input pressure is increased by some percentage to determine the compressor station output pressure. Even when engines and compressors are included within the simulation, the models require the user to input an engine load line or the compressor load line. Few if any simulations offer the ability to incorporate a complete engine or compressor load map, and no references were found that focus on the fuel consumption and pollutant emissions of the compressor station.

The goal of this project is to develop a Virtual Pipeline System Testbed (VPST) for natural gas transmission. This testbed will simulate compressor stations, the pipe that connects these compressor stations, the supply sources, and the end-user demand markets. The compressor station will be described by identifying the make, model, and number of engines, gas turbines, and compressors (centrifugal and reciprocating) that the station is comprised of. System operators and engineers will be able to analyze the impact of system changes on the dynamic

deliverability of gas and on the environment. For example, the user of the virtual pipeline system will able to drill down into a compressor station to describe that compressor station with a high degree of detail.

The investigators of this project have had one in-depth meeting with industry representatives to obtain realistic data and scenarios for developing the simulation methods at K-State, especially for compressor stations. The minutes of this meeting are provided in Appendix B.

2.0 PRIOR WORK

Natural gas systems are becoming more and more complex as the use of this energy source increases. Mathematical modeling is one of the most important tools used to aid in design and operation studies. The systems under consideration actually operate in an unsteady nature, and although much effort has been and continues to be spent on unsteady mathematical models, many design problems can and will be solved by steady-state modeling. Many investigators have studied the problem of compressible fluid flow through pipelines and compressors. Some of these efforts are reported in the following sections.

2.1 Steady-State Solution

For pipelines, the most commonly used equations for steady-state calculations are the Weymouth equation and the Panhandle equations. Some investigations that have focused on steady-state simulation are listed below.

Rhoads (1983), Ouyang and Aziz (1996) and Schroeder (2001) described the equations which govern the flow of compressible fluids through pipes. General flow equations of simple form are developed to account for the pressure drops due to friction, elevation and kinetic energy.

Stoner (1969, 1972) presented a new method for obtaining a steady-state solution of an integrated gas system model made up of pipelines, compressors, control valves and storage fields. He used Newton-Raphson method for solving nonlinear algebraic equations.

Berard and Eliason (1978) developed a computer program that simulated steady-state gas transmission networks using the Newton-Raphson method for solving nonlinear equation. Their program has several features that facilitate efficient, accurate simulation of large nodal systems, including 1) optimal number of nodes, 2) implicit compressor fuel gas consumption calculation, 3) the ability to prorate equally gas volumes entering the network system, and 4) gas temperature distribution calculation.

Hoeven and Gasunie (1992) described some mathematical aspects of gas network simulation using a linearization technique.

Tian and Adewumi (1994) used a one-dimensional compressible fluid flow equation without neglecting the kinetic energy term to determine the flow of natural gas through a pipeline system. This equation provides a functional relationship between the gas flow rates and the inlet and outlet pressure of a given section of pipe; assuming constant temperature and compressibility factor that then describes steady state compressible flow of gas.

Costa et al. (1998) provided a steady–state gas pipeline simulation. In this simulation, the pipeline and compressors are selected as the building elements of a compressible flow network. The model of a pipeline again uses the one-dimensional compressible flow equation to describe the relationship between the pressure and temperature along the pipe, and the flow rate through the pipe. The flow equation and the conservation of energy equation are solved in a coupled fashion to investigate the differences between isothermal, adiabatic and polytropic flow conditions. The compressors are modeled by simply employing a functional relationship between the pressure increase and the mass flow rate of gas through the compressor.

Sung et al. (1998) presented a hybrid network model (HY-PIPENET) that uses a minimum cost spanning tree. In this simulation, a parametric study was performed to understand the role of each individual parameter such as the source pressure, flow rate and pipeline diameter on the optimized network. The authors found that there is an optimal relationship between pipe diameter and the source pressure.

Rios-Mercado et al. (2001) presented a reduction technique for solving natural gas transmission network optimization problems. These results are valid for steady-state compressible flow through a network pipeline. The decision variables are the mass flow rate through each arc (pipeline segment), and the gas pressure level at each pipeline node.

Martinez-Romero et al. (2002) described steady-state compressible flow through a pipeline. They presented a sensibility analysis for the most important flow equations defining the key parameters in the optimization process. They used the software package “Gas Net,” which is based in Stoner’s method with improvements for solving the system of equations. The basic mathematical model assumed a gas network with two elements: nodes and nodes connectors. The connectors represent elements with different pressures at the inlet and outlet, such as pipes, compressors, valves, and regulators.

Cameron (1999) presented TFlow using an Excel-based model for steady state and transient simulation. TFlow comprises a user interface written in Microsoft Excel's Visual Basic for Applications (VBA) and a dynamic linked library (DLL) written in C^{++}. All information needed to model a pipeline system is contained in an Excel workbook, which also displays the simulation result. The robustness for general applications, however, is not readily apparent.

Doonan et al. (1998) used Simulink™ to simulate a pipeline system. The simulation was used to investigate the safety parameters of an alternative control a considerable distance down stream from the main pressure regulating station. The elements used in this model were very limited. Simulink™ is very limited in the knowledge provided about pipeline operation and reliability.

Fauer (2002) suggested a general equation and contributed each variable to make accurate predictions. For providing accurate predictions the model must contain several details that not only describe the pipeline network but also the fluid it transports and the environment in which it operates. He used two steps to reach a useful model, 1) getting the appropriate level of detail in the model and 2) tuning the model to real world results that include steady-state tuning, steady-state tuning with transient factors, transient tuning and on-line tuning.

Greyvenstein and Laurie (1994) used the well-known SIMPLE algorithm of the Patankar method (Patankar, 1980), which is known in Computational Fluid Dynamics (CFD), to deal with pipe network problems. Special attention is given to the solution of the pressure correction equation, the stability of the algorithm, sensitivity to initial conditions and convergence parameters.

2.2 Transient Solution

Wylie et al. (1971) presented a central implicit finite difference method and compared this method with the method of characteristics. They showed that the implicit method is very accurate for large time steps and so in the implicit procedure the maximum practical time increment is limited by the frequency of the variables imposed at the boundary conditions, rather than by a stability criterion as in the method of characteristics.

Tanaka (1983) introduced the notion of “inside”, “outside” and “selected” sections of the gas pipeline from the viewpoint of applying suitable boundary condition at the inlet and outlet ends of the pipe.

Santos (1997) discussed the importance of a transient simulation and the advantages of using a transient simulation. He notes that transient simulation is not only an excellent tool for training operations personal, but it can also act as a helpful tool in on-line systems. He emphasizes its use in the design phase of a gas pipeline. This paper focuses on a single line gas pipeline without storage facilities and with a flow demand that varies with respect to time on an hourly basis so as to show a behavior that could not be considered as a steady-state flow.

Mohitpour et al. (1996) presented the importance of a dynamic simulation on the design and optimization of pipeline transmission systems. In this paper, the authors explain that steady-state simulations are sufficient for optimizing a pipeline when supply/demand scenarios are relatively stable. In general, steady-state simulations will provide the designer with a reasonable level of confidence when the system is not subject to radical changes in mass flow rates on operating conditions. In reality, the mass flow rate changes, hence the most useful and general simulation is one that allows transient behavior.

Price et al. (1996) presented a method to determine the effective friction factor and overall heat transfer flow conditions in the pipeline. This transient flow model was based on a numerical solution of the one-dimensional unsteady flow equations (continuity, momentum and energy), which were discretized using a highly accurate compact finite difference scheme. The work simulated the pipeline in transient mode without considering the effects of turbulent flow.

Osiadacz (1994) described the dynamic optimization of high-pressure gas networks using hierarchical systems theory. The authors explain that the transient optimization is more difficult mathematically than the steady state simulation, but the reward of using a dynamic simulation is that the operator can achieve higher savings. They further explain that it is of great importance to be able to optimize large-scale systems described by partial differential equations as fast as possible in order to achieve real time optimization.

Osiadacz (1987) used the Runge-Kutta Chebyshev (RKC) methods for solving ordinary differential equations resulting from the method of lines applied to partial differential equations of parabolic type.

Osiadacz (1996) compared a variety of transient pipeline models. Numerical solution of the partial differential equations, which characterize a dynamic model of the network, requires significant computational resources. The problem is to find, for a given mathematical model of a pipeline, a numerical method that meets the criteria of accuracy and relatively small computation time. The main goal of this paper is to characterize different transient models and existing numerical techniques to solve the transient equations.

Osiadacz and Chaczykowski (1998, 2001) compared isothermal and non-isothermal transient models for gas pipelines. Adiabatic flow is associated with fast dynamic changes in the gas. In this case, heat conduction effects cannot be neglected. Isothermal flow is associated with slow dynamic changes. Changes of temperature within the gas due to heat conduction between the pipe and the soil are sufficiently slow to be neglected.

Lewandowski (1994) presented an application of an object-oriented methodology for modeling a natural gas transmission network. This methodology has been implemented using a library of C^{++} classes for structured modeling and sensitivity analysis of dynamical systems. The model of a gas pipeline network can be formulated as a directed graph. Each arc of this graph represents a pipeline segment and has associated with it a partial differential equation describing the gas flow through this segment. Nodes of the graph corresponding to the nodes of the gas pipeline network can be classified as: source nodes, sink nodes, passive nodes and active nodes.

Zhou and Adewumi (1995) presented a “new” method for solving one dimensional transient natural gas flow in a horizontal pipeline without neglecting any terms in the conservation of momentum equation. In simulating transient flow of single-phase natural gas in pipelines, most of the previous investigators neglected the inertia term in the momentum equation. This renders the resulting set of partial differential equations linear. Numerical methods previously used to solve this system of partial differential equations include the method of characteristics and a variety of explicit and implicit finite difference schemes. Neglecting the inertia term in the momentum equation will definitely result in a loss of accuracy of the simulation results.

Issa and Spalding (1972), Deen and Reintsema (1983), Thorley and Tiley (1987) and Price et al. (1996) developed the basic equations for one-dimensional, unsteady, compressible flow, including the effects of wall friction and heat transfer. Issa and Spalding (1972) used the Hartree 'hybrid' method, which combines the use of a rectangular grid with the use of characteristics. They suggested that the friction factor and Stanton number can be taken as constants in shock-tube flows. Deen and Reintsema (1983) introduced a technique that reduces the energy equation into a single parameter in the mass equation without the assumption of isothermal or isentropic flow. They used the method of characteristics in conjunction with a finite difference method with second-order truncation error. Price et al. (1996) estimated the effective friction factor and overall heat transfer coefficient for a high pressure, natural gas pipeline during fully transient flow conditions. They used time varying SCADA (Supervisory Control And Data Acquisition) measurements for pipeline boundary condition and used implicit finite difference approximations for solving partial differential equations.

Rachford and Dupont (1974) used a Galerkin finite element method by considering two-dimensional elements in space-time to simulate isothermal transient gas flow. Heath and Blunt (1969) used the Crank-Nicolson method to solve the conservation of mass and momentum equations for slow transients in isothermal gas flow. The main disadvantage of this method is that it does not always give a stable solution according to the Neumann stability analysis of a large time step.

Thorley and Tiley (1987) developed conservation laws for unsteady non-isothermal one-dimensional compressible flow. They also surveyed several popular solution methods for transient pipeline analysis, such as the method of characteristics, explicit and implicit finite difference method, and finite element method. This paper has an excellent literature review for these methods of solutions.

Maddox and Zhou (1983) used steady-state friction loss calculation techniques applied in real time to determine the unsteady state behavior of pipeline systems from pressure drop and material balance relationships.

Kiuchi (1994) described a fully implicit finite difference method for solving isothermal unsteady compressible flow. A Von Neumann stability analysis on the finite difference equations of a pipe

(after neglecting the inertia term in the momentum equation) showed that the equations are unconditionally stable. Kiuchi (1994) compared this method with other methods such as the method of characteristics, Lax-Wendroff method, Guys method and the Crank-Nicolson method and showed that fully implicit methods are very accurate for a small number of sections and a large time step, which is very useful for industrial gas pipelines because of the savings in computation time.

Luongo (1986) presented an isothermal solution for gas pipelines using the Crank-Nicolson method for solving equations. The linear approximation was proven to yield reasonably accurate results, while saving as much as 25% in the computational time.

Tao and Ti (1998) have utilized the electrical analogy between pipeline networks and electrical circuits. The central idea in this approach is that various features of gas pipeline networks are simulated using the notion of electrical resistance. In pipeline networks, resistance components are used to model pipe geometry, the effect of fluid compressibility is simulated via capacitance components and the kinetic energy effects are approximated by inductance components. They converted the partial differential equations into an ordinary differential equation using a method similar to that of Osiadacz (1987), thereby reducing the CPU time significantly.

Hati et al. (2001) investigated the unsteady profiles of pressure and gas mass flux in a horizontal pipe caused by completely or partially shutting and opening a valve in a single pipeline. They used eight different cases of boundary conditions.

Wylie et al. (1974), Yow (1971) used an inertia multiplier modification to the equation of motion with the method of characteristics to improve its computational capabilities for analyzing natural gas pipeline flow.

Modisette (2002) presented the impact of the thermal model on the overall pipeline model for both gas and liquid. He coupled this model with a transient ground thermal model.

Dupont and Rachford (1980) explained the effect of thermal changes induced by transients in gas flow and considered three different environments around the pipe and showed the effect of these conditions on temperature distribution.

Osiadacz and Bell (1995) presented a method based upon decomposition-coordination techniques which are suitable for parallel computation and hence for implementation on parallel processors.

Beam and Warming (1976) developed an implicit finite difference scheme for the efficient numerical solution of nonlinear hyperbolic systems in conversation-law form. The algorithm results in a second order time-accurate, two-level, non-iterative solution using a spatially factored form.

Chang (2001) used the method of characteristics and Total Variation Diminishing (TVD) and compared these two methods. This contributed significantly to technical indigenization and maximization of operators' utilization and understanding in Korea's pipe industry.

McConnell et al. (1992) developed the tracking and prediction simulation models based on SIROGAS and fully integrated their work with the SCADA of an operating high-pressure gas pipeline network.

Ibraheem and Adewumi (1996) developed a numerical procedure to simulate transient phenomena in a 2-D natural gas flow using a special Runge-Kutta method to model accurate evolution of flow characteristics. Thus, the Total Variation Diminishing (TVD) technique can be used with higher-order accuracy in order to resolve sharp discontinuous fronts.

2.3 Centrifugal Compressor and Compressor Station

Botros et al. (1989, 1991) and Botros (1994) presented a dynamic simulation for a compressor station that consists of nonlinear partial differential equations describing the pipe flow together with nonlinear algebraic equations describing the quasi-steady flow through various valves, constrictions, and compressors. This model included a mathematical description of the control system, which consists of mixed algebraic and ordinary differential equations with some controller limits.

Bryant (1997) modeled compressor station control, which had some advantages such as the ability to set individual unit swing priority, the ability to try and meet multiple setpoints, and the

ability to automatically come on-line and off-line. The model used automatic linepack tuning instead of automatic pipeline roughness tuning.

Stanley and Bohannan (1977) discussed the application of dynamic simulation to centrifugal compressor control system design. The simulation studies resulted in design recommendations concerning the number and location of recycles required, sizing of recycle control valves, and set point, gain, and reset settings for control system instrumentation. This paper solves equations in ordinary differential equation form without considering the pipe equations within the compressor station.

Turner and Simonson (1985, 1984) developed a computer program for a compressor station that is added to SIROGAS, which is a program for solving pipeline networks for steady state and transient mode. Schultz (1962) derived the real-gas equations for polytropic analysis and demonstrated their application to centrifugal compressor testing and design.

Odom (1990) reviewed the theory of centrifugal compressor performance, and also presented a set of polynomial equations for the centrifugal compressor map. By using different values for the constant coefficients in these equations, it is possible to model different compressors.

Carter (1996) presented a hybrid mixed-integer-nonlinear programming method, which is capable of efficiently computing exact solutions to a restricted class of compressor models and attempted to place station optimization in the context with regard to simulation.

Letniowski (1993) presented an overview of the design process for a compressor station model that is part of a network model.

Jenicek and Kralik (1995) developed optimized control of a generalized compressor station. The work described an algorithm for optimizing the operation of the compressor station with fixed configuration.

Botros (1990) presented a numerical study of gas recycling during surge control, and furnished a basic understanding of the thermodynamic point of view and showed the variation of gas pressure, temperature and flow.

Phillippi (2002), Mathews (2000) and Murphy (1989) presented the fundamental principles of reciprocating compressors, which include discussions of PV diagrams, capacity, volumetric efficiency, and horsepower.

Hartwick (1968) obtained the resistance factor of valves and gas passage of a reciprocating compressor cylinder by a simple steady flow test. This resistance factor was used to predict isentropic efficiency for dynamic operation. Hartwick (1974) developed general mathematical expressions, to calculate the power loss incurred for each of several mechanical configurations of bypass deactivation.

Metcalf (2000) presented the effect of compressor valves to improve reciprocating compressor performance, compressor efficiency and horsepower consumption, by choosing the best types of valves.

Pierson and Wilcox (1984) developed a computer system for analysis of multi-stage reciprocating compressors which has the ability to generate a sequence of adding clearance to the cylinders in such a way that the compressor is operated within 30% of rated load over a range of suction and discharge pressures.

3.0 TASKS

This project is separated into five distinct tasks: Development of component models, development of the optimization algorithm, software and hardware implementation, development of control modules, and evaluation and analysis of pipeline events. The following sections describe the work that has been completed on each task, and the percentage of the task that has been completed.

Task 1.0: Develop and Analyze Component Models for Integration into the VPST

This task focuses on analyzing existing compressor station and pipeline models and, if necessary, developing new models. Nodes represent modeled components. For example the compressor stations are modeled as a node, and within the compressor station, the engines and compressors are modeled as subnodes. The pipeline that connects two compressor stations is also designated as a node. Where the compressor station node includes mathematical descriptions of engines, compressors, and gas turbines, the pipeline node contains a set of equations that describe turbulent, compressible, and transient flow through the pipeline. Blocking valves and metering stations are also represented by nodes. The interfaces between the nodes are referred to as arcs.

This task is separated into the following subtasks. Each subtask describes a different type of node and the modeling equations that are incorporated into that type of node.

Subtask 1.1: Pipeline Node

Mathematical models are used to design, optimize, and operate increasingly complex natural gas pipeline systems. Researchers continue to develop transient mathematical models that focus on the unsteady nature of these systems. Many related design problems, however, could be solved using steady-state modeling.

Several investigators have studied the problem of compressible fluid flow through the pipeline and have developed a range of numerical schemes, which include the method of characteristics,

finite element methods, and explicit and implicit finite difference methods. The choice partly depends on the individual requirements of the system under investigation.

In this work, the fully implicit finite difference method is used to solve the continuity, momentum, and energy equations for flow within a gas pipeline. This methodology: 1) incorporates the inertia term in the conservation of momentum equation; 2) treats the compressibility factor as a function of temperature and pressure; and 3) considers the friction factor as a function of the Reynolds number. The fully implicit method representation of the equations offers the advantage of guaranteed stability for a large time step, which is very useful for the gas industry.

The results that were obtained were compared with those reported by Kiuchi (1994), who used the fully implicit method for an isothermal solution. The results show that modeling gas in a non-isothermal manner provides accurate pipeline flow calculations, and is extremely necessary for rapid transient processes.

The objective of this portion of the study is to simulate non-isothermal, one-dimensional compressible flow through a gas pipeline by considering: 1) the variable compressibility factor as a function of pressure and temperature; and 2) the friction factor as a function of the Reynolds number. The method of solution is the fully implicit finite difference method, which is very suitable for gas pipeline simulation because of its large step time and low computation time [Thorley and Tiley (1987), Kiuchi (1994)]. The algorithm to solve the nonlinear finite-difference equations of a pipe is based on the Newton-Raphson Method.

The unsteady, compressible, non-isothermal pipeline simulation modeling equations are developed in the following paragraphs. In this project, the continuity, momentum and energy equations for flow within a gas pipeline in an unsteady condition are solved. In this section, the gas parameters and the governing equations for this simulation are explained.

The compositions of a natural gas mixture are usually expressed in molecular fractions. The gas properties that are used for the pipeline simulation are:

Specific gravity (γ_g)

Ratio of specific heats at specified temperature $\left(C_p/C_v\right)$

Critical Pressure $\left(P_c\right)$

Critical Temperature $\left(T_c\right)$

Isentropic Exponent $\left(\sigma\right)$

Compressibility factor $\left(Z\right)$

Lower heating value $\left(LHV\right)$

Specific Gravity (γ_g). Specific gravity is the ratio of the molecular weight of the mixture to the molecular weight of air. We can find the molecular weight of the natural gas mixture by summing the molecular weight of each gas component. Therefore, the specific gravity will be:

$$\gamma_g = \frac{\sum_{i=1}^{n} Mw_i \times y_i}{28.97} \tag{3.1.1}$$

where:

n Number of components

Mw_i Molecular weight of component i

y_i: Molecular fraction of component i

Ratio of Specific Heats. (C_p / C_v). The ratio of specific heats (k) is obtained by dividing the specific heat at constant pressure (C_p) to the specific heat at constant volume (C_v). Then the ratio of specific heats is:

$$K = \frac{C_{pmix}}{C_{vmix}} = \frac{C_{pmix}}{C_{pmix} - 1.98719} \tag{3.1.2}$$

where $\overline{C}_{pmix}$: is the molecular weight of gas mixture specific heat at constant pressure $\left(\text{Btu/lbmol-°R}\right)$.

The molecular heat capacity is obtained by summing the molecular fraction of each individual component times its molar heat capacity at the temperature at which it exists:

$$\overline{C}_{Pmix} = \sum_{i=1}^{n} \overline{C}_{Pi} \times y_i \tag{3.1.3}$$

where:

$$\overline{C}_{Pi} = A + BT_i \tag{3.1.4}$$

The constants *A* and *B* are provided from Table 3.1.1.

Critical Pressure (P_c). The critical pressure is the molecular average critical pressure of the mixture, and is obtained by summing the critical pressure of each component times that component's molecular fraction:

$$P_c = \sum_{i=1}^{n} P_{ci} \times y_i \tag{3.1.5}$$

The critical pressure P_{ci} can be obtained from Table 3.1.1 for each component.

Critical Temperature (T_c). The critical temperature is the molecular average critical temperature of the mixture, and is obtained by summing the critical temperature of each component times that component's molecular fraction:

$$T_c = \sum_{i=1}^{n} T_{ci} \times y_i \tag{3.1.6}$$

Table 3.1.1: Constants for molar heat capacity (Ludwig 1983).

Gas	Formula	Molecular Weight	Critical Pressure (psia)	Critical Temperature (°R)	*A*	*B*
Air		28.97	546.70	238.4	6.737	0.000397
Ammonia	NH_3	17.03	1,638.00	730.1	6.219	0.004342
Carbon Dioxide	CO_2	44.01	1,073.00	547.7	6.075	0.005230
Carbon Monoxide	CO	28.01	514.40	241.5	6.780	0.000327
Hydrogen	H_2	2.016	305.70	72.5	6.662	0.000417
Hydrogen Sulfide	H_2S	34.07	1,306.00	672.4	7.197	0.001750
Nitrogen	N_2	28.02	492.30	226.9	6.839	0.000213
Oxygen	O_2	32.00	730.40	277.9	6.459	0.001020
Sulfur Dioxide	SO_2	64.06	1,142.00	774.7		
Water	H_2O	18.02	3,200.00	1,165.0	7.521	0.000926
Methane	CH_4	16.04	673.10	343.2	4.877	0.006773
Acetylene	C_2H_2	26.04	911.20	563.2	6.441	0.007583
Ethene	C_2H_4	28.05	748.00	509.5	3.175	0.013500
Ethane	C_2H_6	30.07	717.20	549.5	3.629	0.016767
Propene	C_3H_6	42.08	661.30	656.6	4.234	0.020600
Propane	C_3H_8	44.09	617.40	665.3	3.256	0.026733
1-Butene	C_4H_8	56.11	587.80	752.2	5.375	0.029833
Isobutene	C_4H_8	56.11	580.50	736.7	6.066	0.028400
Butane	C_4H_{10}	58.12	530.70	765.3	6.188	0.032867
Isobutane	C_4H_{10}	58.12	543.80	732.4	4.145	0.035500
Amylene	C_5H_{10}	70.13	593.70	853.9	7.980	0.036333
Isoamylene	C_5H_{10}	70.13	498.20	836.6	7.980	0.036333
Pentane	C_5H_{12}	72.15	485.00	846.7	7.739	0.040433
Isopentane	C_5H_{12}	72.15	483.50	829.7	5.344	0.043933
Neopentane	C_5H_{12}	72.15	485.00	822.9	4.827	0.045300
Benzene	C_6H_6	78.11	703.90	1,011.0	-0.756	0.038267
Hexane	C_6H_{14}	86.17	433.50	914.3	9.427	0.047967
Heptane	C_7H_{16}	100.20	405.60	976.8	11.276	0.055400

Isentropic Exponents (σ). The isentropic exponent is obtained by:

$$\sigma = \frac{\left(C_p / C_v\right) - 1}{\left(C_p / C_v\right)} = \frac{K_{av} - 1}{K_{av}} \tag{3.1.7}$$

The isentropic exponent is evaluated at the average temperature between two nodes:

$$K_{av} = K_{50} + \frac{\left(\frac{T(i)+T(j)}{2}\right)-50}{250}\left(K_{300} - K_{50}\right) \tag{3.1.8}$$

The parameters K_{300} and K_{50} are the ratios of specific heats at 300 and 50 degree Fahrenheit.

Compressibility Factor (*Z*). The universal gas law is that it will describe any gas, given a known value of Z. This gas property expresses the deviation of the real gas from the perfect gas law. The two known gas properties required for calculation of Z_{av} are critical temperature, T_c and critical pressure, P_c. The values of reduced temperature Tr, reduced pressure Pr, and reduced density ρr are computed as follows:

$$Tr = \frac{T}{T_c} \tag{3.1.9}$$

$$\mathrm{Pr} = \frac{P}{P_c} \tag{3.1.10}$$

$$\rho r = \frac{0.27\,\mathrm{Pr}}{ZTr} \tag{3.1.11}$$

Therefore, the modification by the Dranchuck et al. (1974) formula provides:

$$Z = 1 + \left(A_1 + \frac{A_2}{Tr} + \frac{A_3}{Tr^3}\right)\rho r + \left(A_4 + \frac{A_5}{Tr}\right)\rho r^2 + \frac{A_6}{Tr^3}\rho r^3 \tag{3.1.12}$$

where:

$A_1 = 0.31506$ $A_4 = 0.5353$

$A_2 = -1.0467$ $A_5 = -0.6123$

$A_3 = -0.5783$ $A_6 = 0.6895$

The result of equation (3.1.12) is shown in Figure. 3.1.1.

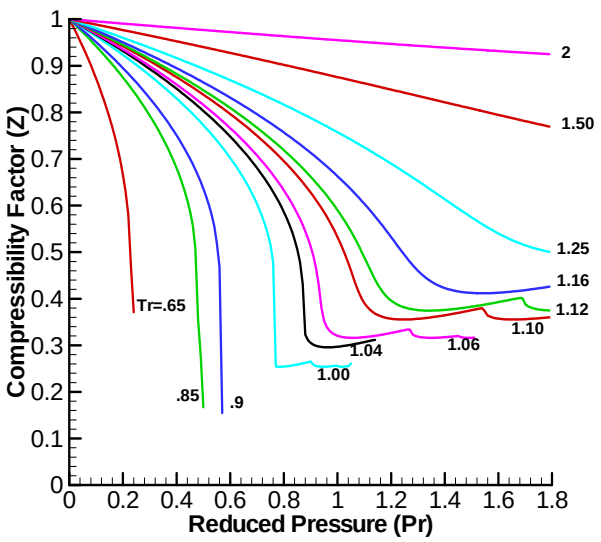

Fig. 3.1.1: Compressibility factor.

Lower Heating Value (LHV**).** The lower heating value is obtained by:

$$LHV = \sum_{i=1}^{n} (LHV)_i \times y_i \qquad (3.1.13)$$

The parameter LHV is the lower heating value for each component $\left(\text{kJ}/\text{kg}\right)$.

The non-isothermal flow of natural gas in pipelines is governed by the time-dependent continuity, momentum, and energy equations, and an equation of state for homogeneous, geometrically one-dimensional flow. By solving these equations, the behavior of gas parameters can be obtained along the pipe network.

Issa and Spalding (1972), Deen and Reintsema (1983), Thorley and Tiley (1987), and Price et al. (1996) developed the basic equations for one-dimensional, unsteady, compressible flow that include the effects of wall friction and heat transfer:

Continuity Equation

$$\frac{\partial \rho}{\partial t} + \frac{\partial}{\partial x}(\rho v) = 0 \qquad (3.1.14)$$

Momentum Equation

$$\rho \frac{\partial v}{\partial t} + \rho v \frac{\partial v}{\partial x} + \frac{\partial P}{\partial x} = -\frac{w}{A} - \rho g \sin\theta \qquad (3.1.15)$$

where $w = \dfrac{f \rho v |v|}{8} \pi D$.

Conservation of Energy

$$\rho\frac{\partial h}{\partial t}+\rho v\frac{\partial h}{\partial x}-\frac{\partial P}{\partial t}-v\frac{\partial P}{\partial x}=\frac{\Omega+wv}{A} \tag{3.1.16}$$

The term Ω is the heat flow into the pipe per unit length of pipe per unit time.

Equation of State

$$\frac{P}{\rho}=ZRT \tag{3.1.17}$$

To obtain the enthalpy h in terms of P , Z , and T , Zemansky (1968) described the thermodynamic identity:

$$dh=CpdT+\left\{\frac{T}{\rho}\left(\frac{\partial\rho}{\partial T}\right)_P+1\right\}\frac{dP}{\rho} \tag{3.1.18}$$

The resulting set of equations is:

$$\left(\frac{\partial P}{\partial t}\right)+v\left(\frac{\partial P}{\partial x}\right)+\rho V_w^{\,2}\left(\frac{\partial v}{\partial x}\right)=\frac{V_w^{\,2}}{CpT}\left[1+\frac{T}{Z}\left(\frac{\partial Z}{\partial T}\right)_P\right]\frac{\Omega+wv}{A} \tag{3.1.19}$$

$$\left(\frac{\partial v}{\partial t}\right)+v\left(\frac{\partial v}{\partial x}\right)+\frac{1}{\rho}\left(\frac{\partial P}{\partial x}\right)=-\frac{w}{A\rho}-g\sin\theta \tag{3.1.20}$$

$$\left(\frac{\partial T}{\partial t}\right)+v\left(\frac{\partial T}{\partial x}\right)+\frac{V_w^{\,2}}{Cp}\left[1+\frac{T}{Z}\left(\frac{\partial Z}{\partial T}\right)_P\right]\left(\frac{\partial v}{\partial x}\right)=\frac{V_w^{\,2}}{CpP}\left[1-\frac{P}{Z}\left(\frac{\partial Z}{\partial P}\right)_T\right]\frac{\Omega+wv}{A} \tag{3.1.21}$$

The parameter V_w is:

$$V_w=\sqrt{\frac{ZRT}{\left\{1-\frac{P}{Z}\left(\frac{\partial Z}{\partial P}\right)_T-\frac{P}{\rho CpT}\left[1+\frac{T}{Z}\left(\frac{\partial Z}{\partial T}\right)_P\right]^2\right\}}} \tag{3.1.22}$$

The continuity, momentum, and energy equations can then be written in terms of the mass flow rate, $\dot{m}$. This is a matter of convenience since the primary interest, in this case, is the mass flow rate as a function of time and location. This is accomplished by replacing the velocity with the mass flow rate:

$$v = \frac{\dot{m}}{\rho A} = \frac{\dot{m} ZRT}{PA} \tag{3.1.23}$$

Therefore:

$$\frac{\partial P}{\partial t} + \frac{\dot{m} ZRT}{PA}\left[1 - \frac{V_w^{\,2}}{ZRT}\left(1 - \frac{P}{Z}\left(\frac{\partial Z}{\partial P}\right)_T\right)\right]\frac{\partial P}{\partial x} + \dot{m} V_w^{\,2}\left(\frac{1}{\dot{m}}\frac{\partial \dot{m}}{\partial x} + \frac{1}{T}\left(1 + \frac{T}{Z}\left(\frac{\partial Z}{\partial T}\right)_P\right)\frac{\partial T}{\partial x}\right)$$

$$= \frac{V_w^{\,2}}{CpT}\left\{1 + \frac{T}{Z}\left(\frac{\partial Z}{\partial T}\right)_P\right\}\left(\frac{\Omega}{A} + \frac{\dot{m} ZRT}{PA^2} w\right) \tag{3.1.24}$$

$$\frac{ZRT}{AP^2}\left\{P\left(\frac{\partial \dot{m}}{\partial t} + \frac{\dot{m} ZRT}{PA}\frac{\partial \dot{m}}{\partial x}\right) - \dot{m}\left(1 - \frac{P}{Z}\left(\frac{\partial Z}{\partial P}\right)_T\right) \times \left(\frac{\partial P}{\partial t} + \frac{\dot{m} ZRT}{PA}\frac{\partial P}{\partial x}\right) + \frac{P\dot{m}}{T}\left(1 + \frac{T}{Z}\left(\frac{\partial Z}{\partial T}\right)_P\right)\right.$$

$$\left. \times \left(\frac{\partial T}{\partial t} + \frac{\dot{m} ZRT}{PA}\frac{\partial T}{\partial x}\right)\right\} + \frac{ZRT}{P}\frac{\partial P}{\partial x} = -\frac{wZRT}{PA} - g\sin\theta \tag{3.1.25}$$

$$\frac{\partial T}{\partial t} + \frac{V_w^{\,2}}{Cp}\left(1 + \frac{T}{Z}\left(\frac{\partial Z}{\partial T}\right)_P\right)\frac{ZRT}{AP^2}\left[P\frac{\partial \dot{m}}{\partial x} - \dot{m}\left(1 - \frac{P}{Z}\left(\frac{\partial Z}{\partial P}\right)_T\right)\frac{\partial P}{\partial x}\right] + \frac{\dot{m} ZRT}{PA}$$

$$\times \left(1 + \frac{V_w^{\,2}}{CpT}\left(1 + \frac{T}{Z}\left(\frac{\partial Z}{\partial T}\right)_P\right)^2\right)\frac{\partial T}{\partial x} = \frac{V_w^{\,2}}{CpP}\left\{1 - \frac{P}{Z}\left(\frac{\partial Z}{\partial P}\right)_T\right\}\left(\frac{\Omega}{A} + \frac{\dot{m} ZRT}{PA^2} w\right) \tag{3.1.26}$$

Complete details about the derivation of these formulas and the specification of the initial values for solving them are presented in Appendix A.

Several investigators have developed various numerical schemes such as the method of characteristics, the finite elements method, the explicit finite difference method, and the implicit finite difference method. The choice depends partly upon the particular requirement of the system under investigation. In this project we use the implicit finite difference method (Chapman et al., 2003).

The major advantage of using an implicit method over the explicit method is that the implicit method is unconditionally stable and imposes no restrictions on the maximum allowable time step. The method, however, can yield unsatisfactory results for sharp transients. In addition, some implicit methods have been known to produce erratic results during the imposition of some types of boundary conditions (Thorley, 1987).

Whereas the explicit finite difference methods are forward difference methods, the fully implicit method is a backward difference method. This method is unconditionally stable. Mohitpour et al. (1996) and Kiuchi (1994) used this method to solve the continuity and momentum equations for a gas pipeline network. This method is very accurate for the gas pipeline industry because their problems usually involve relativity slow transients, and rapidly occurring phenomena are of far less importance than long-term transients (Kiuchi, 1994).

The implicit method guarantees stability for a large time step, but requires using the Newton-Raphson method to solve a set of nonlinear simultaneous equations at each time step.

For this study, the fully implicit method is used to solve the continuity, momentum, and energy equations, and the results are compared with Kiuchi (1994). The fully implicit method consists of transforming equations (3.1.24), (3.1.25), and (3.1.26) from partial differential equations to algebraic equations by using finite difference approximations for the partial derivatives. Figure (3.1.2) shows the mesh used in this transformation. The pipe has N nodes and n time levels.

Then:

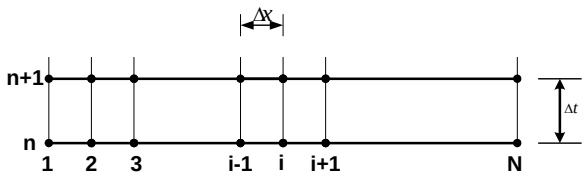

Fig. 3.1.2: Mesh of the solution.

$$\frac{\partial P}{\partial t} = \frac{\left(P_{i+1}^{n+1} + P_i^{n+1} - P_{i+1}^{n} - P_i^{n}\right)}{2\Delta t} \tag{3.1.27}$$

$$\frac{\partial \dot{m}\hat{x}}{\partial t} = \frac{\left(\dot{m}\hat{x}_{i+1}^{n+1} + \dot{m}\hat{x}_i^{n+1} - \dot{m}\hat{x}_{i+1}^{n} - \dot{m}\hat{x}_i^{n}\right)}{2\Delta t} \tag{3.1.28}$$

$$\frac{\partial T}{\partial t} = \frac{\left(T_{i+1}^{n+1} + T_i^{n+1} - T_{i+1}^{n} - T_i^{n}\right)}{2\Delta t} \tag{3.1.29}$$

So,

$$\frac{\partial P}{\partial x} = \frac{P_{i+1}^{n+1} - P_i^{n+1}}{\Delta x} \tag{3.1.30}$$

$$\frac{\partial \dot{m}\hat{x}}{\partial x} = \frac{\dot{m}\hat{x}_{i+1}^{n+1} - \dot{m}\hat{x}_i^{n+1}}{\Delta x} \tag{3.1.31}$$

$$\frac{\partial T}{\partial x} = \frac{T_{i+1}^{n+1} - T_i^{n+1}}{\Delta x} \tag{3.1.32}$$

and

$$P = \frac{P_{i+1}^{n+1} + P_i^{n+1}}{2} \tag{3.1.33}$$

$$\dot{m}\hat{x} = \frac{\dot{m}\hat{x}_{i+1}^{n+1} + \dot{m}\hat{x}_i^{n+1}}{2} \tag{3.1.34}$$

$$T = \frac{T_{i+1}^{n+1} + T_i^{n+1}}{2} \tag{3.1.35}$$

Substituting equations (3.1.27) through (3.1.35) into equations (3.1.24), (3.1.25) and (3.1.26) results in three sets of equations for each node and without considering node *N* there will be *(3N-3)* equations for a pipe. The number of unknown values at time $n+1$, which consists of pressure, temperature and mass flow rate at each node, is 3*N*. Three equations will come from the

boundary condition, and then there are 3*N* unknowns and 3*N* equations. These equations are completely nonlinear and the Newton-Raphson method can be applied to solve these equations for the compressible, non-isothermal transient flows through a pipe.

Kiuchi (1994) applied the fully implicit finite difference method to the isothermal formulation of the conservation equations:

$$\frac{\partial P}{\partial t} + \frac{V_w^2}{A}\frac{\partial \dot{m}}{\partial x} = 0 \tag{3.1.36}$$

$$\frac{1}{A}\frac{\partial \dot{m}}{\partial t} + \frac{\partial}{\partial x}\left(\frac{\dot{m}^2 V_w^2}{PA^2}\right) + \frac{\partial P}{\partial x} + \left(\frac{fV_w^2}{2DA^2}\right)\frac{\dot{m}|\dot{m}|}{P} + \frac{Pg}{V_w^2}\sin\theta = 0 \tag{3.1.37}$$

The speed V_w is $\sqrt{ZRT}$. The first and second terms in the momentum equation (3.1.37) are the inertia terms. Kiuchi, assuming a small flow velocity compared to the wave speed, neglected the second term. In order to compare the model described in this study with the results presented by Kiuchi (1994), the following adjustments were made:

1) The second inertia term was temporarily set to zero; and

2) The flow field was treated as isothermal, so the friction factor was assumed to be constant with a value of 0.008.

The comparison uses the system described by Kiuchi (1994). This system is modeled as a simple straight line 5 km in length, having an internal diameter 500 mm, and holding a gas of molecular weight 18.0 at a pressure of 5 Mpa as shown in Figure 3.1.3. As the outlet valve opens, and the out flow increases from zero to 300,000 m^3/hr, flow rate m^3/hr is shown in the standard condition (100 KPa, 288.15 K), while the inlet pressure is maintained at 5 MPa. After maintaining this condition for 20 min, the outlet valve closes. Solutions are performed using different grid densities (5, 10, 20, 30, 40, 50, 60…) to ensure a grid independent solution. A grid density of 50 is found to be sufficient for this particular problem. Figures 3.1.4 and 3.1.5 show the variation in flow at the center of the pipe length with respect to the number of nodes for the conditions given

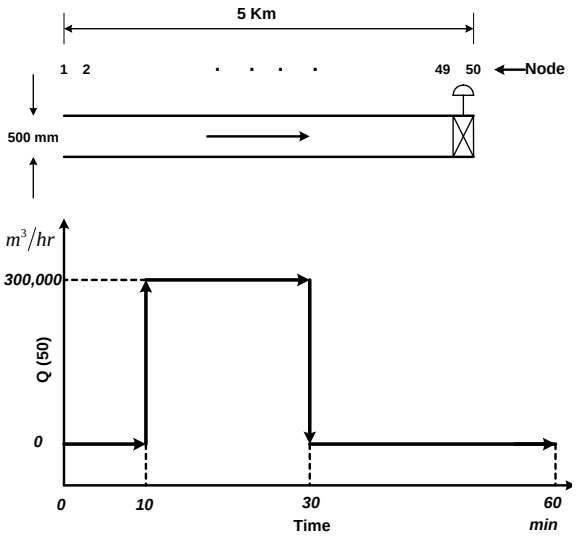

Fig. 3.1.3: Pipe information and boundary condition for flow through the valve.

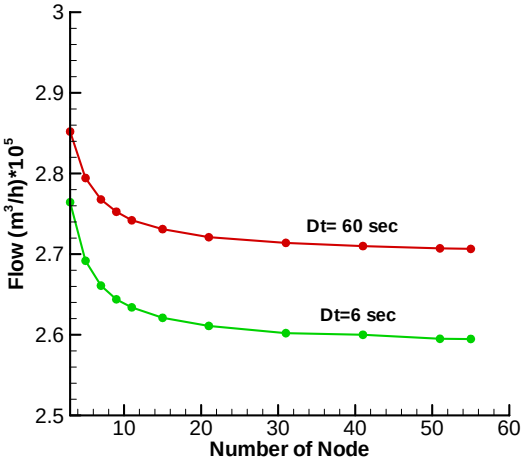

Fig. 3.1.4: Variation of flow at center of pipe length at time 11 min with respect to number of nodes for isothermal condition.

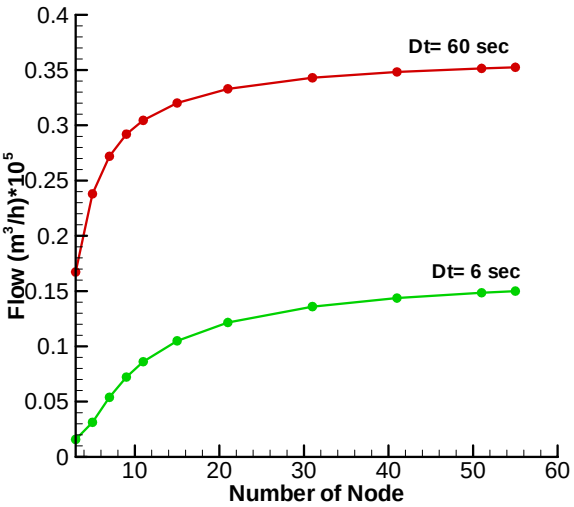

Fig. 3.1.5: Variation of flow at center of pipe length at time 31 min with respect to number of nodes for isothermal condition.

above. This is done at two different times (11 min and 31 min) and the results provide good guidance for finding a suitable node (grid) density for use in the solution process.

Figures 3.1.6 through 3.1.8 compare the results from the current study to those from the Kiuchi Model. Kiuchi compared his method with the Crank-Nicolson method, the method of characteristics, the Lax-Wendroff method, and Guy's method. The Crank-Nicholson method gave an unstable solution in the case of a large time step. The Lax-Wandroff method and the method of characteristics use the explicit method and gave a correct solution when the pipes were divided into sufficiently small sections for both rapid and slow transient phenomena; however, both required significant computation time. Kiuchi (1994) showed that Guy's method, which uses the implicit method, has good stability for a small time step and has greatly dampened oscillations.

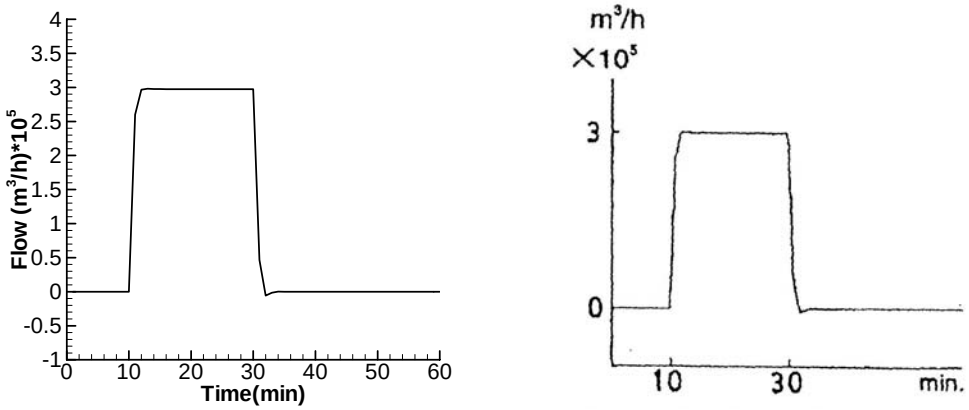

(a) (b)

Fig. 3.1.6: Comparison of present work (a) with Kiuchi model (b) for Δ*t* = 1.0 min.

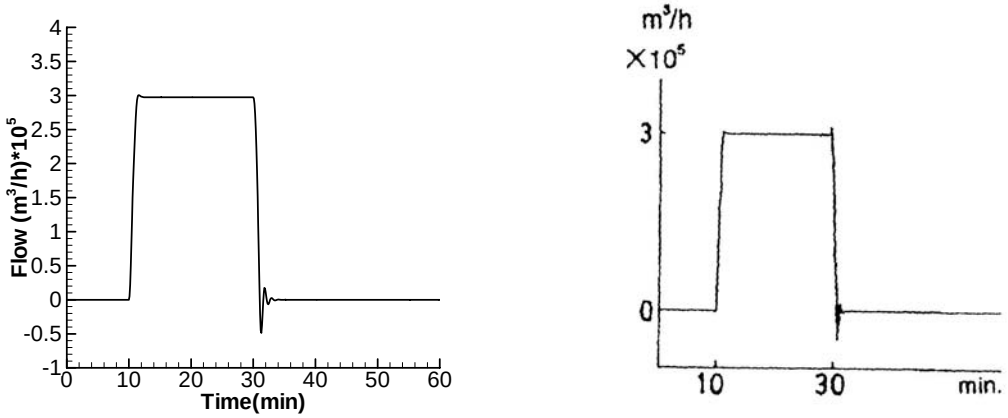

(a) (b)

Fig. 3.1.7: Comparison of present work (a) with Kiuchi model (b) for Δ*t* = 0.1 min.

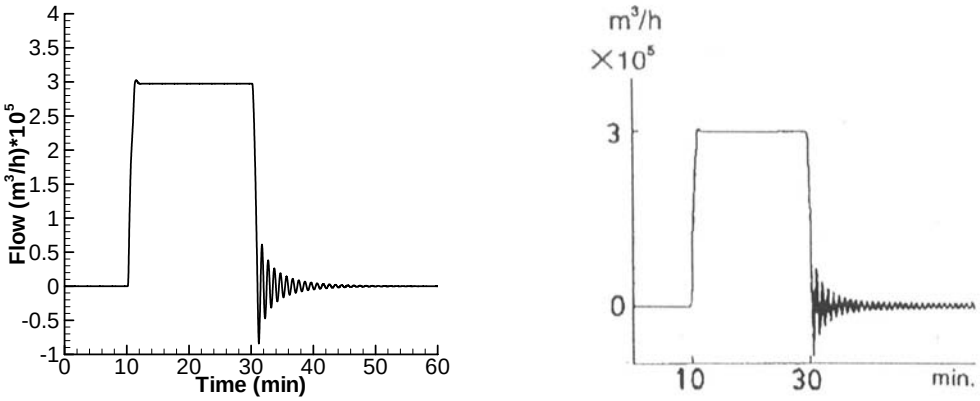

(a) (b)

Fig. 3.1.8: Comparison of present work (a) with Kiuchi model (b) for Δ*t* = 0.01 min.

Figures 3.1.6, 3.1.7 and 3.1.8 show the variation of flow rates at node 1 (pipe inlet) with respect to time for different time steps. As shown, the results of the present work compare very closely to the Kiuchi solutions. As the time step decreases, the flow rate oscillation at this condition increases. Eventually this oscillation is damped due to conservation of mass.

The Kiuchi study neglected the second term (the inertia term) of equation (3.1.37) and assumed a uniform and constant friction factor. The present study investigates the effect of the inertia term as well as friction variation. Figures 3.1.9, 3.1.10, 3.1.11 and 3.1.12 show the effect of the time step on the flow rate at node 1 and the effect of pressure changes at all nodes.

During valve opening and closing, all the gas properties attempt to change due to the condition change. The system requires some finite time to adjust itself to the new condition and reach steady state. However, different types of behaviors take place before the flow reaches the steady condition, as shown at different time steps in Figures 3.1.9, 3.1.10, 3.1.11, and 3.1.12. For a large time step, the small effect of some parameters such as the inertia term may not be noticeable within the flow before it reaches the steady state condition. In this case, the effect of the inertia term simply vanishes between the time steps, as Figures 3.1.9 and 3.1.10 depict. Therefore, the existence or absence of the inertia term in the momentum equations will not affect the results. On the other hand, for small time steps the effect of this parameter is noticeable and in fact plays an important rule in the fluctuations in amplitude and in damping before reaching steady state, as shown in Figures 3.1.11 and 3.1.12.

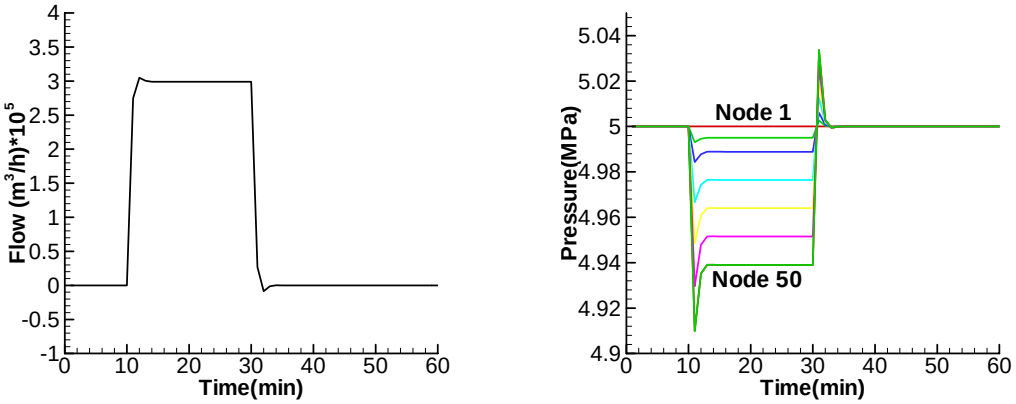

(a) (b)

Fig 3.1.9: Solution for isothermal model including inertia term with Δt = 1.0 min.

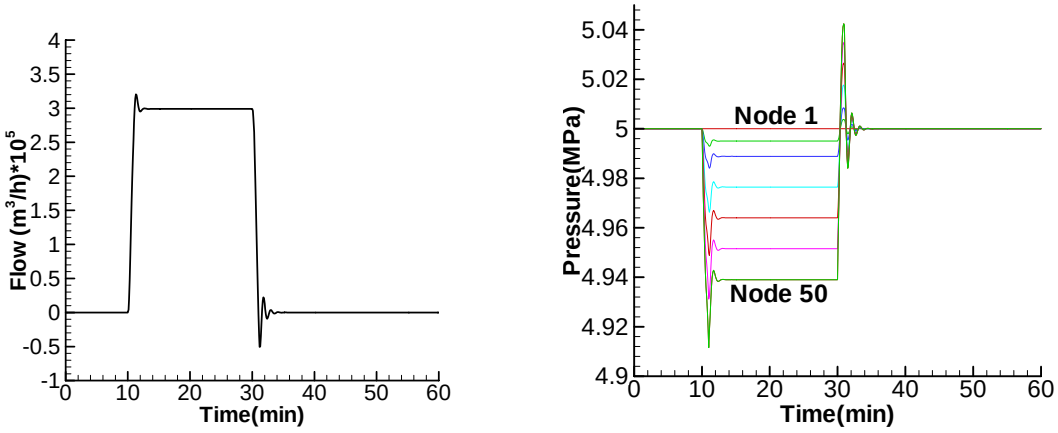

(a) (b)

Fig 3.1.10: Solution for isothermal model including inertia term with Δt = 0.1 min.

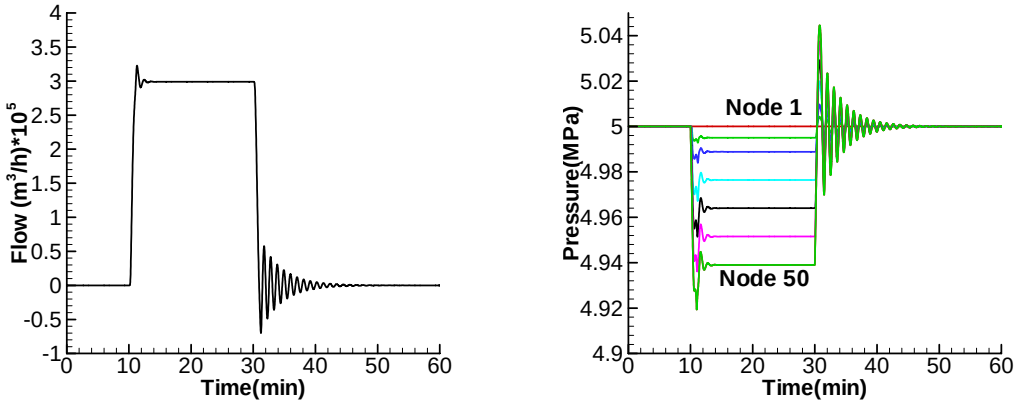

(a) (b)

Fig 3.1.11: Solution for isothermal model including inertia term with Δt = 1 sec.

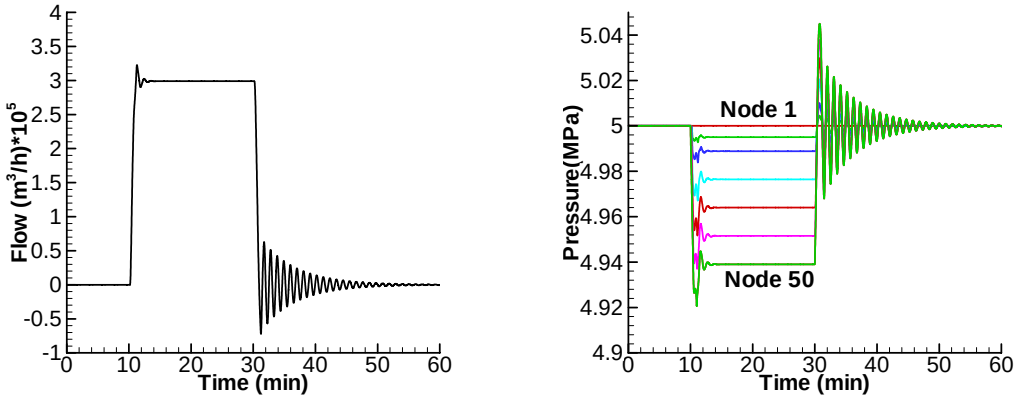

(a) (b)

Fig 3.1.12: Solution for isothermal model including inertia term with Δt = 0.01 min.

The energy equation (3.1.26), which is coupled to the momentum and continuity equations, is used to account for the temperature variation along the pipe. Specifically, the governing equations are solved using the fully implicit method. The mass flow rate and pressure boundary conditions are similar to the isothermal case.

Figure 3.1.13 shows the temperature boundary condition for the inlet flow as the valve is opened. The equivalent heat transfer coefficient between the pipe and its surroundings is 200 W/ m^2K.

The effects of non-isothermal conditions on the flow are illustrated in Figures 3.1.14 through 3.1.19. Figures 3.1.14, 3.1.16, and 3.1.18 show the effect of the time step on the flow rate at node 1 at different times. Figures 3.1.15, 3.1.17, and 3.1.19 show the same effect on the temperature and compressibility variation. The figures show that the flow rate is significantly affected by the temperature variations until the flow reaches steady state. While the mass flow rate in the isothermal case suddenly jumps to the steady state condition, the mass flow rate of the non-isothermal case gradually increases until steady state is reached. This occurs because the density varies with respect to temperature. By opening and closing the valve, the flow pressure and temperature change. This results in a significant density change. As the density change slowly transfers from one part of the flow to the other parts, the properties of the flow change accordingly. Hence, the temperature effect on the pipeline flow analysis must be taken into account since ambient conditions vary not only along with the seasons, but also between day and night time.

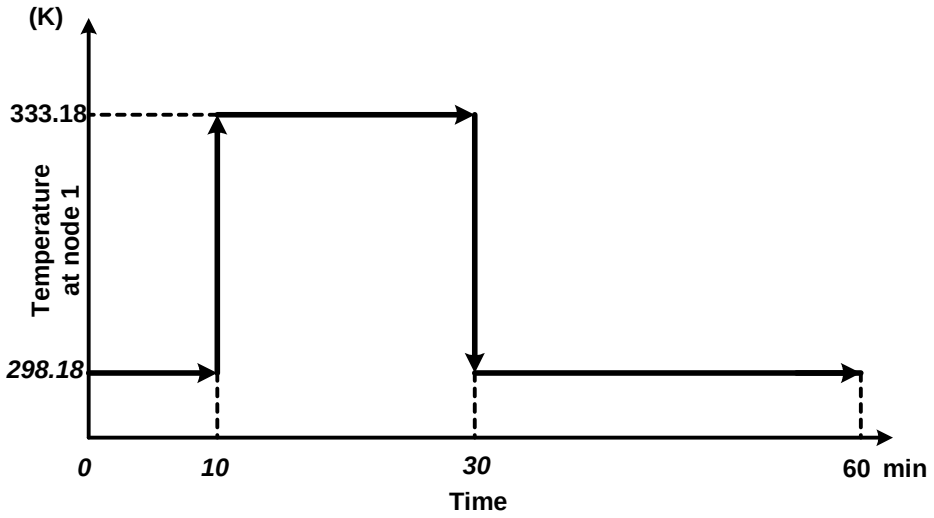

Fig 3.1.13: Temperature boundary condition at node 1.

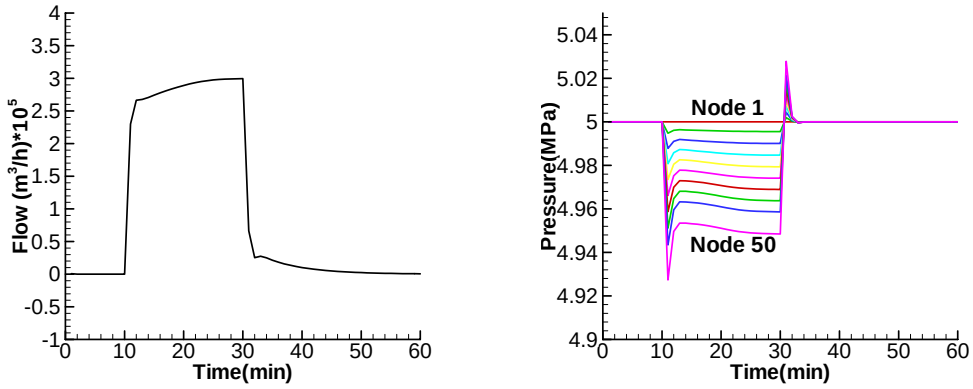

(a) (b)

Fig 3.1.14: Flow (a) and Pressure distribution (b) for non-isothermal condition and Δt = 1.0 min.

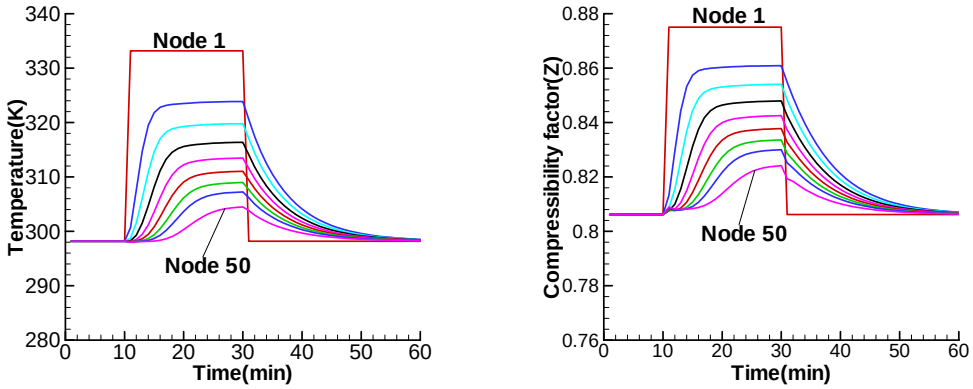

(a) (b)

Fig 3.1.15: Temperature (a) and Compressibility factor (b) for non-isothermal condition and Δt = 1.0 min.

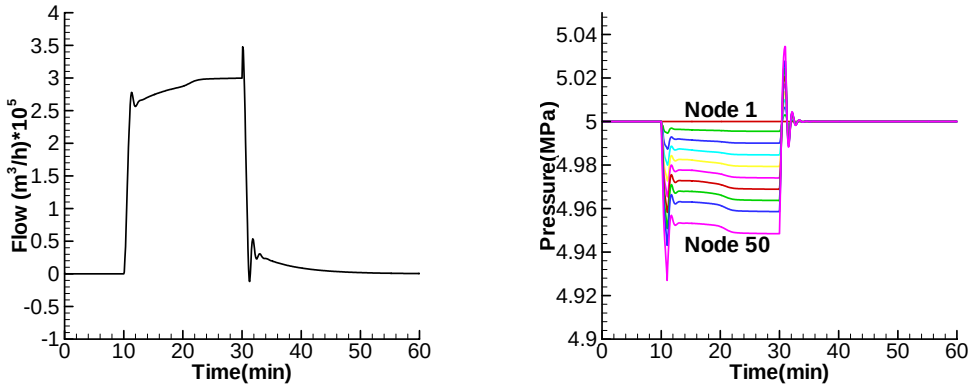

(a) (b)

Fig 3.1.16: Flow (a) and Pressure distribution (b) for non-isothermal condition and Δt = 0.1 min.

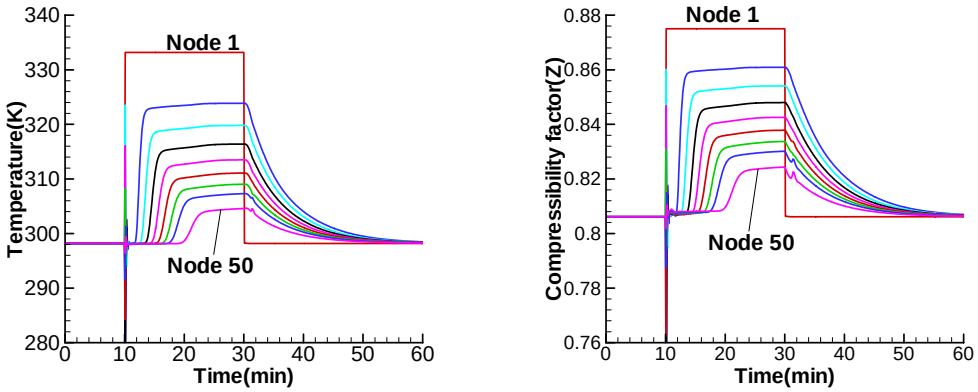

(a) (b)

Fig 3.1.17: Temperature (a) and compressibility factor (b) for non-isothermal condition and Δt = 0.1 min.

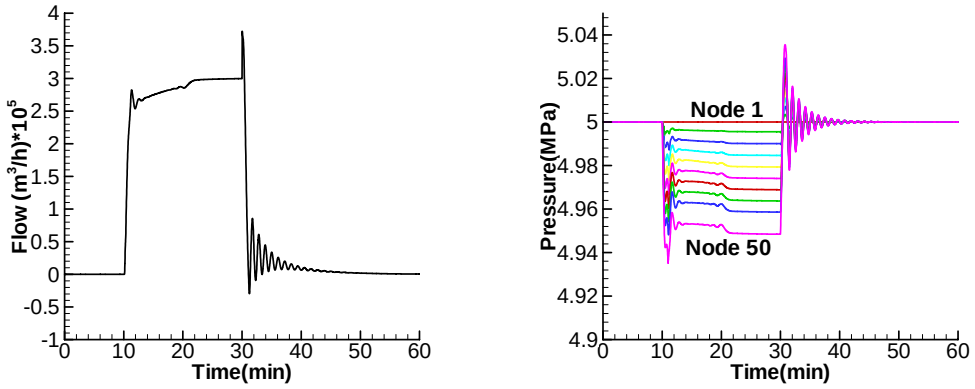

(a) (b)

Fig. 3.1.18: Flow (a) and pressure distribution (b) for non-isothermal condition and Δt = 1.0 sec.

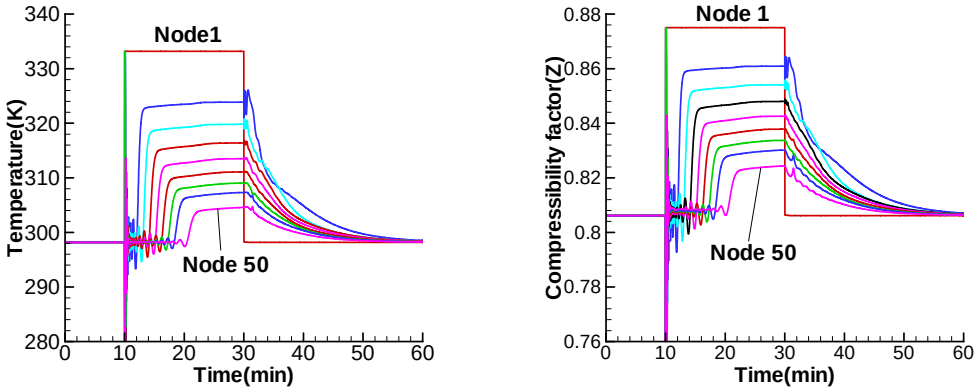

(a) (b)

Fig. 3.1.19: Temperature (a) and compressibility factor (b) for non-isothermal condition and Δt = 1.0 sec.

The flow rate and pressure variation with respect to pipe length and time are shown in Figure 3.1.20. As the length of pipe increases, the pressure drop due to the opening of the valve increases. A longer time is required to reach a steady state condition. Similarly, when the valve is closed, the pressure takes longer to reach the final value for longer pipe lengths. Therefore, pipes with longer lengths do not experience sudden pressure changes. The flow rate behaves similarly.

Subtask 1.2: Compressor Station Node

The compressor station is somewhat more complex than the pipeline node since there can be several different configurations of engines, gas turbines, and compressors. To complicate the problem, one or more engines may operate at part-load. The compressor station node is further subdivided into additional subnodes, with each subnode representing a reciprocating engine, gas turbine, centrifugal compressor, or reciprocating gas compressor.

Reciprocating Engine Submodel. Prior research has resulted in the development of a robust turbocharger-reciprocating engine computer simulation (T-RECS) package (Chapman and Keshavarz-Valian, 2003), which model uses energy, momentum, and mass conservation equations to conduct a cycle analysis of the gases within the engine cylinder. It calculates the airflow rate through the engine system, the exhaust gas temperature, the power generated by the engine, and fuel consumed by the engine. The simulation completes a cycle analysis that

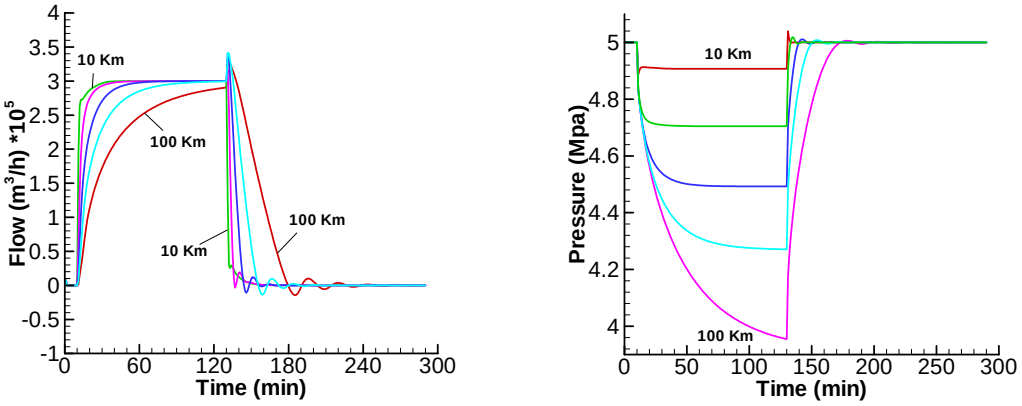

(a) (b)

Fig. 3.1.20: Flow distribution in the head of pipe (a) and pressure distribution in the end of pipe (b) for different pipe length respect to time.

calculates the in-cylinder pressure and temperature throughout the engine cycle. The T-RECS program was funded by the Gas Research Institute (now the Gas Technology Institute) and was validated with information from the Pipeline Research Council International, Inc.

Inputs to this simulation can be as detailed as the specification of the spark advance for the spark plug, or as easy as the selection of a generic 2- or 4-stroke cycle engine that generates a particular power output. Since the computational effort is of the order of 50 seconds, the engine subnode will present only a small addition to the computational effort necessary for the entire VPST.

Gas Turbine Submodel. As with the reciprocating engine node, the goal of the gas turbine engine node is to provide estimates of power, exhaust gas temperature, fuel consumption, and emissions. These inputs are based on operating conditions and the specific design of the gas turbine. Euler's equations for turbomachinery, velocity triangles, and combustion analysis are used to determine the gas turbine output conditions (Mattingly, 1999). The combination of Euler's equations and velocity triangles provides a balance between the conservation of energy and angular momentum. Empirical relationships allow compressor and turbine efficiencies to be incorporated into the model.

Centrifugal Compressor Submodel. The compressor equations are used for two types of solutions. One solution type is to define pipeline conditions across the compressor (flow, discharge pressure, suction pressure, and suction temperature) with the goal to determine whether the operating point is on the compressor map and, if so, to determine the fuel consumption of the driver (gas turbine, engine). The other solution type is the specification of the driver to operate at full load power, with the goal to determine the pressure ratio produced by the compressor at a specified ratio.

The key parameters that are necessary to describe compressor performance are isentropic head, isentropic efficiency, rotational speed and power. Considering suction, s, and discharge, d, for the compressor shown in Figure 3.1.21 yields:

$$Head = \frac{T_s R Z_s}{\sigma}\left(\left(\frac{P_d}{P_s}\right)^{\sigma} - 1\right) \tag{3.1.38}$$

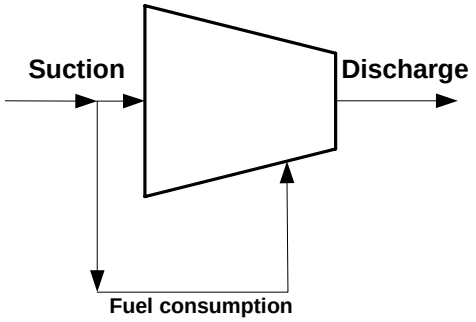

Fig. 3.1.21: Schematic of compressor and fuel consumption.

where:

Head	Isentropic head $\left(\mathrm{kJ}/\mathrm{kg}\right)$
T_s	Suction Temperature (K)
P_s	Suction Pressure (Pa)
P_d	Discharge Pressure (Pa)

Taking $R = \dfrac{\bar{R}}{M_G}$ and $\gamma_g = \dfrac{M_G}{M_{air}}$, results in:

$$Head = 0.28704 \frac{T_s Z_s}{\sigma \gamma_g} \left(\left(\frac{P_d}{P_s} \right)^{\sigma} - 1 \right) \tag{3.1.39}$$

The volumetric flow rate through the compressor is expressed in terms of the mass flow rate and standard pressure and temperature is:

$$Q_{st} = \frac{\dot{m}_{dc} R}{\dfrac{P_{sc}}{Z_{sc} T_{sc}}} \tag{3.1.40}$$

where:

P_{sc}	Standard Pressure (101,325 Pa)
T_{sc}	Standard Temperature (288.15 K)
Z_{sc}	1.00

Then:

$$Power = \frac{Head \times \dot{m}_{ac}}{\eta_{is}\eta_{mech}} \qquad (3.1.41)$$

where:

$Power$	Power (Kw)
η_{is}	Isentropic efficiency
η_{mech}	Mechanical efficiency (~ 0.98)

One method to input centrifugal compressor characteristics into a pipeline simulation model is to digitize the entire head versus capacity and store it as a table. On the other hand, a simplified but still accurate representation of the head versus capacity curve, however, can be obtained through the use of normalized characteristics. Figure 3.1.22 shows a sample compressor map.

Three normalized parameters can be used to describe a compressor map $Head/N^2$, Q_{ac}/N, and η_{is}. Using standard polynomial cure-fit procedures for each centrifugal compressor (Odom, 1990) relationships between these three parameters are:

$$\frac{Head}{N^2} = b_1 + b_2\left(\frac{Q_{ac}}{N}\right) + b_3\left(\frac{Q_{ac}}{N}\right)^2 \qquad (3.1.42)$$

and:

$$\eta_{is} = b_4 + b_5\left(\frac{Q_{ac}}{N}\right) + b_6\left(\frac{Q_{ac}}{N}\right)^2 \qquad (3.1.43)$$

The parameters b_1, b_2, b_3, b_4, b_5, and b_6 are the coefficients of the centrifugal compressor

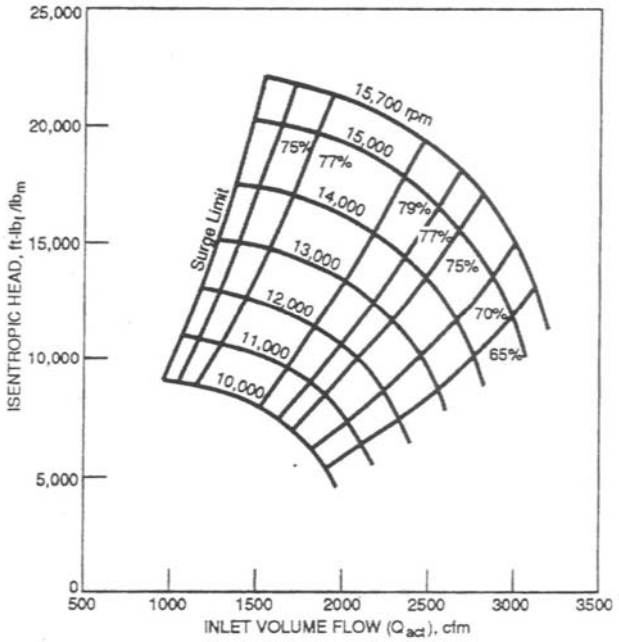

Fig. 3.1.22: Compressor Map (Odom 1990).

map that characterize a particular compressor. With these coefficients, the compressor speed and isentropic efficiency can be calculated as functions of the isentropic head and inlet volumetric flow.

The fuel consumption for the driver is obtained by:

$$\dot{m}_f = \frac{Power}{LHV \times \eta_{dr}} \qquad 3.1.44)$$

where:

$\dot{m}_f$ Fuel consumption $\left(\mathrm{kg}/\mathrm{s}\right)$

η_{dr} Efficiency of driver (engine or gas turbine)

The discharge temperature is obtained by:

$$T_d = T_s + \frac{T_s}{\eta_{is}/100}\left[\left(\frac{P_d}{P_s}\right)^{\sigma} - 1\right] \qquad (3.1.45)$$

The mass balance between suction and discharge of the compressor is:

$$\dot{m}_{ac})_s = \dot{m}_{ac})_d + \dot{m}_f \qquad (3.1.46)$$

where $\dot{m}_f$ is the fuel consumed by the compressor-engine system.

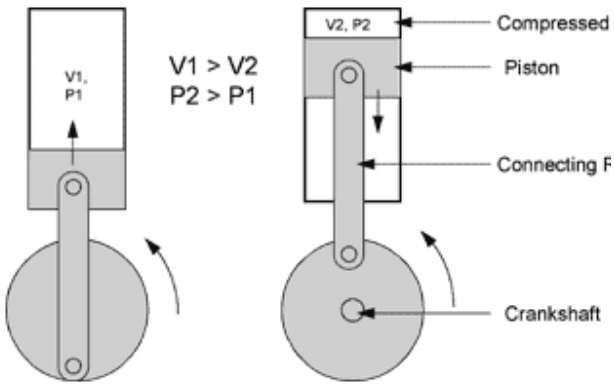

Fig. 3.1.23: Schematic of reciprocating compressor.

Reciprocating Gas Compressor Submodel. Reciprocating gas compressors are somewhat more complicated than the centrifugal compressors. Figure 3.1.23 illustrates the working mechanisms of a reciprocating compressor. These compressors generally contain unloading pockets that can be opened and closed to decrease or increase the compressor load. Reciprocating compressors are positive displacement machines that

increase air pressure by reducing volume. Substantial information exists on methods to determine various performance factors of these compressors, such as the power required and the temperature and pressure rise across the reciprocating compressors as functions of design and operating conditions.

Figure 3.1.24 shows the *p*-*V* diagram for the ideal and actual processes in a reciprocating compressor. Some information and definitions for this process are:

1. Volumetric efficiency (VE): the ratio of inlet volume to displacement
2. Cylinder clearance volume (CL): the volume of gas left in the cylinder at the discharge end of the stroke, which includes the space between the piston and cylinder head, the volume of the valves, valve pockets and any added clearance. Clearance volume is

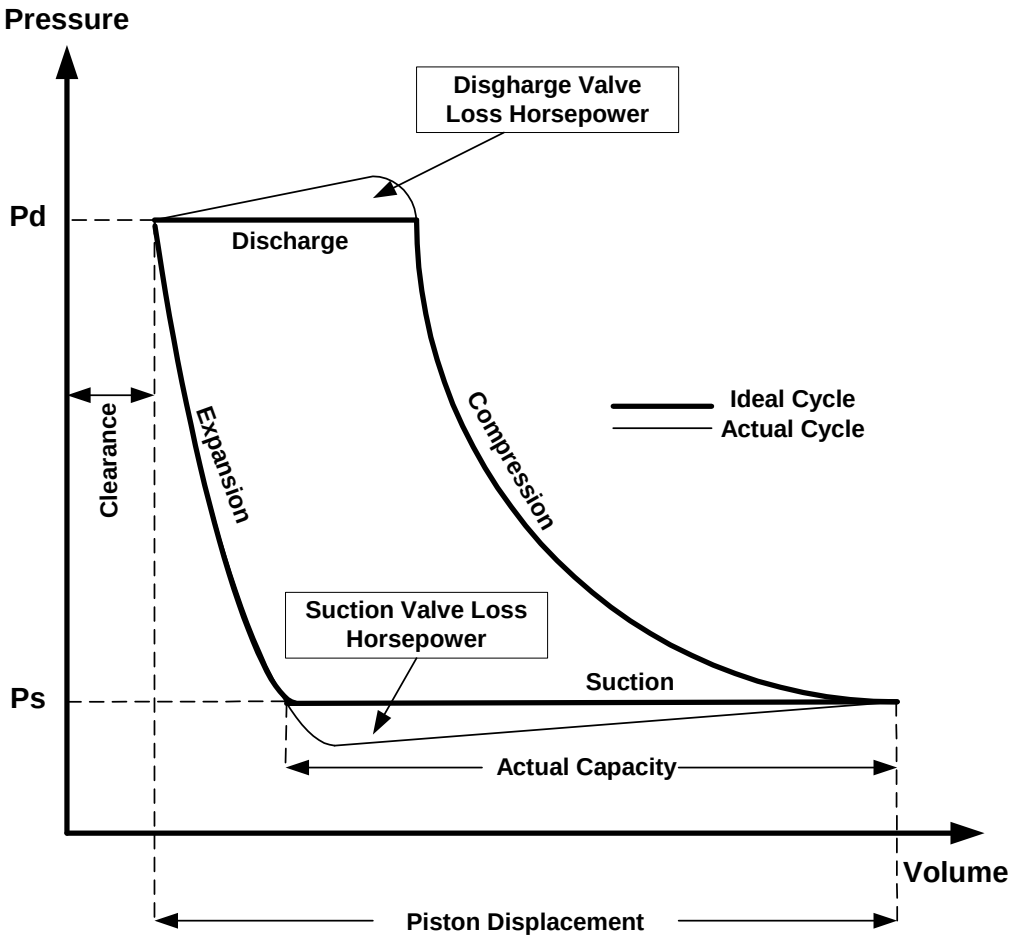

Fig. 3.1.24: Reciprocating compressor *P-V* diagram for ideal and actual condition.

generally expressed as a percentage of the swept volume of a given cylinder end.

3. Valve loss horsepower (VLHP): the power that created by the pressure drop encountered as gas flows through the suction and discharge valve.
4. Adiabatic Horsepower (AHP): the power that created from *p*-*V* diagram for adiabatic condition (Ideal) without considering valve loss regions.

The procedure to determine the horsepower consumed by a reciprocating compressor is:

1. Estimate suction volumetric efficiency (Ariel, 2001):

$$VE_s = 0.98\left(\frac{(98 - R_c)}{100} - CL\left[\left(\frac{Z_s}{Z_d}\right)R_c^{1/k} - 1\right]\right) \quad (3.1.47)$$

where:

CL Clearance

R_c Compression ratio

2. Estimate suction volumetric efficiency (Ariel, 2001):

$$VE_s = 0.98\left(\frac{(98 - R_c)}{100} - CL\left[\left(\frac{Z_s}{Z_d}\right)R_c^{1/k} - 1\right]\right) \quad (3.1.47)$$

where:

CL Clearance

R_c Compression ratio

Z_s Compressibility factor at suction side condition

Z_d Compressibility factor at discharge side condition

k Adiabatic exponent

3. Estimate the discharge volumetric efficiency (Phillippi, 2002):

$$VE_D = \frac{VE_s}{\left(\frac{Z_s}{Z_d}\right) R_c^{1/k}} \tag{3.1.48}$$

4. Estimate the adiabatic horsepower (Phillippi, 2002):

$$AHP = \frac{(144)(K)(P_s)(PD)(VE_s)(Z_s + Z_d)}{(33000)(k-1)(2 \times Z_s)} \left[(R_c)^{\frac{(k-1)}{k}} - 1 \right] \tag{3.1.49}$$

where P_s is the suction pressure (psia). The piston displacement is defined as (Ariel, 2001):

$$PD = \frac{V_{Swept} \times N}{1728} \tag{3.1.50}$$

where N is the rotational speed of the compressor crankshaft (rpm). The swept volume that is used in equation (1-50) is defined as:

$$V_{Swept} = V_{HE} + V_{CE} \tag{3.1.51}$$

where:

$$V_{HE} = A_P \times S$$

$$V_{CE} = A_P \times S - A_R \times S$$

V_{HE} Head end volume (in^3)

V_{CE} Crank end Volume (in^3)

A_P Piston area (in^2)

A_R Rod area (in^2)

S Stroke (in)

5. Estimate the suction valve loss horsepower (Phillippi, 2002):

$$SVLHP = \Delta P_s \left(A_P \right)\left(VE_s \right)\left(S \times N \right) \tag{3.1.52}$$

where ΔP_s is the pressure drop across the suction valve event.

6. Estimate the discharge valve loss horsepower (Phillippi, 2002):

$$DVLHP = \Delta P_d \left(A_P \right)\left(VE_d \right)\left(S \times N \right) \tag{3.1.53}$$

where ΔP_d is pressure drop into discharge valve event.

7. Estimate the compression efficiency (Phillippi, 2002):

$$E_c = \frac{\mathrm{AHP} \times \mathrm{E_{mech}}}{\mathrm{AHP+SVLHP+DVLHP}} \tag{3.1.54}$$

where $\mathrm{E_{mech}}$ is the mechanical efficiency.

8. Estimate the indicated horsepower (Phillippi, 2002):

$$IHP = AHP + SVLHP + DVLHP \tag{3.1.55}$$

9. Estimate brake horsepower:

$$BHP = \frac{IHP}{E_{mech} \times E_c} \tag{3.1.56}$$

10. Estimate mass fuel consumption from equation (3.1.44):

These equations that describe the performance of reciprocating and centrifugal compressors are based on the assumption of a quasi-steady flow at each time step of the numerical solution.

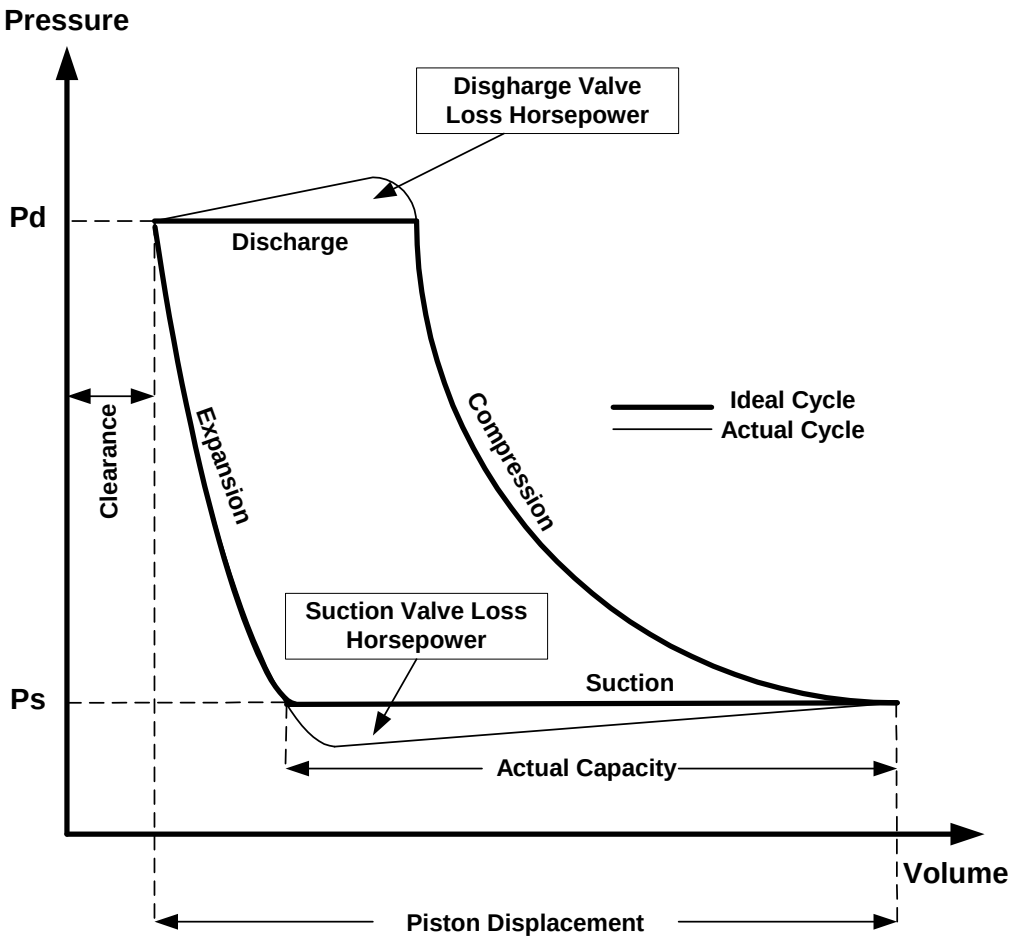

Fig. 3.1.24: Reciprocating compressor *P-V* diagram for ideal and actual condition.

Compression Unit. A compression unit is defined as a combination of a compressor and its driver. Four possible combinations are:

1. Reciprocating compressor driven by reciprocating engine
2. Centrifugal compressor driven by gas turbine
3. Reciprocating compressor driven by gas turbine
4. Centrifugal compressor driven by reciprocating engine

Items 1 and 2 are the most commonly found compression units in a natural gas pipeline system and hence were the primary focus areas for modeling in this project. A compression unit could be an integral type as many reciprocating engines and reciprocating compressor combinations are

or could be a non-integral type where the compressor is connected to the driver using an external coupling. A comprehensive compression unit database supplements the individual submodels described earlier. The user has the choice of choosing predefined units from the database or creating new units by choosing appropriate submodels constrained by any one of the four possible unit combinations. The primary data that the compression unit database includes are the unit speed and the unit rated power. The individual driver and compressor submodel database includes manufacturers' basic data, operating information and modeling information. The operating information includes the input parameters required for submodel simulation. The modeling information consists of the coefficients obtained as a result of digitizing performance data for both compressor and the driver.

Subtask 1.3: Blocking Valve Node

The blocking valve is modeled as a boundary condition for the network. Figure 3.1.25 schematically illustrates the blocking valve that is used for the simulation. When the valve is open, the conservation of mass, energy, and momentum reduce to: $\dot{m}_1 = \dot{m}_2$, $P_1 = P_2$, and $T_1 = T_2$. When the valve is closed, the conservation of mass, energy, and momentum are not applicable since there is no connection between the inlet and the outlet of valve. The mass flow rate at the valve outlet at the time when the valve is closed is zero, however, mass continues to increase at the valve entrance until a steady-state condition is reached. The equation, $\dot{m}_2 = 0$, is used to model the valve closing event.

Figure 3.1.26 shows a blocking valve that is positioned between two long pipes. Each 500 mm diameter pipe is 50 km long. Each pipe is separated into 50 computational nodes. The constant boundary conditions are:

- Inlet pressure at Pipe 1 (Point 1): 6 MPa

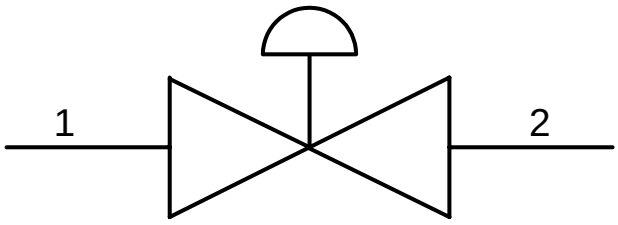

Fig. 3.1.25: Blocking valve.

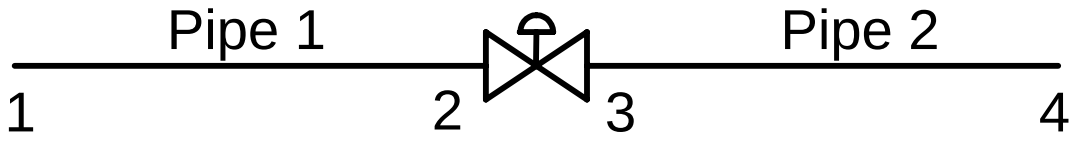

Fig. 3.1.26: Schematic of valve and two pipes connected.

- Inlet temperature at Pipe 1 (Point 1): 333.33 K
- Outlet pressure at Pipe 2 (Point 4): 4 MPa

The valve is opened for 41 minutes and 40 seconds, after which the valve is suddenly closed. The valve then remains closed for an additional 33 minutes, 20 seconds. At time = 75 minutes the valve opens and remains open until the simulation is stopped.

Figure 3.1.27 shows the pressure distribution for various nodes ranging from Node 1 (inlet) to Node 50 (exit). The pressure at each node reaches a steady state condition in the time period when the valve is initially open. The pressure gradient between nodes 1 and 50 occurs due to the frictional losses in the pipe. At time 41 minutes and 40 seconds when the valve closes, the pressure at each computational node increases to reach to inlet pressure. At 75 minutes, when the valve re-opens, the pressure at all computational nodes again trend to the steady state conditions. A similar characteristic occurs in the pipe downstream of the valve.

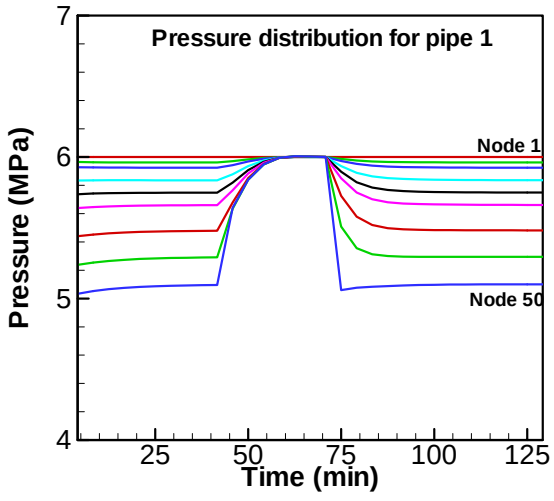

Fig. 3.1.27: Pressure distribution for inlet pipe (Pipe 1).

Figure 3.1.28 exhibits the mass flow rate variation with respect to time for the computational nodes along the inlet pipe that is upstream of the blocking valve (Pipe 1). Prior to closing the valve, the mass flow rate at all nodes asymptotically approaches the steady state flow rate of 112.6 kg/s. At time 41 minutes and 40 seconds the valve closes and the mass flow rate at Node 50 (end of pipe that is connected to the valve) suddenly

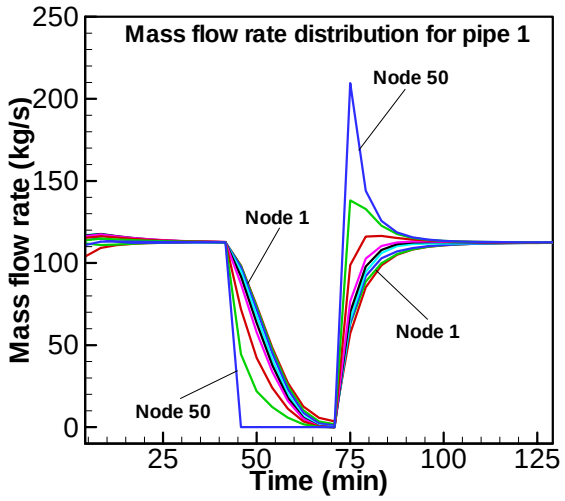

Fig. 3.1.28: Mass flow rate distribution for inlet pipe (Pipe 1).

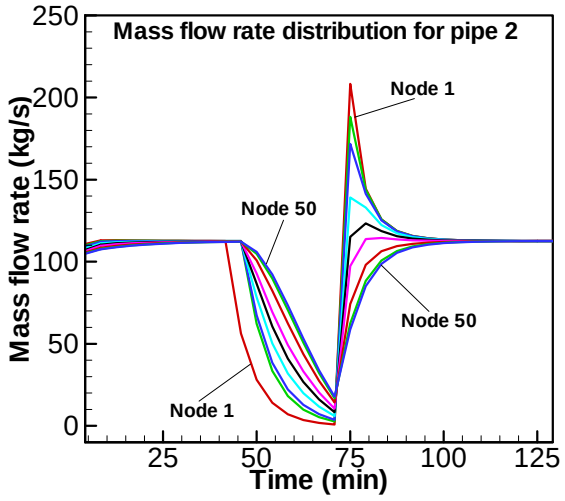

Fig 3.1.29: Mass flow rate distribution for outlet pipe (Pipe 2).

drops to zero. Since the fluid is compressible, the flow rate at the upstream nodes asymptotically approach zero, essentially packing the pipe with gas. At 75 minutes, the blocking valve re-opens and the mass flow rate at each computational node again asymptotically approach the steady state flow rate of 112.6 kg/s. Figure 3.1.29 illustrates the similar characteristic for the down stream section of pipe (Pipe 2).

Subtask 1.4: Regulator and Metering Station Node

The pressure regulator impacts VPST by creating a prescribed down stream pressure. The regulator is modeled in a similar manner to the blocking valve, since the conservation equations reduce to: $\dot{m}_1 = \dot{m}_2$. $P_1 \neq P_2$, and $T_1 \cong T_2$.

Figure 3.1.30 schematically illustrates a regulator that is positioned between two 5 km long, 500 mm diameter pipes to control the pressure at the regulator outlet pressure. Each pipe is separated into 20 nodes with the following time-invariant constant boundary conditions:

- Inlet pressure at Pipe 1 (Point 1): 6 MPa
- Inlet temperature at Pipe 1 (Point 1): 333.33 K

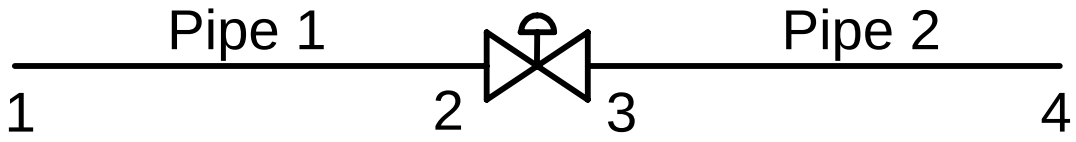

Fig. 3.1.30: Schematic of regulator and two pipes connected.

- Outlet pressure at regulator (Point 3): 4.5 MPa
- Outlet pressure at pipe 2 (Point 4): 3.5 MPa

Figure 3.1.31 shows the transient response of the mass flow rate in Pipe 1. As show in this figure, the mass flow rate at different nodes exhibits a transient fluctuation until all nodes reach the steady-state condition 10 minutes when the mass flow rate is 326.36 kg/s. The behavior is similar in Pipe 2 (Figure 3.1.32) and after 10 minutes all mass flow rates reach steady-state conditions.

Figures 3.1.33 and 3.1.34 illustrate the pressure distribution within the inlet and outlet pipes. The pressure distribution for each node is different with respect to time due to the compressibility effects and friction losses within the pipes. As shown in these figures, the node pressures asymptotically approach the steady state pressure.

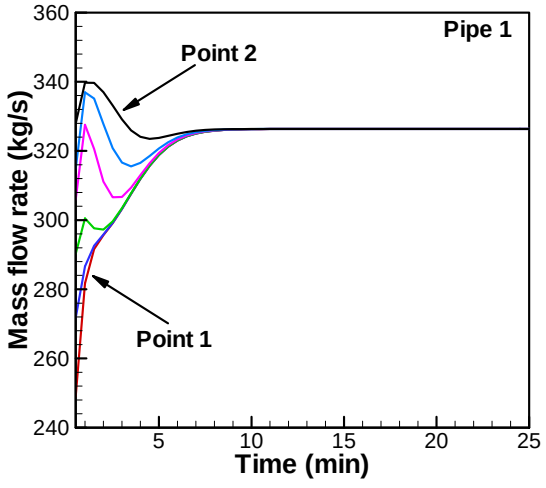

Fig. 3.1.31: Mass flow rate variation with respect to time at Pipe 1.

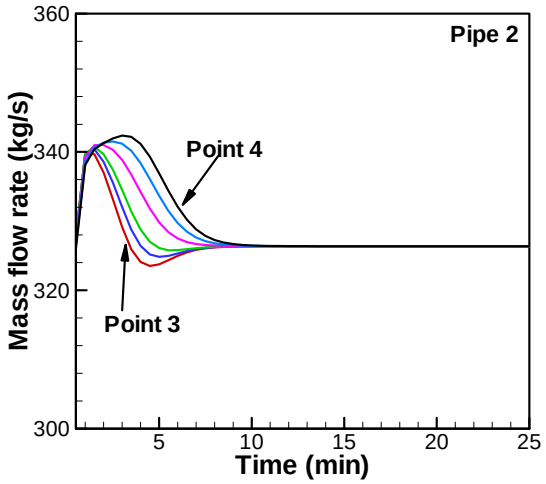

Fig. 3.1.32: Mass flow rate variation with respect to time at Pipe 2.

At the end of simulation, the pressure at Point 1 becomes 5.27 MPa at Pipe 1. The same behavior occurs at Pipe 2, but at this pipe the pressure at the inlet and outlet is fixed. Therefore there is no transient variation in pressure for other nodes as shown in Figure 3.1.34.

The same type of information is depicted for the temperature distribution for inlet and outlet pipes as shown in Figure 3.1.35 and Figure 3.1.36. Because of heat transfer between the pipe and environment, the temperature at each node is different. After about 10 minutes, the temperature at Point 2 becomes 321 K and 312 K at Point 4.

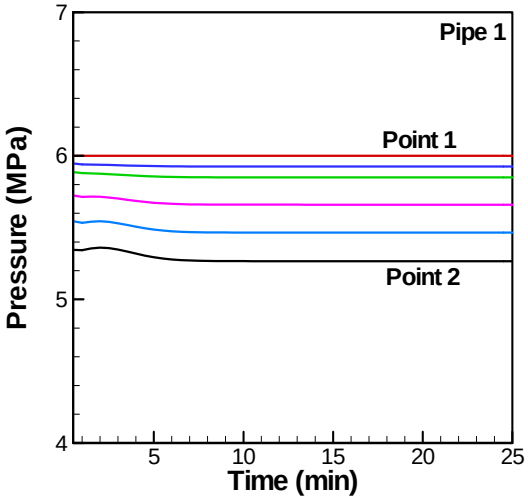

Fig. 3.1.33: Pressure distribution with respect to time in Pipe 1.

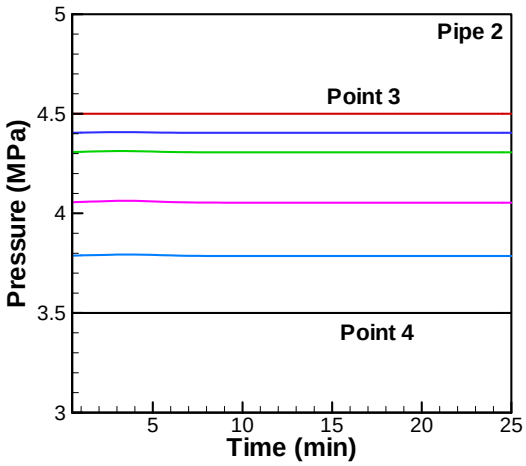

Fig. 3.1.34: Pressure distribution with respect to time in Pipe 2.

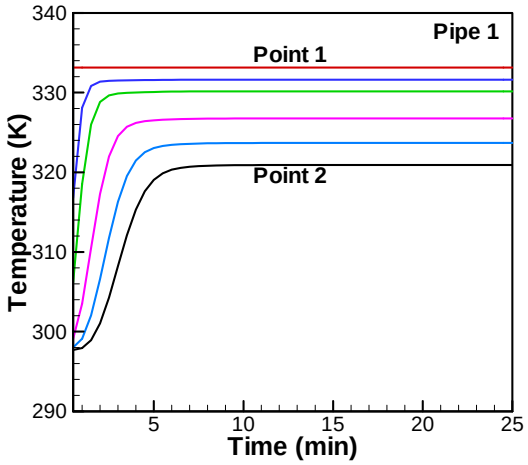

Fig. 3.1.35: Temperature distribution with respect to time at Pipe 1.

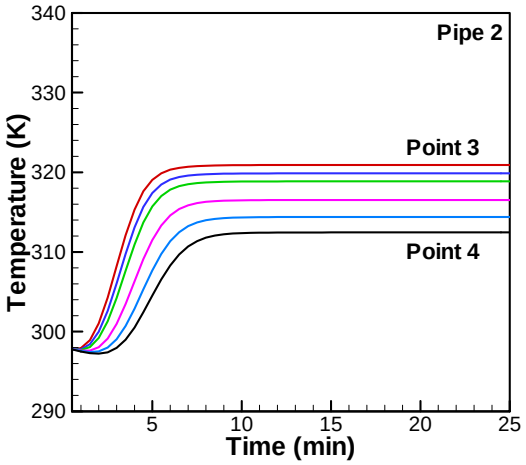

Fig. 3.1.36: Temperature distribution with respect to time at Pipe 1.

Task 2.0: Develop Optimization Algorithm

The analysis and simulation tools developed under Task 1.0 are used as a foundation to formulate new methods for performing optimization and reliability studies on the pipeline. This allows VPST to function not only as an analysis tool, but also as a design and operational planning tool. Based on interactions with industry personnel, three key needs were identified:

1. Develop optimal network performance methods through appropriate equipment selection
2. Develop methods to optimize the location and design of mid-station compression
3. Develop methods to optimize network reliability with respect to equipment failure.

It is worth noting that none of these capabilities are currently available, even though they are highly desirable to the natural gas pipeline industry. In all the above optimizations, the goal is to maximize gas flow while keeping losses within limits. Alternatively, losses may be minimized subject to limits on flow rate. Clearly, this is a constrained optimization problem, and can be solved as such. However, the industry routinely converts this to the roughly equivalent unconstrained problem of maximizing the pressure in the pipeline. The original intention was to support all of these optimization problem formulations. However, the project scope was later redefined in consultation with industry representatives and DOE, and the focus of the optimization was shifted to operational optimization, with particular emphasis on cost reduction through minimization of fuel consumption. It is important to note that currently available commercial packages do not provide the capability for fully automated optimization of operational parameters; rather, they provide computational support for human decision making. In other words, the current generation of software in this area allows a human operator to simulate pipe flow in a network without detailed modeling of equipment such as compressors and drivers. Any decisions on how to optimize the operation of equipment must be made by the human operator based on simplified simulation of a few scenarios. Thus, the solutions that are arrived at are generally not truly optimal, and require considerable user involvement. This study advances this methodology in that the software, using detailed equipment modeling and rigorous mathematical optimization, automatically generates truly optimal solutions with practically no user involvement. This represents a significant advancement in the state-of-the-art in this field.

The formulation and numerical solution scheme discussed earlier provides the ability to simulate the behavior of the system under a variety of conditions. Thus, it provides the necessary analysis capability to support optimization. In general, two types of optimization problems are of interest in pipeline networks: design optimization and operation optimization. In design optimization, the goal is to optimize the pipeline design by selecting appropriate layouts, equipment, etc. In operation optimization, the network and station configuration is given, and the goal is to operate the pipeline network in an optimal manner.

In this work, only operation optimization is considered. The optimal operation of a network involves meeting all performance requirements that are placed on the network, while minimizing an objective function. The operating parameters whose values can be adjusted to achieve this optimal operating point are referred to as "design variables" in the optimization problem.

In order to optimize the operation of the network, the problem is formulated in the format of a standard nonlinear programming problem (NLP). This standard form is:

Find the values of the design variables $[b_1,b_2,\ldots,b_r]^T$ to:

Minimize an objective function $f(\boldsymbol{b})$

Subject to the constraints: $h_j(\boldsymbol{b}) = 0$, $j = 1,\ldots, m$

and $g_j(\boldsymbol{b}) \leq 0$, $j = m+1,\ldots,n$

The formulation of the network operation problem in the standard NLP form must be done carefully to ensure that the NLP formulation captures all the relevant aspects of the associated network problem.

Formulation of the Optimization Problem. The formulation of the optimization problem is done in three steps. First, the design variables whose values are to be determined by the optimization process are defined. Next, the objective function whose value is to be minimized is specified. Finally, the necessary constraints to ensure that the optimal solution found is meaningful are formulated.

Definition of design variables: In defining the design variables, it is important to choose only those variables whose values can be directly controlled while operating the actual network; otherwise, the solution cannot be implemented. At the same time, the set of design variables must be large enough to provide a reasonably extensive design space so that there is more scope for optimization. With these considerations in mind, the compressor speeds were selected as the design variables for this formulation.

Specification of objective function: Many possible objective functions can be used to define the optimality of the network operation. These could include to: minimize fuel consumption, minimize emissions, minimize maximum pressure, and minimize station discharge temperature. While any of these can be used as the objective function for the method described herein, this report will use the objective function to minimize total fuel consumption for all examples.

Formulation of constraints: The constraints in the NLP play a critical role to ensure that the optimal operating point found is actually usable and free of undesirable conditions. In this particular case, for example, the fact that each compressor in the system can only operate in the speed range for which the compressor is designed must be taken into account. In addition, a constraint is employed to ensure that each compressor station maintains a mass flow rate that is above a preset threshold. The bounds on the compressor speeds and the requirement on the mass flow rate are directly introduced as constraints in the NLP. Other requirements, such as the suction and discharge pressures that each compressor station must maintain, are handled outside the NLP by fixing their values in the simulation. This reduces the chances of over constraining the problem and improves computational efficiency.

Based on the preceding discussion, the pipeline operation optimization problem can be stated as:

> Let the number of compressor stations in the pipeline network be N and let the number of compressors in station j be NC_j. Let n_{ik} be the speed of compressor k in station i. Further, let $nmin_{ik}$ and $nmax_{ik}$ represent the allowable minimum and maximum speeds of compressor k in station i. Let the fuel consumption rate of station i be m_{fi}. Finally, let the mass flow rate at station i be m_i and let the specified minimum allowable mass flow rate at station i be $mmin_i$.

Then, the set of design variables is defined by:

$$\{n_{ik}\},\ i = 1, \ldots, N;\ k = 1, \ldots, NC_i$$

while the objective function is given by:

$$f = \Sigma(m_{fi}),\ i = 1, \ldots, N$$

and the constraints are:

$$nmin_{ik} \leq n_{ik} \leq nmax_{ik},\ i = 1, \ldots, N;\ k = 1, \ldots, NC_I$$

$$mmin \leq m_i,\ I = 1, \ldots, N$$

Solution of the Optimization Problem. Once the network operation problem has been formulated as an optimization problem as outlined above, it can be solved using any of a variety of available methods. This work utilized the sequential unconstrained minimization technique (SUMT) with an exterior penalty function. A directed grid search method was used for the unconstrained minimization that is required by the SUMT approach.

One of the advantages of this solution approach is that it can be used in a gradient-based form or in a non-gradient form, depending on the type of method used for solving the unconstrained optimization sub-problem. Since the derivatives of the objective function and constraint functions with respect to design are not easily available, the non-gradient directed grid search method was chosen.

Overall, this method worked very well and was found to be very robust. While this method is not very efficient, its reliability, robustness, and ability to work without derivative information outweigh this one disadvantage.

Optimization Examples. The optimization examples presented in this report have been carefully selected to illustrate specific points. Table 3.2.1.summarizes the examples.

The first example is a simple two compressor proof-of-concept problem with a known optimum. The second example consists of a fourteen compressor station, and is designed to illustrate the

Table 3.2.1: Different cases for compressor station optimization.

Example 1	Compressor station with two similar compressors
Example 2	Compressor station with 14 compressors, incl. shutdown of one and two compressors
Example 3	Compressor station with three different compressors
Example 4	Two compressor stations in series, with each compressor station as in example 3

application to situations where unit shutdowns have to be taken into account. In the third example, a compressor station with three dissimilar compressors is examined. This is a common situation in practice and the optimum operating condition is difficult to find by other means. Finally, the fourth example considers two compressor stations in series to compare the results obtained by optimizing both stations simultaneously ("network level optimization") with the results obtained by optimizing each station separately ("station level optimization").

Example 1: The system considered here is a single compressor station with two identical compressors as shown in Figure 3.2.1. The compressor speed limits for this case are given in Table 3.2.2, and the goal of the optimization is to minimize the total fuel consumption while maintaining a station throughput of 85 kg/s (292.69 MMSCFD).

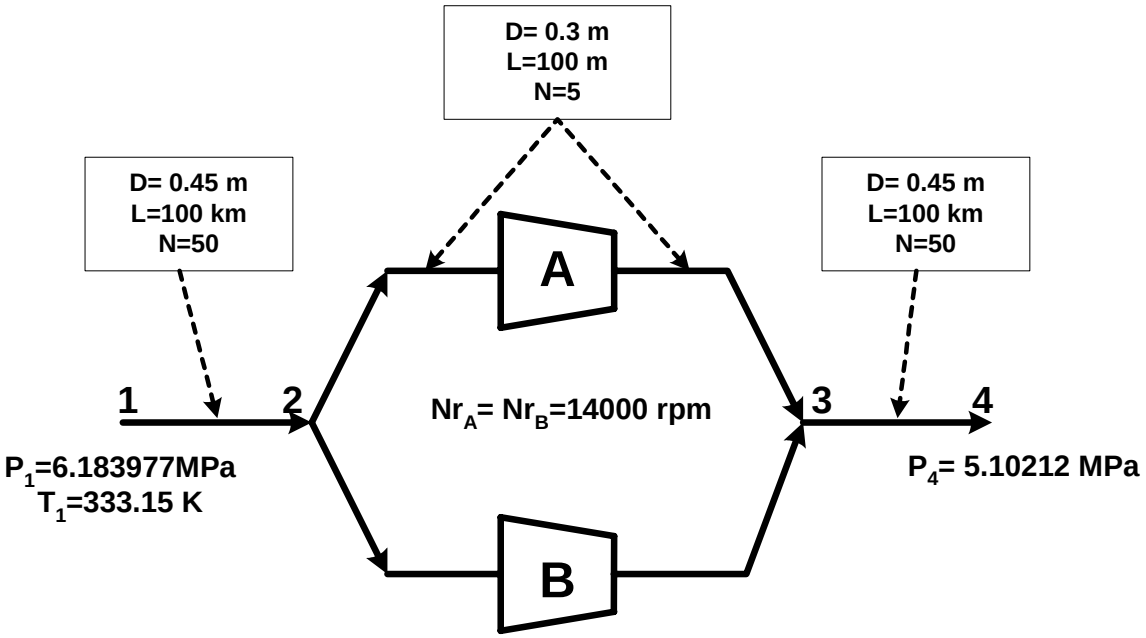

Fig. 3.2.1: Station configuration for Example 1.

Table 3.2.2: Input data for Example 1.

	N_{rA}	N_{rB}
Initial Value	14,000 rpm	14,000 rpm
Maximum Value	15,000 rpm	15,000 rpm
Minimum Value	10,000 rpm	10,000 rpm
Minimum Mass Flow Rate	85 kg/s (292.69 MMSCFD)	

It is clear that the solution we expect in this case is for both units to operate at the lowest possible fuel consumption rate that maintains the desired throughput. The optimization results for this example are shown in Table 3.2.3.

It is seen that the speeds of both compressors are reduced to 13,400 rpm, resulting in a throughput of 85.04 kg/s (292.81 MMSCFD), which is the minimum allowable value. Thus, we may conclude that the numerical optimization worked well and gave the correct solution for this simple case. It can also be seen from Table 3.2.3 that the efficiency of each unit improved from 78.71% to 78.86%, while the outlet temperature dropped from 352.46 K to 347.97 K.

Example 2: This system is a single compressor station with fourteen identical compressors as that of Example 1. The maximum and minimum speed for each compressor is 15,000 rpm and 10,000 rpm, respectively. The goal of the optimization is to minimize the total fuel consumption

Table 3.2.3: Final result for speed, isothermal efficiency, outlet temperature and fuel consumption for Example 1.

	Initial	**Final**
N_{rA} (rpm)	14,000	13,400
N_{rB} (rpm)	14,000	13,400
Fuel Consumption (kg/s- MMSCFD) x10^3	26.85 - 92.46	23.91 - 82.32
Mass Flow Rate (kg/s- MMSCFD)	87.04 - 299.70	85. 04 - 292.81
η_{isA}	78.71	78.86
η_{isB}	78.71	78.86
Discharge Temperature T_3 (K)	352.46	347.97

while maintaining a station throughput of 600 kg/s (2066.06 MMSCFD).

In this example the possibility that the optimum operating condition for this station may require the shutdown of one or more units is taken into consideration. Accordingly, the optimization model is run separately using 9, 10, 11, 12, 13, and 14 compressors as shown in Table 3.2.4. By comparing the optima thus obtained, we can see that the best solution is to operate twelve compressors, with five compressors running at 13,725 rpm and the remaining seven compressors running at 13,750 rpm. Generally, it is believed that running fewer units in a compressor station is a way to improve the efficiency of the station. This example shows that this heuristic is not necessarily true, and by using numerical optimization we can find solutions that are much more fuel efficient. It can also be seen from Table 3.2.4 that at the optimum (i.e. with only 12 compressors running at their optimized speeds), the efficiency of each unit is about 79.95%. It is also seen from Table 3.2.4 that in this case, the outlet temperature dropped from 356.33 K to 347.04 K. Most importantly, the total fuel consumption is reduced from 1.94 kg/s (6.68 MMSCFD) at the initial speeds for the 12-compressor case to 1.55 kg/s (5.32 MMSCFD) at the optimum. It should also be noted that the second best solution is that obtained using 11 or 13 compressors, followed by the solutions obtained using 10 or 14 compressors; the worst optimum is the one for the 9-compressor case.

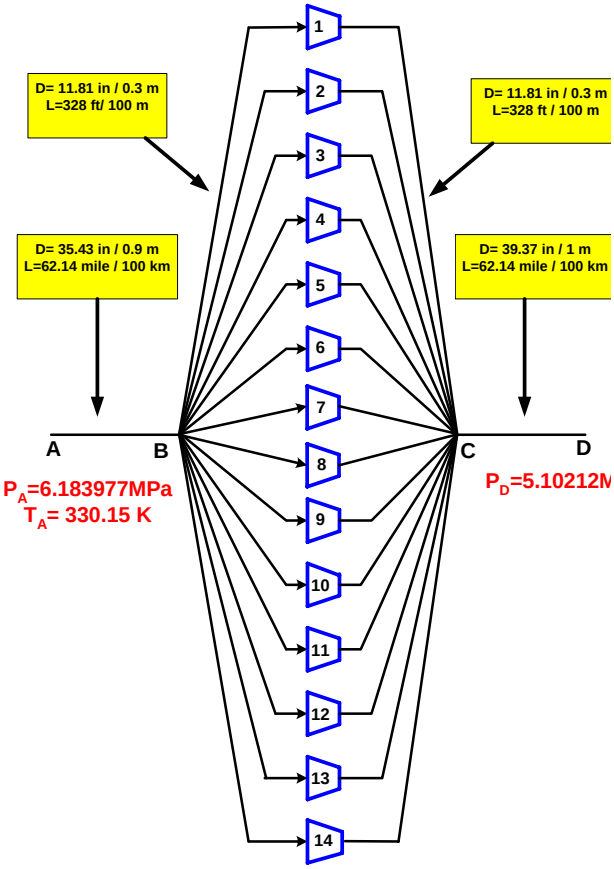

Fig. 3.2.2: Station configuration for Example 2.

Table 3.2.4: Final result for speed, isothermal efficiency, outlet temperature, and fuel consumption for optimization Example 2.

	14 Compressors On-line		13 Compressors On-line		12 Compressors On-line	
	Initial	Final	Initial	Final	Initial	Final
N_{r1} (rpm)	15,000	13,475	15,000	13,537.5	15,000	13,725
N_{r2} (rpm)	15,000	13,450	15,000	13,575	15,000	13,725
N_{r3} (rpm)	15,000	13,475	15,000	13,575	15,000	13,725
N_{r4} (rpm)	15,000	13,475	15,000	13,575	15,000	13,725
N_{r5} (rpm)	15,000	13,475	15,000	13,575	15,000	13,725
N_{r6} (rpm)	15,000	13,475	15,000	13,575	15,000	13,750
N_{r7} (rpm)	15,000	13,475	15,000	13,575	15,000	13,750
N_{r8} (rpm)	15,000	13,475	15,000	13,575	15,000	13,750
N_{r9} (rpm)	15,000	13,475	15,000	13,575	15,000	13,750
N_{r10} (rpm)	15,000	13,475	15,000	13,575	15,000	13,750
N_{r11} (rpm)	15,000	13,475	15,000	13,575	15,000	13,750
N_{r12} (rpm)	15,000	13,475	15,000	13,575	15,000	13,750
N_{r13} (rpm)	15,000	13,475	15,000	13,575	0	0
N_{r14} (rpm)	15,000	13,475	0	0	0	0
Fuel Consumption (kg/s- MMSCFD) x10^3	2.06 – 7.09	1.57– 5.39	2.00 – 6.91	1.55– 5.35	1.94 – 6.68	1.55 – 5.32
Mass flow Rate (kg/s- MMSCFD)	579.12 – 1,994.15	550.51– 1,895.64	577.53– 1,988.68	550.51– 1,895.64	574.60 – 1,978.58	550.51 – 1,895.64
η_{is1}	78.47	78.88	79.382	79.43	79.90	79.94
η_{is2}	78.47	78.50	79.382	79.62	79.90	79.94
η_{is3}	78.47	78.88	79.382	79.62	79.90	79.94
η_{is4}	78.47	78.88	79.382	79.62	79.90	79.94
η_{is5}	78.47	78.88	79.382	79.62	79.90	79.94
η_{is6}	78.47	78.88	79.382	79.62	79.90	79.95
η_{is7}	78.47	78.88	79.382	79.62	79.90	79.95
η_{is8}	78.47	78.88	79.382	79.62	79.90	79.95
η_{is9}	78.47	78.88	79.382	79.62	79.90	79.95
η_{is10}	78.47	78.88	79.382	79.62	79.90	79.95
η_{is11}	78.47	78.88	79.382	79.62	79.90	79.95
η_{is12}	78.47	78.88	79.382	79.62	79.90	79.95
η_{is13}	78.47	78.88	79.382	79.62	0	0
η_{is14}	78.47	78.88	0	0	0	0
Discharge Temperature T_c (K)	358.94	347.39	357.75	347.09	356.33	347.04

Table 3.2.4: Final result for speed, isothermal efficiency, outlet temperature, and fuel consumption for optimization Example 2 (continued).

	11 Compressors On-line		10 Compressors On-line		9 Compressors On-line	
	Initial	Final	Initial	Final	Initial	Final
N_{r1} (rpm)	15,000	14,000	15,000	14,400	15,000	15,000
N_{r2} (rpm)	15,000	14,000	15,000	14,400	15,000	15,000
N_{r3} (rpm)	15,000	14,000	15,000	14,400	15,000	15,000
N_{r4} (rpm)	15,000	14,000	15,000	14,400	15,000	15,000
N_{r5} (rpm)	15,000	14,000	15,000	14,400	15,000	15,000
N_{r6} (rpm)	15,000	14,000	15,000	14,400	15,000	15,000
N_{r7} (rpm)	15,000	14,000	15,000	14,400	15,000	15,000
N_{r8} (rpm)	15,000	14,000	15,000	14,400	15,000	15,000
N_{r9} (rpm)	15,000	14,000	15,000	14,400	15,000	15,000
N_{r10} (rpm)	15,000	14,025	15,000	14,425	0	0
N_{r11} (rpm)	15,000	14,025	0	0	0	0
N_{r12} (rpm)	0	0	0	0	0	0
N_{r13} (rpm)	0	0	0	0	0	0
N_{r14} (rpm)	0	0	0	0	0	0
Fuel Consumption (kg/s- MMSCFD) x10^3	1.86–6.40	1.553–5.35	1.75 – 6.03	1.57 – 5.42	1.61 – 5.55	1.61 – 5.55
Mass flow rate (kg/s- MMSCFD)	569.74–1,961.84	550.51–1,895.64	532.08 – 1,935.49	550.51–1,895.64	550.64 – 1,895.64	550.51–1,895.64
η_{is1}	79.83	79.74	78.95	78.80	76.95	76.95
η_{is2}	79.83	79.74	78.95	78.80	76.95	76.95
η_{is3}	79.83	79.74	78.95	78.80	76.95	76.95
η_{is4}	79.83	79.74	78.95	78.80	76.95	76.95
η_{is5}	79.83	79.74	78.95	78.80	76.95	76.95
η_{is6}	79.83	79.74	78.95	78.80	76.95	76.95
η_{is7}	79.83	79.74	78.95	78.80	76.95	76.95
η_{is8}	79.83	79.74	78.95	78.80	76.95	76.95
η_{is9}	79.83	79.74	78.95	78.80	76.95	76.95
η_{is10}	79.83	79.70	78.95	78.80	0	0
η_{is11}	79.83	79.70	0	0	0	0
η_{is12}	0	0	0	0	0	0
η_{is13}	0	0	0	0	0	0
η_{is14}	0	0	0	0	0	0
Discharge Tempereature T_c (K)	354.59	347.37	352.42	348.17	349.6	349.6

Example 3: The system considered here is a single compressor station with three dissimilar compressors. Thus, the station configuration is just one of the two clusters shown in Figure 3.2.3. In this case, the three units are not identical and they each have different compressor maps. This is more realistic, since few compressor stations have all their compressors identical. This also makes it more difficult to find the optimum operating configuration since we now have no notion of symmetry. The compressor speed limits for this case are given in Table 3.2.5, and the goal of the optimization is to minimize the total fuel consumption while maintaining a station throughput of 170 kg/s (585.38 MMSCFD).

The results obtained by optimization are shown in Table 3.2.6. The optimal solution for this examples provides three different speeds for the three compressors (12,650, 11,650, and 10,650 rpm), and the final mass flow rate is close to its minimum allowable value at 170.7 kg/s (585.62 MMSCFD).

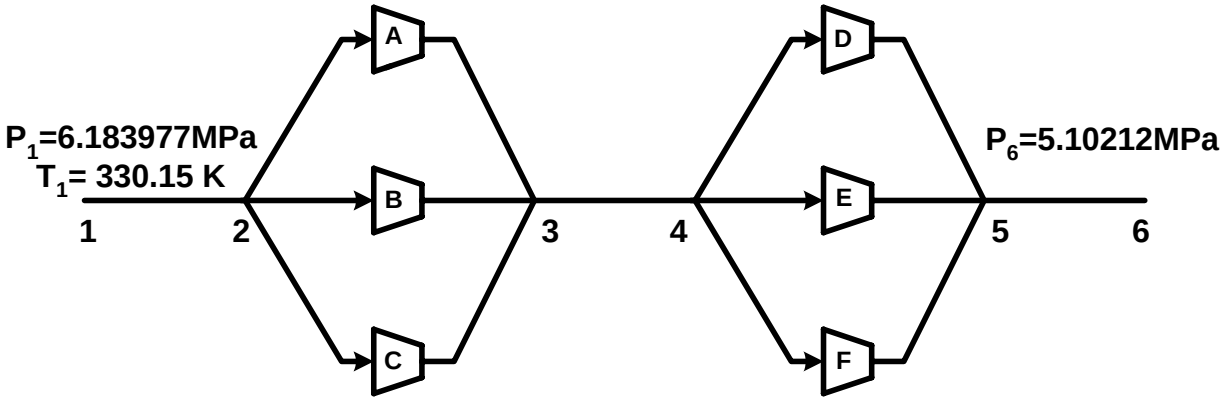

Fig. 3.2.3: Station configuration for Examples 3 and 4.

Table 3.2.5: Input data for Example 3.

	N_{rA}	N_{rB}	N_{rC}
Initial Value (rpm)	13,000	12,000	11,000
Maximum Value (rpm)	15,000	15,000	15,000
Minimum Value (rpm)	10,000	10,000	10,000
Minimum Mass Flow Rate	170 kg/s – 585.38 MMSCFD		

Table 3.2.6: Final result for speed, isothermal efficiency, outlet temperature, and fuel consumption for Example 3.

	Initial	Final
N_{rA} (rpm)	13,000	12,650
N_{rB} (rpm)	12,000	11,650
N_{rC} (rpm)	11,000	10,650
Fuel Consumption (kg/s- MMSCFD) x10^3	42.86 – 147.59	39.39 - 135.65
Mass Flow Rate (kg/s- MMSCFD)	173.12- 596.13	170.07- 585.62
η_{isA}	79.75	79.60
η_{isB}	79.35	79.35
η_{isC}	76.98	76.97
Discharge Temperature T_3 (K)	342.67	340

The fuel consumption in this example is reduced from 42.86x10^{-3} kg/s (147.59x10^{-3} MMSCFD) to 39.39x10^{-3} kg/s (135.65x10^{-3} MMSCFD). As seen in Table 3.2.6, the efficiency of the first unit actually drops from 79.75% to 79.60% at the optimal solution, while the efficiency of the other two units does not change much. The outlet temperature decreases from 342.67 K to 340 K.

Example 4: In the previous examples, only the problem of optimizing the compressors in one compressor station was considered. To optimize the pipeline network, a "network-level optimization" of compressor speeds must be performed. That is, the speeds of all the compressors in all the compressor stations must be simultaneously optimized. This is numerically very difficult and computationally very expensive. On the other hand, this task will be considerably simplified if it is possible to obtain high quality solutions through "station-level optimization", which is the independent optimization of the compressor speeds in each station. In order to compare network-level optimization with station-level optimization, a small network consisting of two compressor stations, each of which is identical to the compressor station in Example 3 (Fig. 3.2.3) is considered. Thus, the solution obtained in Example 3 provides the optimal speeds obtained by station-level optimization for this problem. The compressor speed limits for this example are identical to the limits in Example 3, as shown in Table 3.2.7. Numerical optimization is used to find the optimal speeds of all six compressors simultaneously,

which is the application of network-level optimization to this network. The goal of the optimization is to minimize the total fuel consumption in both stations combined while maintaining a line throughput of 170 kg/s (585.38 MMSCFD).

The results obtained by optimization are shown in Table 3.2.8. Te optimal compressor speeds obtained in network-level optimization are very close to those obtained by station-level optimization in Example 3. The fuel consumption in this example is reduced from 85.51×10^{-3} kg/s (294.44×10^{-3} MMSCFD) to 77.76×10^{-3} kg/s (267.76×10^{-3} MMSCFD). These are almost exactly double the values obtained for a single station in Example 3. Therefore, it may concluded that in this example, station-level optimization is a viable alternative to network-level optimization. This is a very important and encouraging result in terms of the feasibility of optimizing compressor speeds in large networks using the developed methods.

These examples show the effectiveness and ease of use of the new optimization methodology that has been developed and implemented. The capabilities that have been developed here far exceed those found in the current generation of commercial software in terms of modeling detail, quality of solution, automation of solution process, and ease of use.

Table 3.2.7: Input data for Example 4.

	N_{rA}	N_{rB}	N_{rC}	N_{rD}	N_{rE}	N_{rF}
Initial Value	13,000	12,000	11,000	13,000	12,000	11,000
Maximum Value	15,000	15,000	15,000	15,000	15,000	15,000
Minimum Value	10,000	10,000	10,000	10,000	10,000	10,000
Minimum Mass Flow Rate	170 kg/s – 585.38 MMSCFD					

Table 3.2.8 Final result for speed isothermal efficiency, outlet temperature, and fuel consumption for Example 4.

	Initial	Final
N_{rA} (rpm)	13,000	12,600
N_{rB} (rpm)	12,000	11,600
N_{rC} (rpm)	11,000	10,600
N_{rD} (rpm)	13,000	12,600
N_{rE} (rpm)	12,000	11,650
N_{rF} (rpm)	11,000	10,650
Fuel Consumption (kg/s- MMSCFD) x10^3	85.51– 294.44	77.76 – 267.76
Mass Flow Rate (kg/s- MMSCFD)	173.41 - 597.14	170.01 – 585.42
η_{isA}	79.69	79.39
η_{isB}	79.35	79.34
η_{isC}	76.95	76.9
η_{isD}	79.76	79.67
η_{isE}	79.35	79.35
η_{isF}	76.99	76.96
Discharge Temperature T_3 (K)	342.44	339.11
Discharge Temperature T_5 (K)	342.67	339.83

Task 3.0: Software and Hardware Implementation

Task 3.0 focuses on the development and implementation of the software architecture that will solve the system of equations developed in Tasks 1.0 and 2.0. The VPST is a collection of software modules that model the activity of compressor stations and line pipe. The software architecture that supports the simulations of these pipeline components must accommodate design, construction, and operation of the overall model and its interconnections. Viewing the overall pipeline as an acyclic directed graph, i.e., gas only flows in one direction, VPST is composed of nodes such as compressors stations and pipes, and the interconnections between these nodes. The interconnections, or interfaces, are referred to as arcs. In the design phase the user must be able to graphically specify the interconnections; in construction, the user should be able to configure the models that run within each node; and in execution, input data and output data are supplied through online databases and the user should be able to visualize the performance through graphical output.

Overview

The Pipeline Editor is a feature-rich graphical user interface (GUI) that is designed to provide pipeline designers with a graphical view of their pipeline systems and simulation data. The Pipeline Editor can be used to graphically build the pipeline system, manipulate an already built graph, and simulate the model using Parallel or Sequential Simulators and to display the results of such simulation graphically. The Pipeline Editor is developed using the JGraph and Swing packages. The editor is an easy to use application that can be started from any computer using an Internet browser. Once started, the Pipeline Editor will connect to the Optimizer and the Sequential and Parallel Simulators. The application requires Java Web Start 1.2 for execution.

GUI – Description

The Pipeline Editor is the graphical user interface to the virtual pipeline simulation testbed. The editor provides all the necessary components to draw a complete pipeline system and acts as an interface between the user and the Parallel and Sequential Simulators. The interface that consists of one window with two toolbars and one menu bar is shown in Figure 3.3.1.

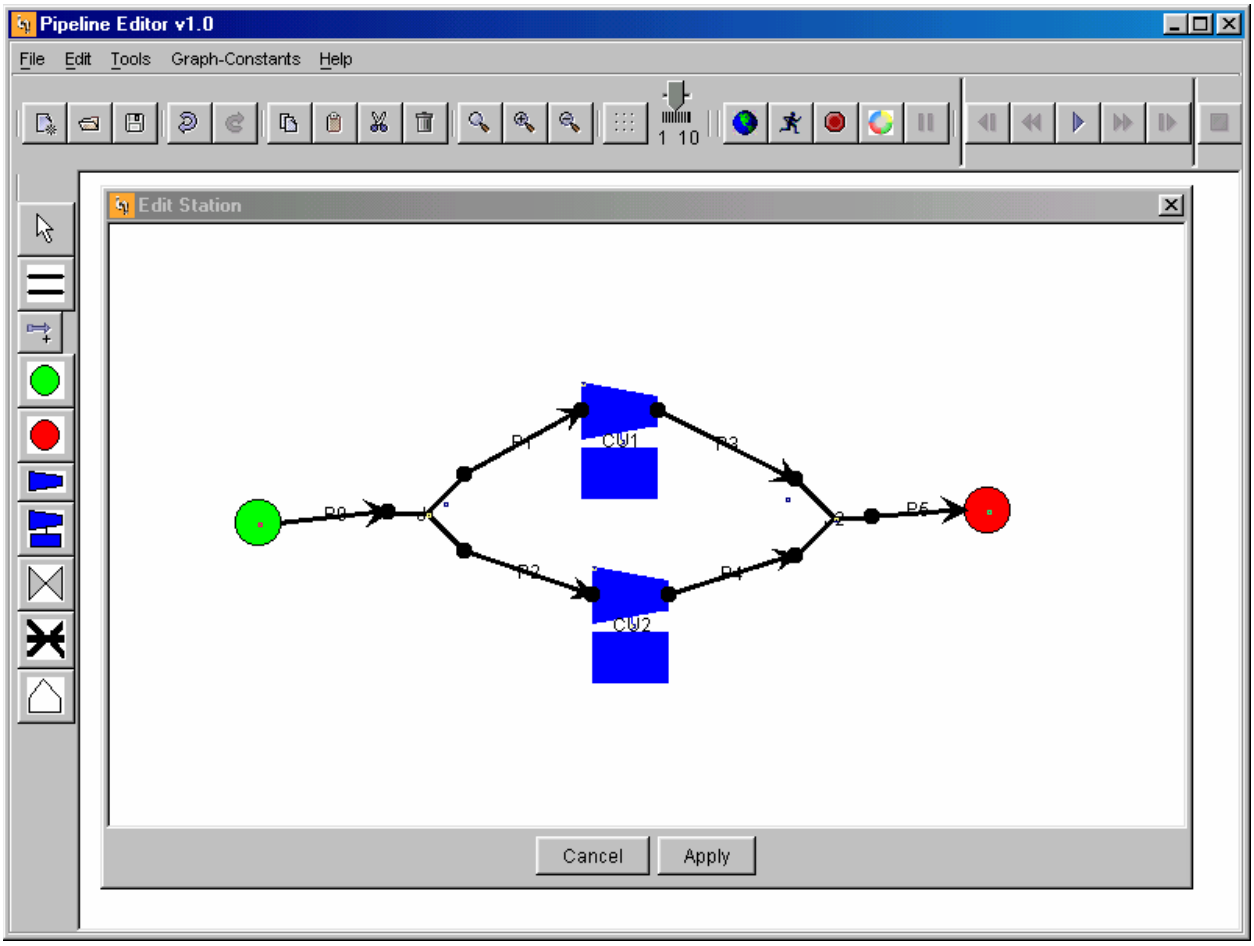

Fig. 3.3.1: Screenshot of the graphical user interface.

The vertical toolbar has one button for each supported component. The components can be inserted by dragging and dropping or double-clicking on these buttons. The horizontal toolbar contains all the buttons for editing and zooming. The vertical toolbar also contains the command buttons for parallel and sequential simulation. The menu bar offers the same functionality as the two toolbars in addition to the save/open function. The interface also offers the possibility to use the keyboard via some shortcut keys.

Various elements of an actual pipeline can be graphical illustrated with the Pipeline Editor. Table 3.3.1 lists these components. The components also are shown in the screenshot of the Pipeline Editor, Figure 3.3.1.

The user can draw a component by clicking on the component icon in the toolbar or by dragging the component onto the drawing pad. The compressor and compression unit components can

Table 3.3.1: Pipeline Editor Components.

Component	Description	Comment
	Compression Unit	Composed of a compressor and a driver
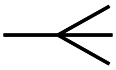	Connector	Represents an *n*-way combining and splitting junction
→	Pipe	
	Valve	Connects two pipes and can be either opened or closed
	Compressor	
	Receipt Point	
	Delivery Point	

only be connected to pipelines, but each can accept several pipelines connections. Similarly, a connector can be connected only to pipelines and can accept as many pipelines as there are total connections. Pipes should have another component other than pipes connected at each end.

The user can delete any component in the pipeline system by: 1) right-clicking on the component and selecting remove ; 2) clicking on the remove icon in the toolbar; or 3) using the delete key.

To edit the characteristics of any component inside the pipeline system, the user should use the right-click menu. Features available for editing depend on the component selected.

The user can move any component of the pipeline system inside the drawing space using a dragging move. All the components connected to the component being moved will move accordingly and stay connected.

Actions can be undone (or re-done) on any component of the pipeline system by clicking on an icon in the toolbar. If no action is available, then the button will be in disabled state.

To copy, cut or paste pipeline components, the Pipeline Editor includes buttons in the toolbar or the user may use the standard keyboard shortcuts. In addition, the toolbar includes buttons to zoom-in or zoom-out of an area of the pipeline system.

Within the Pipeline Editor, the user may launch the optimizer or the simulator. The toolbar includes a button to launch simulator and another button to launch the simulator. Once the simulator button is clicked the user is prompted to to launch the Sequential or Parallel Simulator.

In addition, the user has the ability to select a host of other functionalities to facilitate the viewing of the simulation results.

GUI – Design

The three main packages in architecture are: JGraph, Pipeline Editor, and Optimizer. In order to have a better understanding of the design, the design and features of JGraph are explained before providing details of the Pipeline Editor and the Optimizer packages.

JGraph Design

Jgraph is a powerful open source Swing-style Java library for the visualization of graphs. The implementation of JGraph is entirely based on the source code of the JTree class, although it is not an extension of JTree but rather a a modification of JTree's source code. The components for trees and lists mostly are used to display data structures, whereas this graph component typically is used to modify a graph and handle modifications in an application-dependent way.

The main features of JGraph are:

- **Inheritance**: JTree's implementation of pluggable look and feel support and serialization is used without changes. The UI-delegate implements the current look and feel, and serialization is based on the Serializable interface, the XMLEncoder and the XMLDecoder classes for long-term serialization.
- **Modification:** The existing implementation of in-place editing and rendering was modified to work with multiple cell types.
- **Extension:** JGraph's marquee selection and stepping-into groups extend JTree's selection model.
- **Enhancement:** JGraph is enhanced with data transfer, attributes, and history that are Swing standards not used in JTree.

- **Implementation:** The layering, grouping, handles, cloning, zoom, ports and grid are new features, which are standards-compliant with respect to architecture, and coding conventions.

Pipeline Editor Design

Most classes of the Pipeline Editor extend from the JGraph classes in order to provide a custom graph needed to draw the pipeline network. Only a few classes directly extend some Swing classes. Figure 3.3.2 shows the class diagram of the Pipeline Editor.

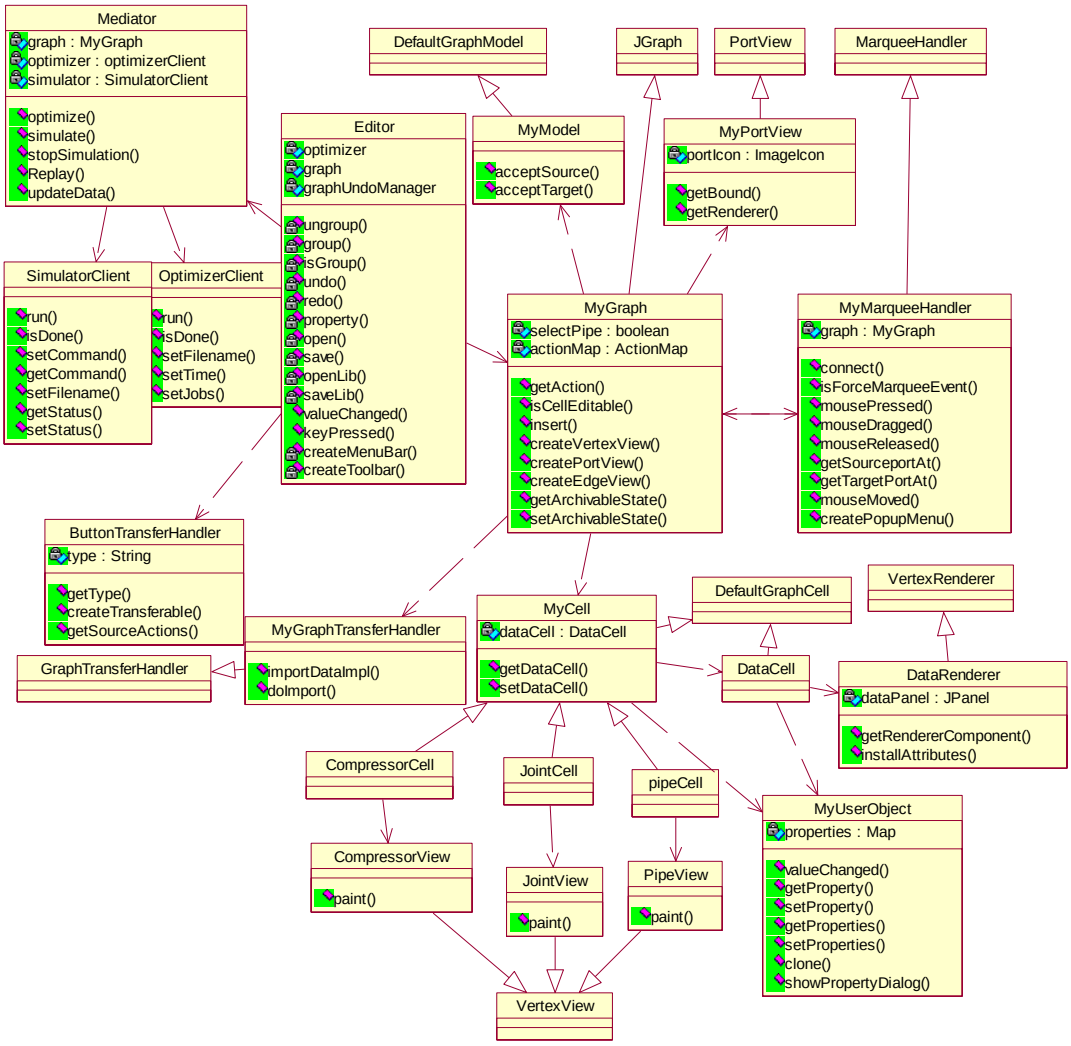

Fig. 3.3.2: Class diagram of the Pipeline Editor.

A description and function of each class of the Pipeline Editor follows. For the classes that extend the JGraph classes only the purpose of the extension is provided.

- **Class Editor:** This is an extension of JPanel and is the primary class representing the application's main panel. It includes the graph panel (JGraph) and the toolbars.
- **Class MyGraph:** An extension of JGraph, this class provides a custom graph model and contains all the necessary methods to create and insert custom components in the graph.
- **Class MyMarqueeTransferHandler:** This class extends MarqueeTransferHander. It creates popup dialogs and provides a custom mouse handler for the graph and custom edges used to represent pipes.
- **Class MyModel:** This extension of GraphModel defines the criteria to accept the connection edge (pipe) and cell (component).
- **Class MyPortView:** This class extends PortView and defines a custom representation of ports.
- **Class MyGraphTransferHandler:** This extension of GraphTransferHandler provides drag and drop support for the graph.
- **Class ButtonTransferHandler:** An extension of TransferHandler, it is used for dragging the buttons from the toolbar.
- **Class DataCell:** Extended from DefaultGraphCell, this class defines a cell use to display data from the simulation. This cell is a JPanel.
- **Class DataRenderer:** An extension of VertexRenderer, it is used to render the DataCell as a JPanel that contains information to be displayed.
- **Class MyCell:** This class extends DefaultGraphCell and is an abstract class for all the custom cells representing the components. Each MyCell object has a reference to a DataCell.

- **Class CompressorCell:** An extension of MyCell, this class represents a component cell (compressor). Each component cell has a DataCell and a MyUserObject to holds information about the cell. There is similar class for each component (pipe, connector, compression unit, etc.).

- **Class CompressorView:** This class extends VertexView and defines the shape of the compressor. Similarly, a class exists for each component (pipe, connector, compression unit, etc.) in the pipeline system.

- **Class MyUserObject:** Extended from Object:Holds this class stores the properties of the associated object (component) in a map for future reference and displays the property dialog for each component.

- **Class Optimizer:** This class creates JobComponent objects from component cells taken from the graph. Each component cell has a corresponding JobComponent and holds a reference to BranchBound class to start the optimization.

Optimizer Design

In order to be simulated using the Parallel Simulator, a graph has to be optimized first. Given a set of jobs with execution and computation times and a set of machines, the function of the Optimizer is to find the optimal job distribution among those machines. The jobs are the pipelines components (pipes, joints, compressors, etc.). Each job has some computation time and some communication time. The computation time depends on the characteristic of the component and the machine on which it is executed. The communication time depends on the amount of information exchanged and whether or not the connected component are on the same machine (local communication) or not (remote communication). Given these constraints, the optimizer finds an optimal distribution of jobs among machines that minimizes the workload of each processor. The Optimizer uses the Depth-First Branch and Bound algorithm to find the best distribution. Figure 3.3.3 shows the class diagram of the Optimizer.

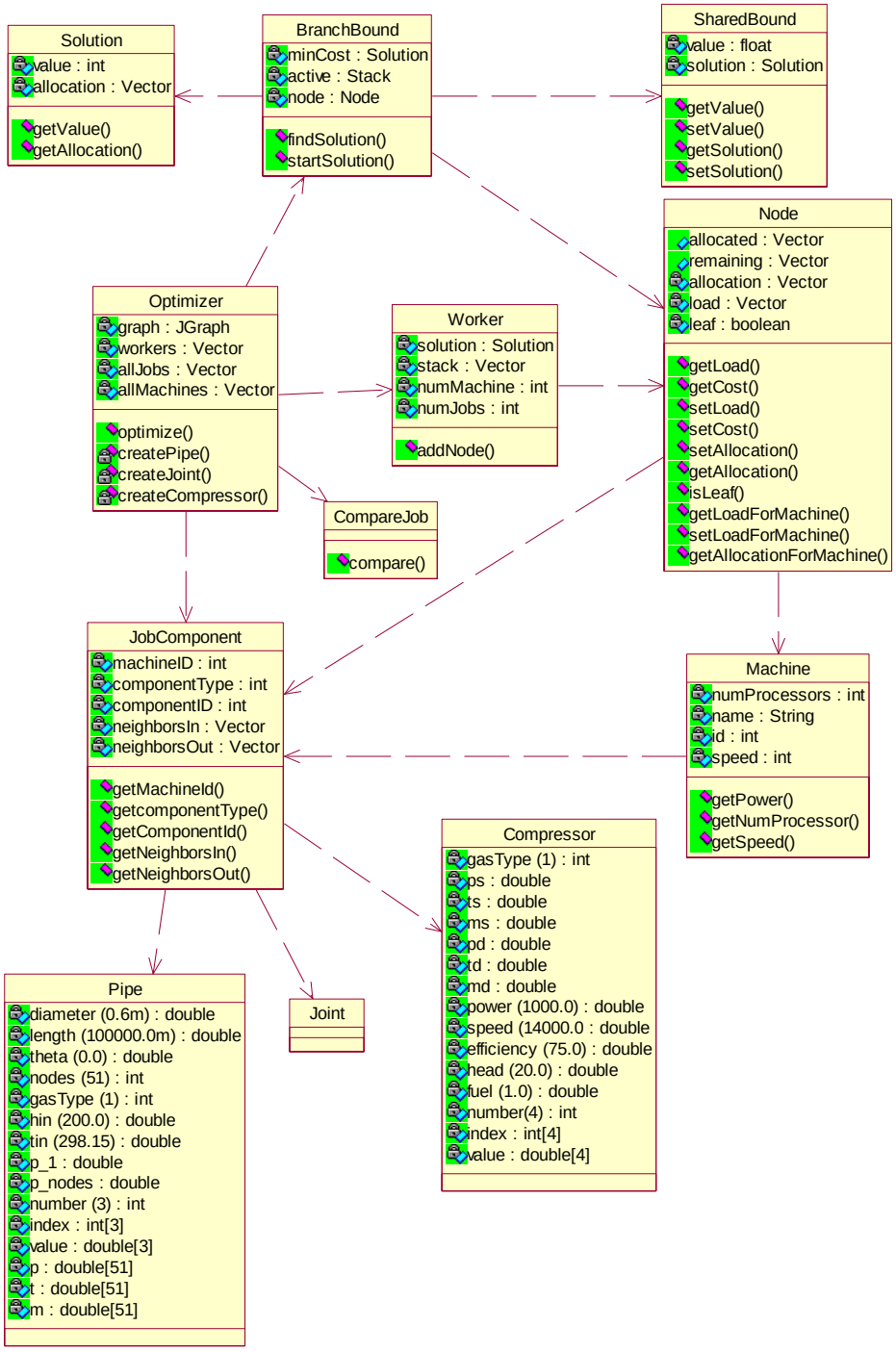

Fig. 3.3.3: Class diagram of the Optimizer.

A description and function of each class of the Optimizer follows.

- **Class BranchBound:** This class implements the branch and bound algorithm and holds a reference to the current solution found.
- **Class Solution:** This class represents a solution to the branch and bound algorithm. And contains the minimal allocation found.
- **Class Node:** The class holds the current allocation, which is the array of machine with their corresponding jobs. The allocation can be partial (non-leaf node) or complete (leaf node). For a non-leaf node, the jobs are non-allocated yet stored inside the node.
- **Class Machine:** This holds all the information about a machine and stores all the jobs allocated to this machine so far.
- **Class JobComponent:** An abstract class representing a job, this class includes sub-classes, which are component objects (pipe, compressor, etc.).
- **Class Pipe extend JobComponent:** This class holds all the properties and initial values of a pipe. There is a similar class for each component (compressor, connector, etc.).
- **Class Worker:** An extension of Thread, this class includes worker objects that are threads searching a part of the tree. They threads exchange new bounds via a shared memory (class SharedBound) and hold a stack of nodes representing the representative part of the tree.
- **Class SharedBound:** This class holds the minimal bound found so far by the Worker objects and also holds the allocation (Solution object) corresponding to this bound.
- **Class CompareJob:** This class is used to specify how jobs should be compared. Jobs are compared by number of neighbors and by weight. When the jobs are sorted, this helps reduce the number of nodes visited to reach the solution.

Simulator Design

Parallel Simulator. The communication between the Pipeline Editor and the Parallel Simulator is through sockets. Since the Pipeline Editor actually simulates the pressure and flow distribution that is happening in a real pipeline system which involves some tedious computations, the simulation will be done on several powerful computers in order to meet the timing constraints. The input is first passed to a Job-Control Optimizer which efficiently distributes the computation among several machines. The graph cannot be simulated using the parallel simulator without optimizing.

The Job-Control Optimizer takes as input the component objects representing the pipeline components in the input graph. It outputs a list of job objects. The difference between the component objects and the job objects is that the job objects contain in addition to the properties of a component, information about the machine on which it should be executed, the components connected to it, the execution time and the associated file containing the source code of its execution. The optimizer will run to completion once started.

The job allocation optimization is a discrete optimization problem. The system uses the Branch and Bound algorithm to find the best distribution given some time and communication constraints. The solution may not be optimal but will be close to the optimal one. The optimizer adequately balances computation and communication time among all the processors. It outputs a list of all jobs along with the machines on which they should be executed in order to have the best distribution.

The parallel simulation involves solving a set of partial differential equations that mathematically models the pressure and flow rate distribution in each component of the real pipeline system. The computation will be done on several powerful computers and result will be transmitted back to the GUI for display. Communication between the GUI and the parallel simulator is through sockets. The parallel simulator uses the optimized file with the .opt extension. There are two separate threads called SimulatorClient and SimulatorDataClient to handle communication between the GUI and the Simulator. The SimulatorClient class receives commands from the GUI and passes it to the Simulator while the SimulatorDataClient receives the results from the Simulator and passes it to the GUI. This is necessary to prevent the GUI from freezing. Though

there are three separate threads that comprise the Pipeline Editor, there is only a single socket between the Pipeline Editor and the Parallel Simulator.

The following functions are available for Parallel simulation:

- **Simulate:** This will start the simulation. There are separate buttons for parallel and sequential simulation
- **Stop:** This command will stop the simulation.
- **Pause:** This will pause the simulation. The paused simulation can be resumed later or stopped altogether. The skip forward, skip backward, step forward, step backward commands can be issued only in the paused replay state.
- **Resume:** There is only a single button for both pause and resume commands. This command will resume a paused simulation.
- **Replay:** This command is used to replay the simulation from beginning. It can be issued by clicking on the replay button. The step forward, step backward, skip forward, skip backward commands can be issued only during replay.
- **Step Forward:** This command will skip one time step forward during replay.
- **Step Backward:** This command will skip one time step backward during replay.
- **Skip Forward:** This command is used to skip more than one time step forward during replay. The number of steps to skip can be inputted through a textbox adjacent to the skip forward button.
- **Skip Backward:** This works similar to the skip forward command except that the direction of the skip is backward.
- **Speed:** This command can be used to vary the speed of replay. Speed can be increased or decreased by varying the position of the speed slider.

Sequential Simulator: The communication between the Sequential Simulator is through text files in ASCII format. When designing on the GUI a graph that models a pipeline network, the user may select to simulate using the Sequential Simulator. This single command will start a three-step process. First, the GUI will output an input-data file that represents the components in the pipeline network. This file will contain the properties of the components of the input graph in a predefined standard format. This file will be inputted to the Sequential Simulator, which will process it and output the results in an output-data file in a predefined standard format. This file will in turn be read by the GUI and the results will be displayed graphically. The constant data necessary for sequential simulation should be entered through the graph-constants menu in the menu bar.

All the functionalities available with the Parallel Simulator are available with the Sequential Simulator. The same set of buttons can be used for both the Sequential and Parallel Simulations. Only one of the two types of simulation can be executed at any given time.

Task 4.0: Develop Control Model

This task was part of the original work plan. However, during the renegotiation of the project scope in 2004, the budget was reduced and, therefore, this task was removed from the work scope.

Task 5.0: Analysis and Evaluation

At this point, the analysis capability of the VPST is nearly complete. A simple compressor station model has been developed that includes many of the sub-models. This model severs as a basis to begin to investigate optimization opportunities within the station. This last task demonstrates the use of the VPST by testing a variety of design concepts on a pipeline system.

Subtask 5.1: Develop Base Pipeline System

This sub-task includes three parts: 1) develop various modeling parameters described in Task 1.0; 2) develop a virtual compressor station to analyze the flow characteristics through a

compressor station; and 3) identify bottlenecks that restrict compressor station flow. Figure 3.5.1 shows a schematic of a typical compressor station with known parameters and boundary conditions. The compressor station is located between two pipes that are 100 km in length. The pipe specifications of this compressor station are shown in Table 3.5.1. The variable boundary condition with respect to time is applied at the head (beginning) of the inlet pipe that supplies gas to the compressor station and is shown in Figure Fig 3.5.2. This point is referred to as Node 1 in the following discussion. The mass flow rate is initially 500 kg/s (1,102.31 lbm/s) and remains constant for 125 minutes. Then the flow rate gradually increases to 600 kg/s (1,322.77 lbm/s) at a time of 166.7 minutes. The mass flow rate then remains constant for another 125 minutes, after which it suddenly decreases to 400 kg/s (881.85 lbm/s). The mass flow rate remains constant for the next 41.7 min, and then at the time of 375 min, the mass flow rate suddenly increases to initial value of 500 kg/s (1,102.31 lbm/s). The flow rate then remains constant until the end of the simulation at an elapsed time of 500 min.

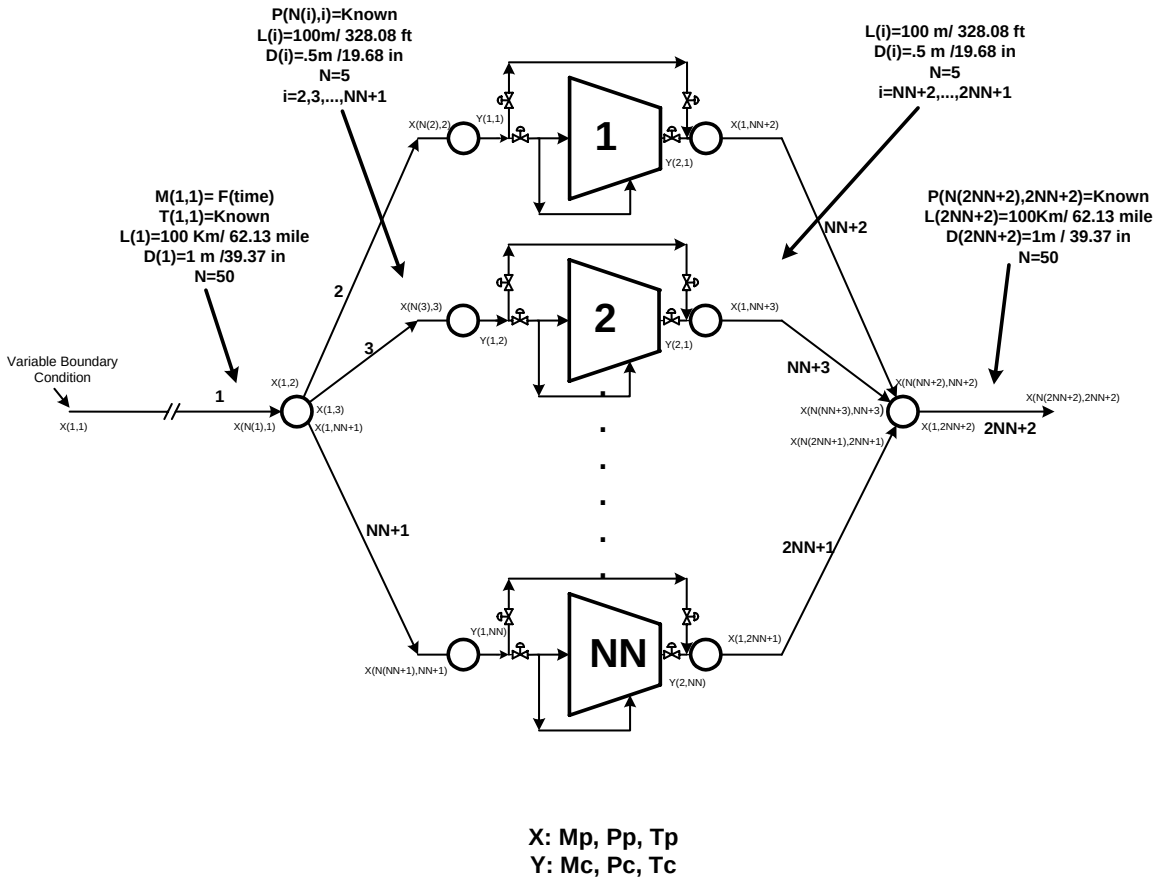

Fig. 3.5.1: Schematic of compressor station.

Table 3.5.1: Pipe specifications.

Pipe	Diameter	Length	Number of Nodes
Inlet pipe to the compressor station	1.00 m (39.37 in)	100 km (62.13 mi)	50
Outlet pipe from the compressor station	1.00 m (39.37 in)	100 km (62.13 mi)	50
Inlet pipe to each compressor	0.50 m (19.68 in)	100 m (328.08 ft)	5
Outlet pipe from each compressor	0.50 m (19.68 in)	100 m (328.08 ft)	5

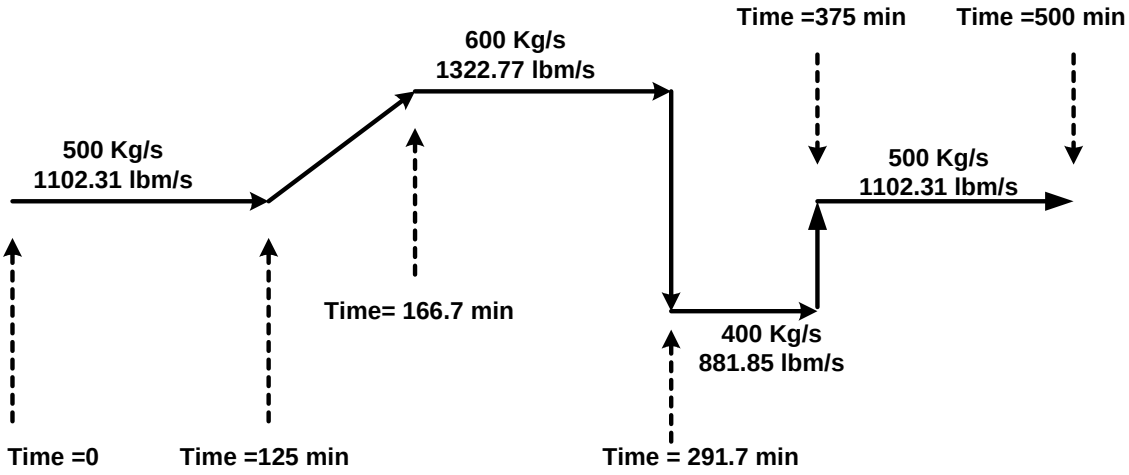

Fig. 3.5.2: Changing mass flow rate at Node 1 with respect to time.

This simulation used different types of compressors to demonstrate the difference in gas parameters and performance data. Specifically, two different compressor stations are considered. One used centrifugal compressors and the other uses reciprocating compressors. The specifications of the centrifugal and reciprocating compressors are shown in Tables 3.5.2 and 3.5.3, respectively.

Table 3.5.2: Centrifugal compressor specifications.

	b_1	b_2	b_3	b_4	b_5	b_6
Compressor Map Coefficients	0.3542×10^{-4}	0.1013×10^{-2}	-0.4768×10^{-2}	17.269	916.64	3350.8

Table 3.5.3: Reciprocating compressor specifications.

Speed	Stroke/Bore	Suction/Discharge Pressure Loss	Rod Diameter	Clearance	Cylinders
300 rpm	14/12.5 in (355.6/317.5 mm)	5% / 5%	3 in (76.2 mm)	0.1 - 1.6	8

The compressor station includes nine identical compressors, all of which operate at the initial condition of 500 kg/s of natural gas flow through the station (Fig. 3.5.2). As will be shown in the following section, the control scheme shuts down and starts compressors to match the demand conditions while maintaining the compressor operating parameters within the specific limits.

Subtask 5.2: Demonstrate VPST with the Base Pipeline System

In order to prove the usability of VPST, the model was tested over a series of cases determined from Subtask 5.1, as well as on larger scale examples. These cases demonstrate the VPST capabilities, and the types of results that can be obtained.

Example 1 Base System: Some results for the virtual compressor station described in Subtask 5.1 are shown in Figures 3.5.3 through 3.5.15. Figure 3.5.3 shows the change in mass flow rate with respect to time for the inlet pipe to the compressor station when different types of compressors are used. When the inlet pipe inlet mass flow rate is constant at 500 kg/s (1102.31 lbm/s), the flow rate in the pipe gradually increases to the inlet value.

Figure 3.5.3 shows the change in mass flow rate for the inlet pipe from the compressor station. This variation is similar to that shown in Figure 3.5.4, which is the change in mass flow rate for the outlet pipe.

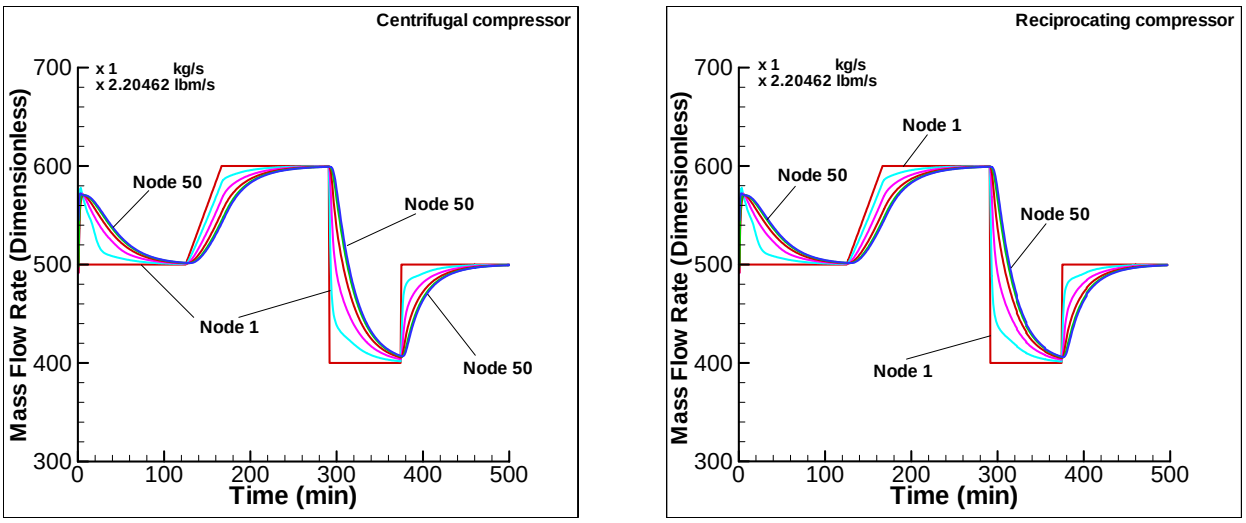

Fig. 3.5.3: Mass flow rate at the inlet pipe for different types of compressors.

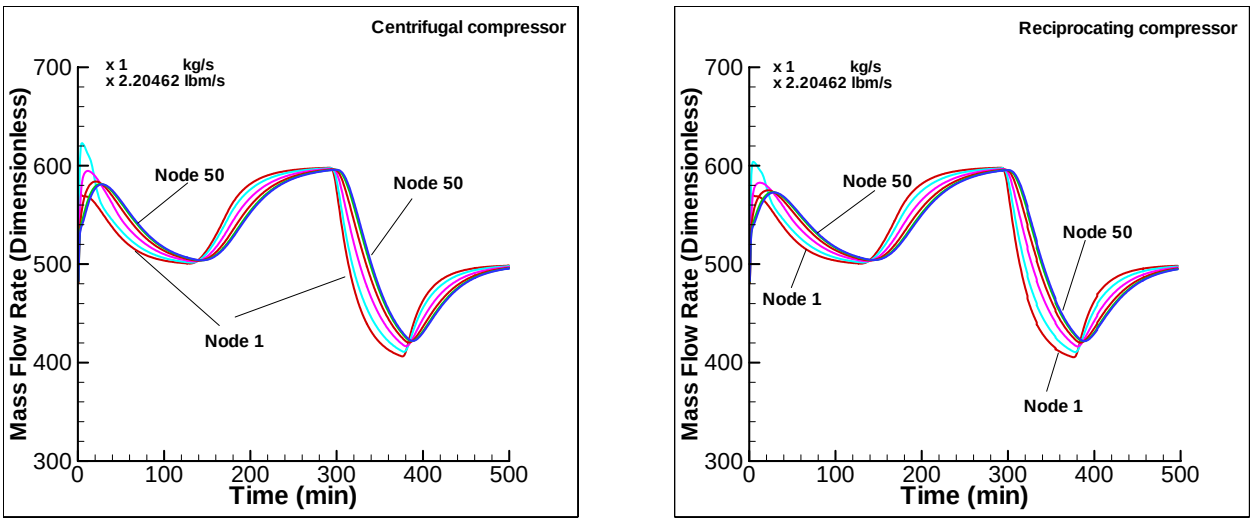

Fig. 3.5.4: Mass flow rate at the outlet pipe for different types of compressors.

Figure 3.5.5 shows the compressor station fuel consumption as a function of each compressor type. The mass fuel consumption is almost the same and is about 0.2% of the total mass flow rate entering the compressor station (note that this percentage is for only one compressor station). The jumps that are shown in this figure are because of starting and shutting down of reciprocating compressors.

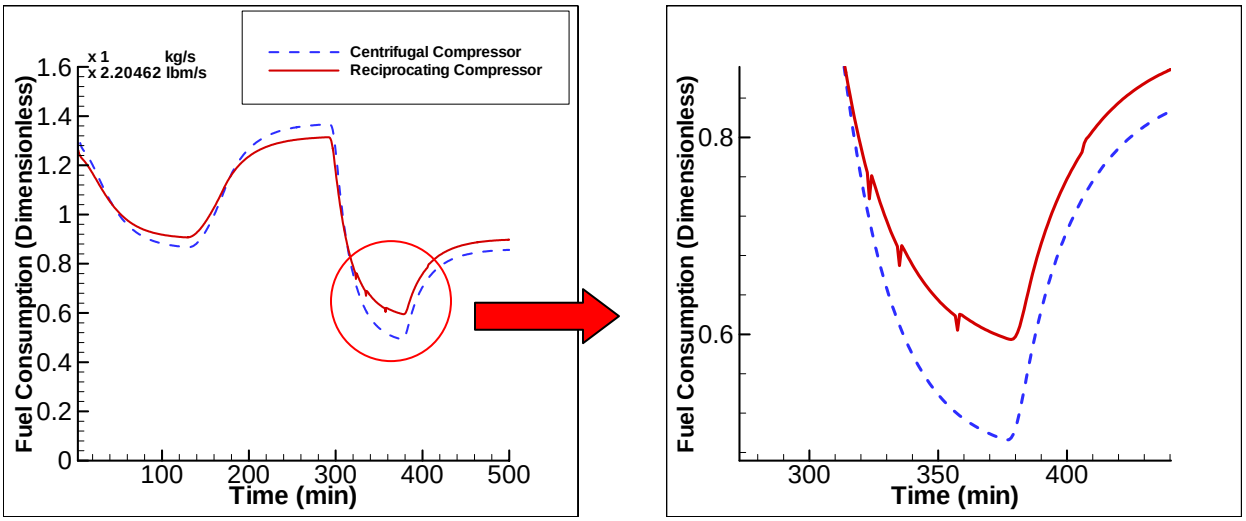

Fig. 3.5.5: Fuel consumption for different type of compressors.

Figures 3.5.6 and 3.5.7 illustrate the pressure distribution within the inlet pipe and the outlet pipe, respectively. The pressure distribution for each node is different with respect to time due to the compressibility effects. The pressure distribution is the same for each type of compressor and is not impacted by changing the number of compressors. Consequently, the type of compressor and the number of compressors does not have any effect on the up and down stream of compressor station. This is because, in this simulation, the mass flow rate at the inlet to the pipe at node 1 is precisely controlled.

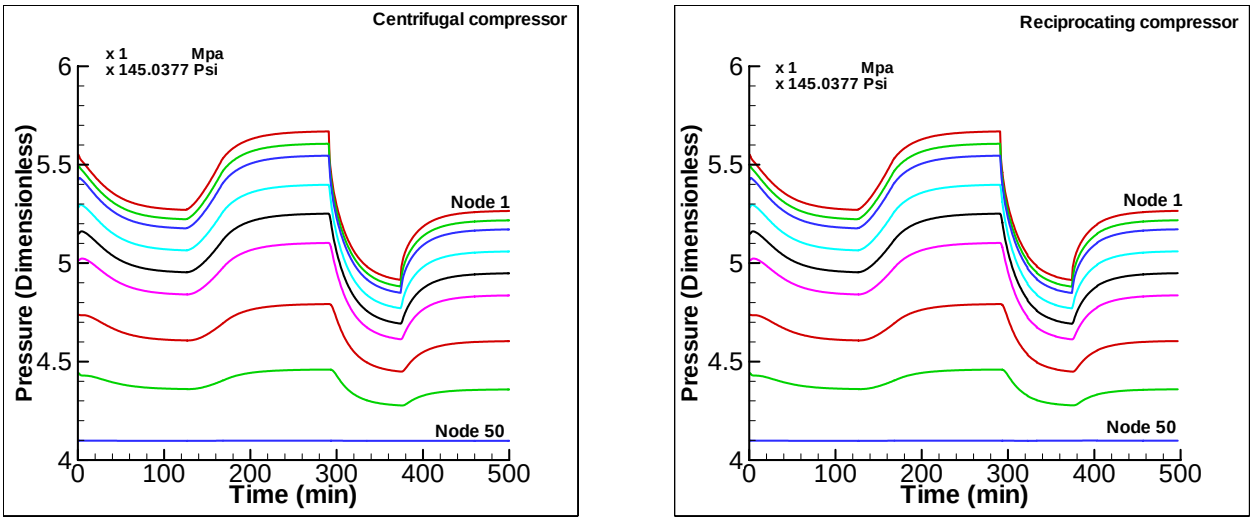

Fig. 3.5.6: Pressure distribution within the inlet pipe for different types of compressors.

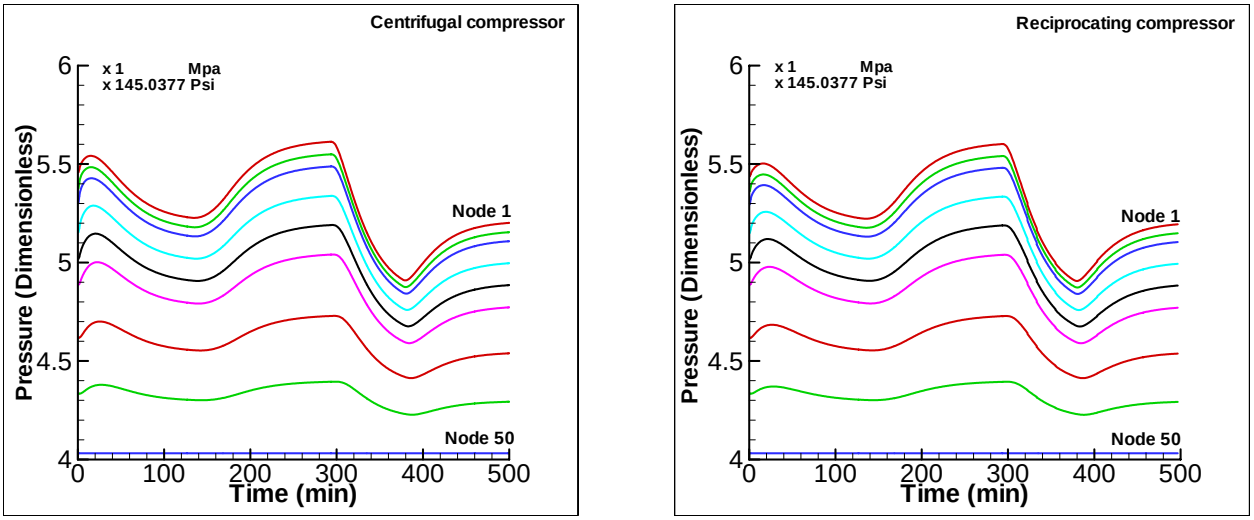

Fig. 3.5.7: Pressure distribution within the outlet pipe for different types of compressors.

The same type of information is available for the temperature distribution and compressibility factor distribution for the inlet and outlet pipes. Figures 3.5.8 through 3.5.11 show these conditions for the temperature and compressibility factor distributions.

Figure 3.5.12 shows the change of power with respect to time for different compressor types. For this simulation, the centrifugal compressors require more power than the station using reciprocating compressors. The value of power for reciprocating compressor depends with some parameter such as valve loss horsepower, which is different for each compressor. Consequently, this is not a general statement, but can only be stated for this particular case.

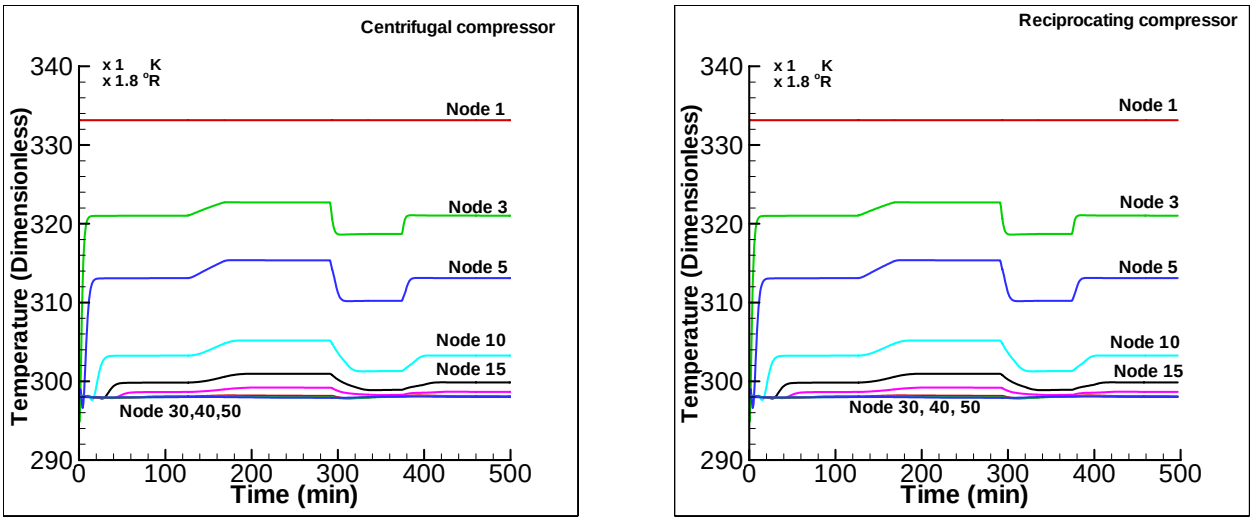

Fig. 3.5.8: Temperature distribution within the inlet pipe for different types of compressors.

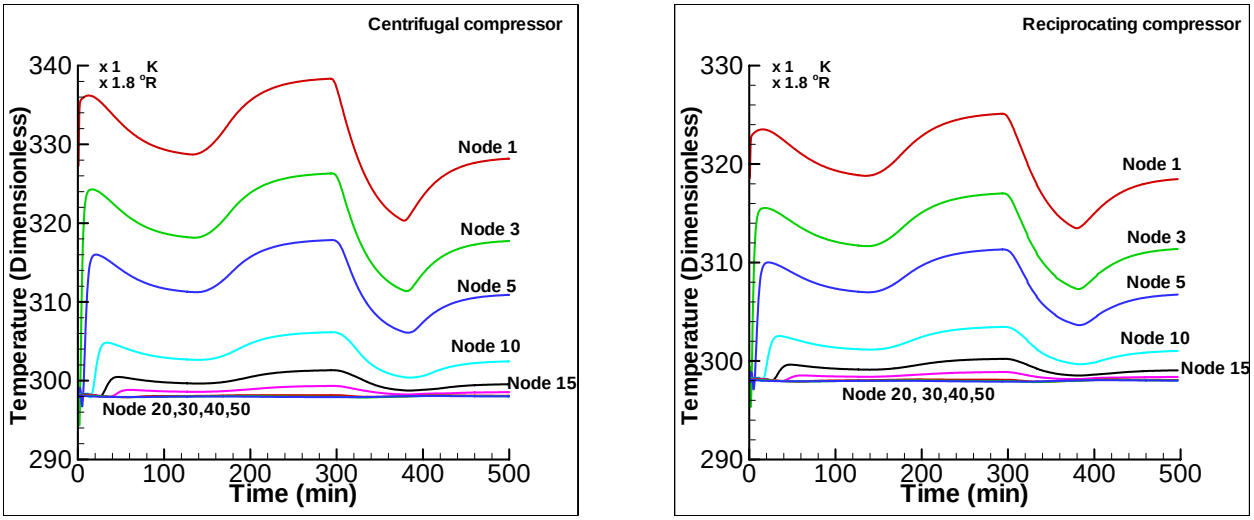

Fig. 3.5.9: Temperature distribution within the outlet pipe for different types of compressors.

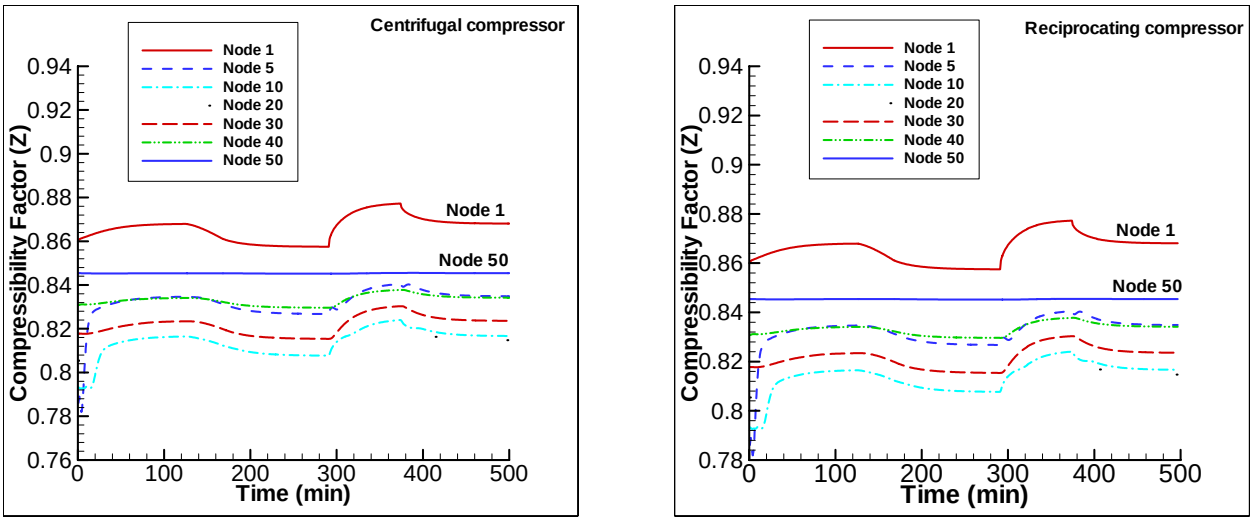

Fig. 3.5.10: Compressibility factor within the inlet pipe for different types of compressors.

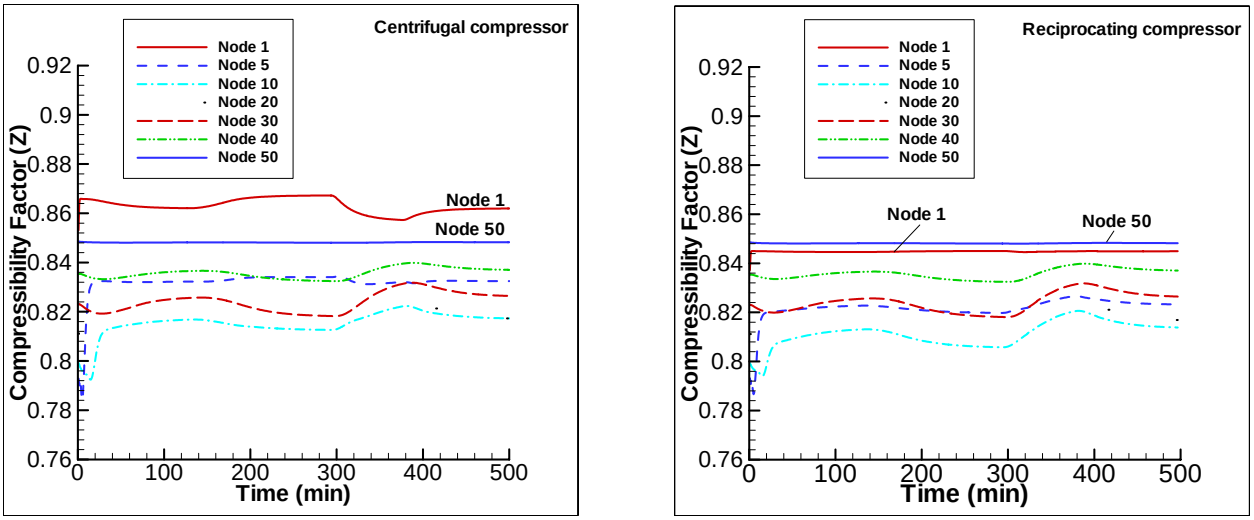

Fig. 3.5.11: Compressibility factor within the outlet pipe for different types of compressors.

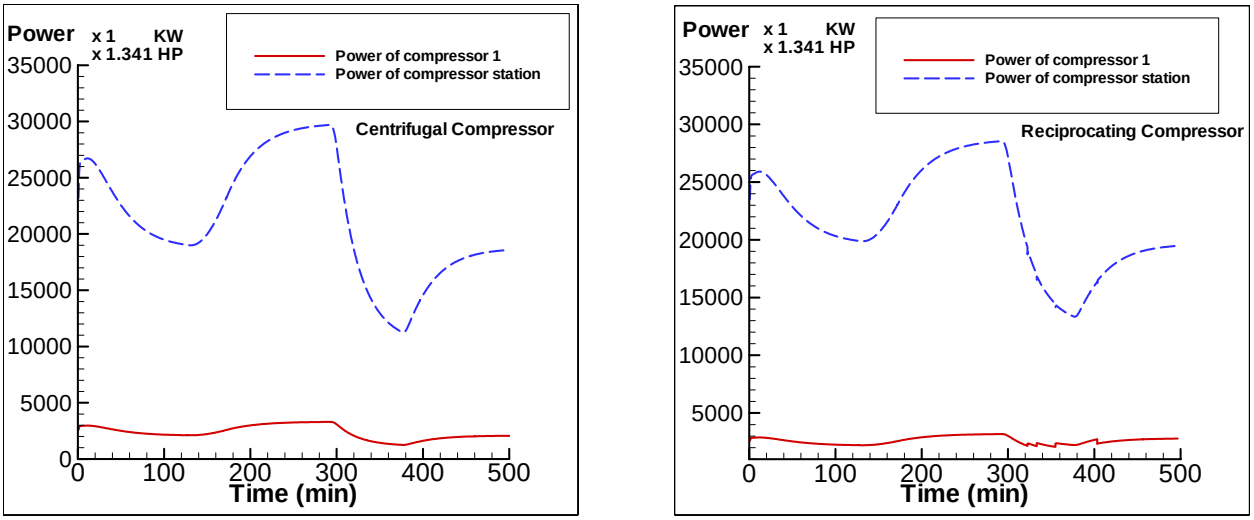

Fig. 3.5.12: Change of power with respect to time for different types of compressors..

At 125 minutes, the mass flow rate at Node 1 starts to gradually increase to 600 kg/s (1,322.77 lbm/s). Comparing reciprocating compressors with that of centrifugal compressors shows that each exhibits different characteristics, such as mass flow rate and pressure distributions because each compressor has a different control limit. For example, the limit control for a centrifugal compressor is speed, but for the reciprocating compressor the control limit is via cylinder pocket clearance. When the control scheme calls for increased mass flow rate, the centrifugal compressor speed gradually increases as shown in Figure 3.5.13, and the pocket clearance

decreases in the reciprocating compressors. Fortunately, speed does not reach the upper or lower limit in the centrifugal compressor.

After 292 minutes, the mass flow rate requirement is suddenly decreased from 600 kg/s (1322.77 lbm/s) to 400 kg/s (881.85 lbm/s). The centrifugal compressors decrease in speed and the pocket clearance of the reciprocating compressors increase. However, because of the clearance limitation in the reciprocating compressors, these compressors are not able to adjust to the sudden decrease in mass flow rate through pocket clearance alone. Instead, three of the compressors in this compressor station are shut down as show in Figure 3.5.14.

Figure 3.5.15 shows changing isentropic efficiency with respect to time and compressor map for centrifugal compressor. The variation in this figure depends on the changing mass flow rate and compressor speed.

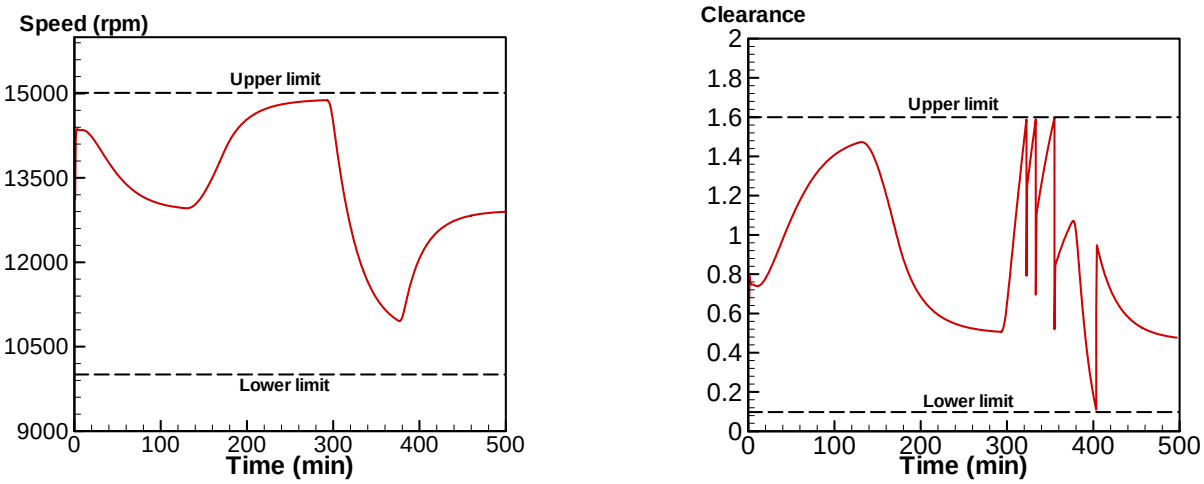

Fig. 3.5.13: Change in speed of centrifugal compressor and change in clearance for a reciprocating compressor with respect to compressor map.

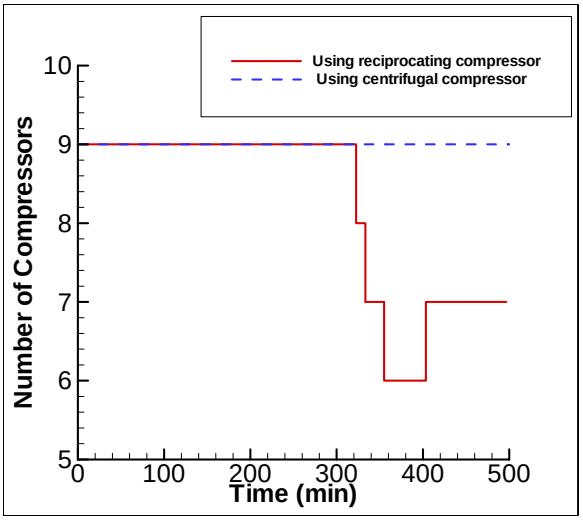

Fig. 3.5.14: Change in the number of branches with respect to time for different types of compressors.

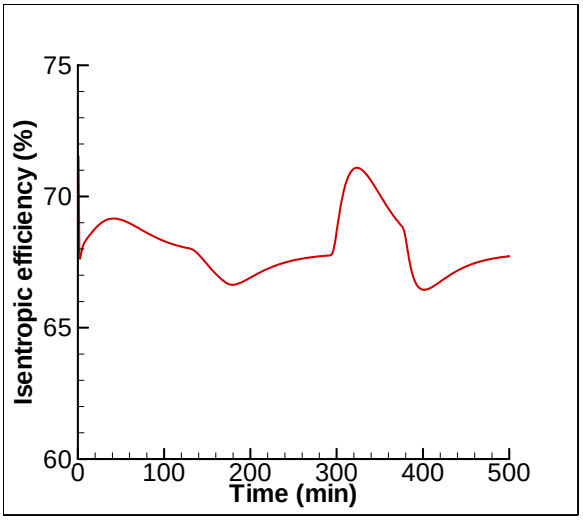

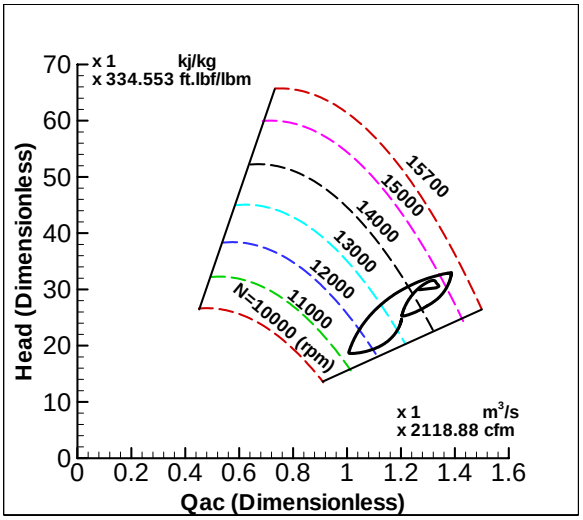

Fig. 3.5.15: Isentropic efficiency plot and compressor map for a centrifugal compressor.

Example 2 Ten Compressor Stations Each with Three Compression Units: This example demonstrates the applicability of the VPST for a relatively large pipeline section. The pipeline considered has 10 compressor stations, and within each compressor there are 3 centrifugal compressors driven by gas turbines. All the compression units are identical. Figure 3.5.16 shows the schematic of such a network. All compressor stations are connected using pipes that are 100

km in length. In each compressor station the design is same as the one shown in Figure 3.5.1 with *NN* equal to 3. The specifications of all the pipes are provided in Table 3.5.4. All pipes are assumed to be horizontal, i.e., the angle of inclination of all the pipes is 0.0 radians. The specifications of the compression unit are specified in Tables 3.5.5 through 3.5.8.

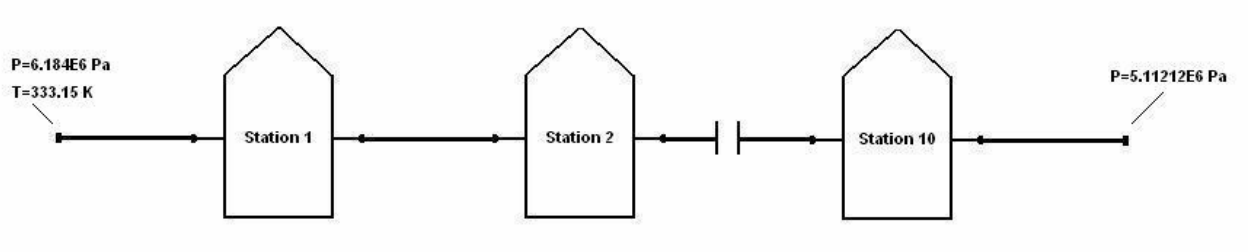

Fig. 3.5.16: Schematic of the 10-station network.

Table 3.5.4: Pipe specifications.

Pipe	Diameter	Length	Number of Nodes
Inlet pipe to the compressor station	0.45m (17.72in)	100 km (62.13 mile)	50
Outlet pipe from the compressor station	0.45m (17.72in)	100 km (62.13 mile)	50
Inlet pipe to each compression unit	0.25m (9.84in)	100 m (328.08ft)	5
Outlet pipe from each compression unit	0.25m (9.84in)	100m (328.08ft)	5

Table 3.5.5: Centrifugal compressor specifications.

	b_1	b_2	b_3	b_4	b_5	b_6
Compressor Map Coefficients	0.3542×10^{-4}	0.1013×10^{-2}	-0.4768×10^{-2}	17.269	916.64	3,350.8

Table 3.5.6: Lower and higher gas turbine map coefficients.

	A_1^L	A_2^L	A_3^L	A_4^L	A_5^L	A_6^L
Lower Gas Turbine Map Coefficients	0.002085	0.00113089	-7.358E-7	22126.6	-35.7514	0.0246
	A_1^H	A_2^H	A_3^H	A_4^H	A_5^H	A_6^H
Higher Gas Turbine Map Coefficients	0.004036	0.0013639	-9.5537E-7	21834.2	-38.8951	0.0293973

Table 3.5.7: Adjustment coefficients for lower and higher gas turbine map equations.

	b_1^L	b_2^L	b_1^H	b_2^H
Gas Turbine Map Coefficients	2.0	3.5	1.0	-0.5

Table 3.5.8 :Other gas turbine parameters.

Heat Rate	η_{mech}	T_B	T_{EN}
4.0 kJ/kg	0.98	260.9278 K	298.15 K

The natural gas flowing through the system is a mixture of methane, ethane and propane in the ratio of 0.7:0.25:0.05, respectively. The gas parameters are specified in Table 3.5.9.

Figure 3.5.16 also shows the boundary conditions used for the simulation. The boundary conditions used are constant throughout the simulation. The pressure and temperature at the head node of the pipe leading to the first compressor station and the pressure at the end node of the pipe leading out of the last compressor station are treated as boundary conditions. The boundary condition information is provided in Table 3.5.10. By changing the boundary conditions the dynamic behavior of any compressor station in the network can be studied. As the network is large, the time step for the simulation is taken as 2,000 seconds.

Table 3.5.9: Natural gas properties.

	Mole Fraction	Molecular Weight	Specific Heat at 50	Specific Heat at 300	Critical Pressure	Critical Temp	Density	Lower Heating Value
Methane	0.70	16.042	8.414E3	10.01E3	667.8	343.04	0.7168	55,601
Ethane	0.25	30.068	12.17E3	16.34E3	707.8	549.76	1.356	51,958
Propane	0.05	44.097	16.88E3	23.56E3	616.3	665.68	2.019	50,409

Table 3.5.10: Boundary conditions for 10 compressor stations each with 3 compression units.

Component	ID	Node #	Parameter	Value
Pipe	'PA'	1	Pressure	6.184E6 Pa
Pipe	'PA'	1	Temperature	333.15 K
Pipe	'PBS'	2	Pressure	5.11E6 Pa

As mentioned in earlier sections, the dynamic simulation of the compressor station network involves: 1) nonlinear partial differential equations that describe the pipe flow; and 2) nonlinear algebraic equations that describe the compression units and junctions. The pressure, temperature and mass flow rate variations over the line pipe were explained in earlier sections. The main aim is to study the behavior of the compression unit parameters with respect to time for different compressor stations. For this, one compression unit from each compressor station is selected and its parameters are studied over a time period. Figures 3.5.17 through 3.5.22 show the variations of speed, power, efficiency, fuel consumption, head, discharge pressure, discharge temperature and discharge mass flow rate for a compression unit from each of the 10 compressor stations with respect to time. All the parameters are across a selected single compression unit.

For all the parameters, the compression unit in the compressor station reaches steady state. As the unit gets further downstream, more time is required to reach steady state. Thus, the first compressor station reaches steady state condition first and the tenth compressor station reaches steady state last.

The mass flow rate decreases as it passes each compressor station as some of the fuel is consumed by the gas turbine. The power and speed needed for the compression unit decreases as we go from one compressor station to the next. This can be seen in Fig 3.5.17. The compression unit in station 1 needs more power and works at a higher speed, than the one in station 10, because the mass flow is more.

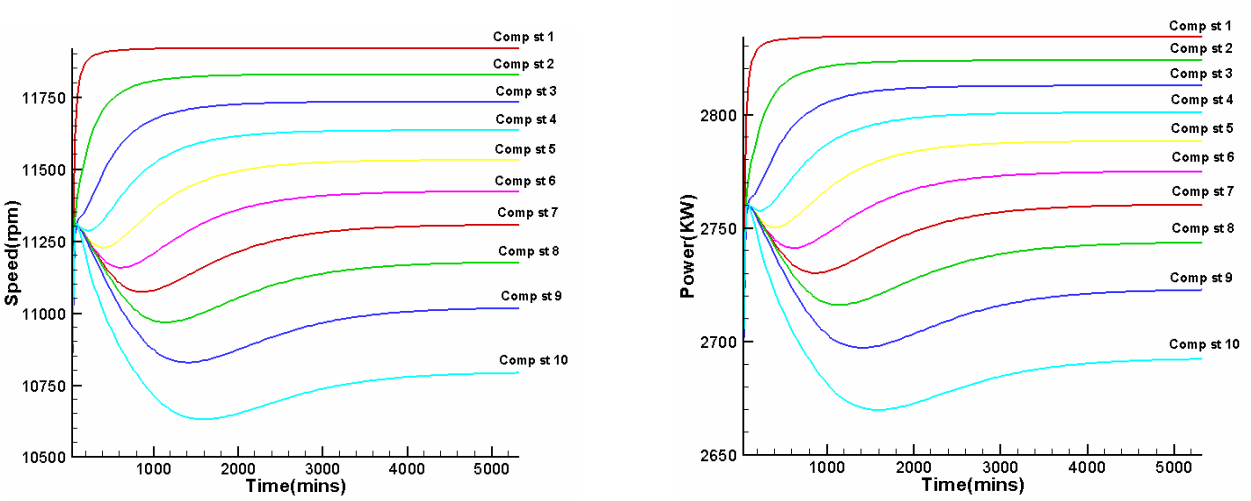

Fig 3.5.17 Comparisons of speed and power at each compressor station over time.

The head of the compressor depends on its suction and discharge pressure. The difference between the suction and discharge pressures for the compressors in the first station should be more than in the last station. Thus, the head of the compression unit decreases as the compressor station number increases as seen in Figures 3.5.18 and 3.5.19.

Fuel consumption depends on the head of the compression unit. Figure 3.5.20 shows that though the fuel consumption increases along the compressor stations the difference is not great. As the compression unit in the first station works with a higher difference between the suction and discharge pressures, the discharge temperature is higher as compared to the last station, as shown in Figure 3.5.21.

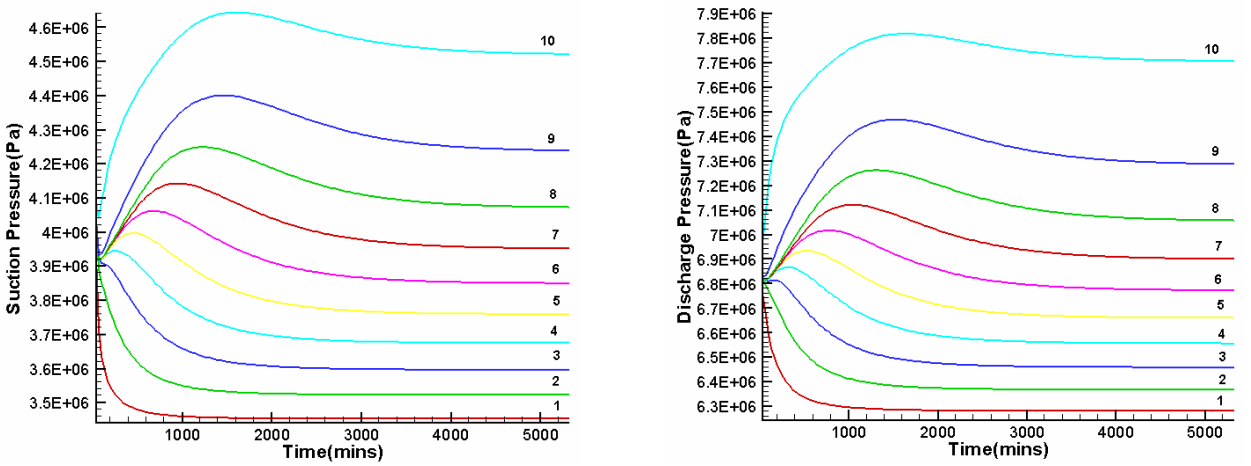

Fig. 3.5.18: Comparisons of suction and discharge pressures at each compressor station over time.

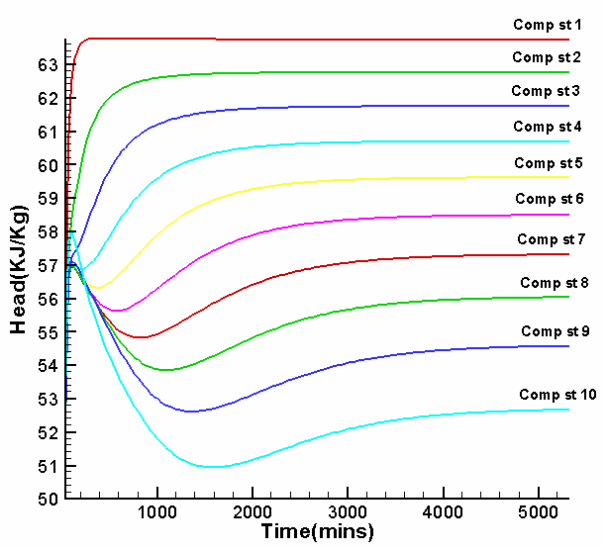

Fig. 3.5.19: Comparison of head at each compressor station over time.

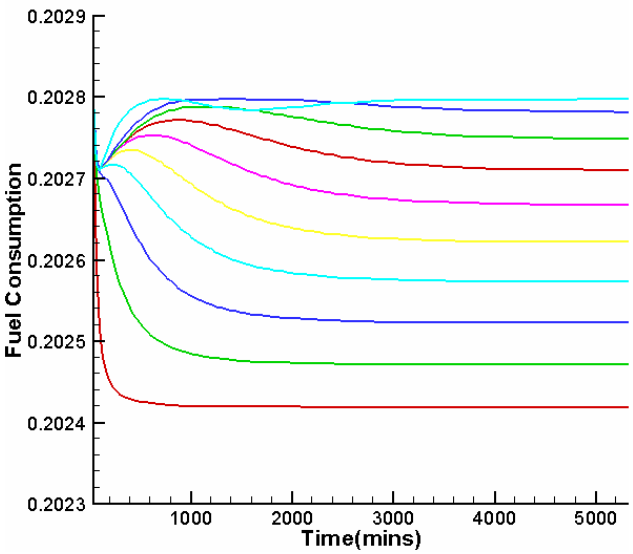

Fig. 3.5.20: Comparison of fuel consumption at each compressor station over time.

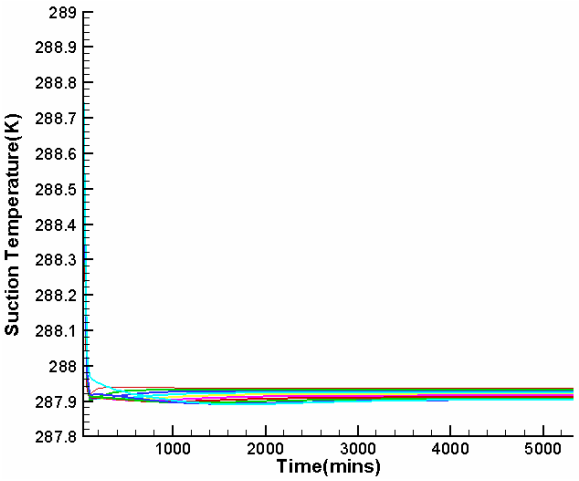

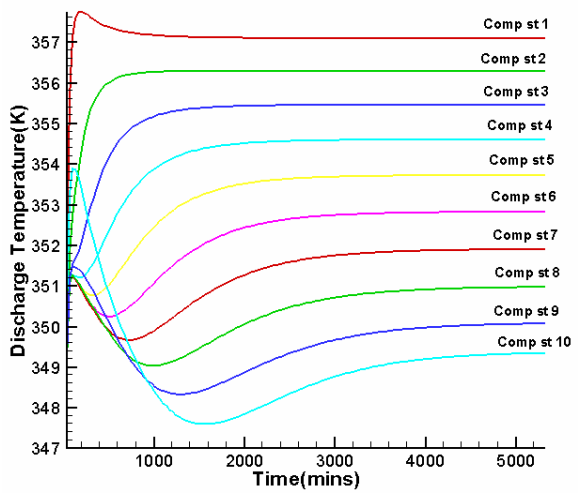

Fig. 3.5.21: Comparison of suction and discharge temperatures at each compressor station over time.

The suction mass flow rate for a compression unit is greater than the discharge mass flow rate as a small percent of the gas is used by the gas turbine to drive the compressor. This can be seen in Fig 3.5.22.

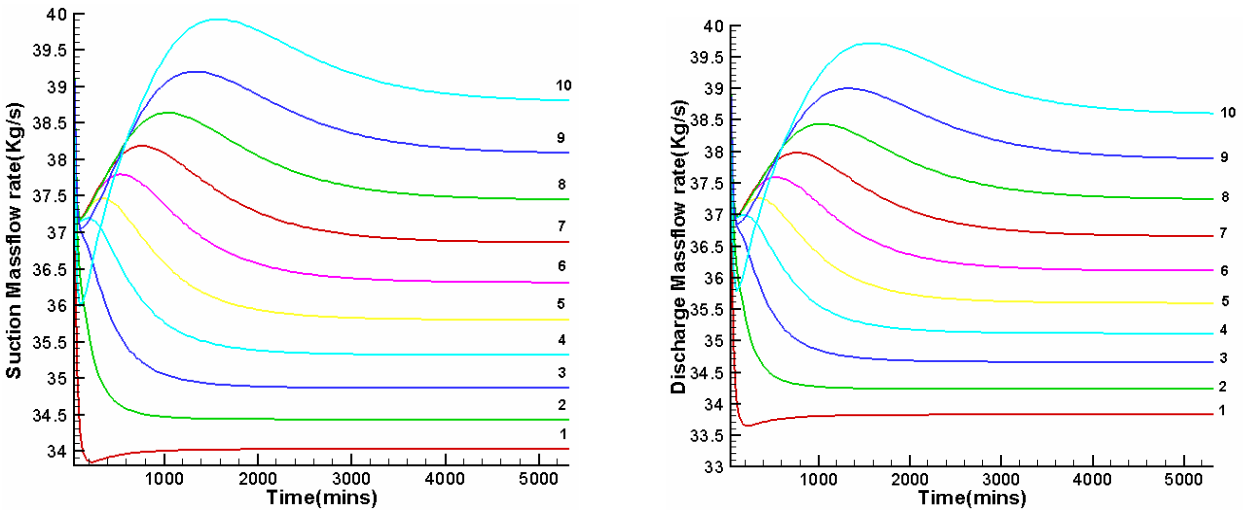

Fig. 3.5.22: Comparison of suction and discharge mass flow rates at each compressor station over time.

Example 3 Ten Compression Stations Each with Five Compression Units: In this example the pipeline has 10 compressor stations, and within each compressor station there are 5 compression units consisting of centrifugal compressors driven by gas turbines. All the compression units are identical. The schematic of the network is the same as that in Fig 3.5.16. All compressor stations are connected using long pipes that are 100 km in length. In each compressor station the design is the same as the one shown in Figure 3.5.1 with *NN* equal to 5. The specifications of all the pipes are the same as in Table 3.5.4. The angle of inclination of all the pipes is 0.0 radians. The specifications of the compression units are the same as in Tables 3.5.5 to 3.5.7. The natural gas flowing is a mixture of methane, ethane and propane in the ratio 0.7:0.25:0.05, respectively. The natural gas parameters are same as in Table 3.5.8.

Figure 3.5.16 also shows the boundary conditions used for the simulation. The boundary conditions used are constant throughout the simulation. The boundary condition information is provided in Table 3.5.10. By changing the boundary conditions the dynamic behavior of any compressor station in the network can be studied. As the network is large, the time step for the simulation is taken as 2,000 seconds.

The pressure, temperature and mass flow rate variations over the line pipe are as explained in the previous example. The variation of the compression unit parameters with respect to time for different compressor stations needs to be observed. For this, one compression unit from each compressor station is selected and its parameters are studied over a time period. Figures 3.5.23 through 3.5.28 show the variations of speed, power, fuel consumption, head, discharge pressure, discharge temperature and discharge mass flow rate for a compression unit from each of the 10 compressor stations with respect to time. All the parameters are for a selected single compression unit in the compressor station.

The mass flow rate decreases as it passes each compressor station as some of the fuel is consumed by the gas turbine. Thus the power needed for the compression unit decreases from one compressor station to the next, and hence the speed at which it runs decreases. This can be seen in Figure 3.5.23. The compression unit in the first station needs more power and runs faster than the last station, as the mass flow is more.

The head of the compressor depends on its suction and discharge pressure. The difference between the suction and discharge pressures for the compressors in the first station should be more than for the same in the last station. Thus, the head of the compression unit decreases as the compressor station number increases. Figures 3.5.24 and 3.5.25 show this trend.

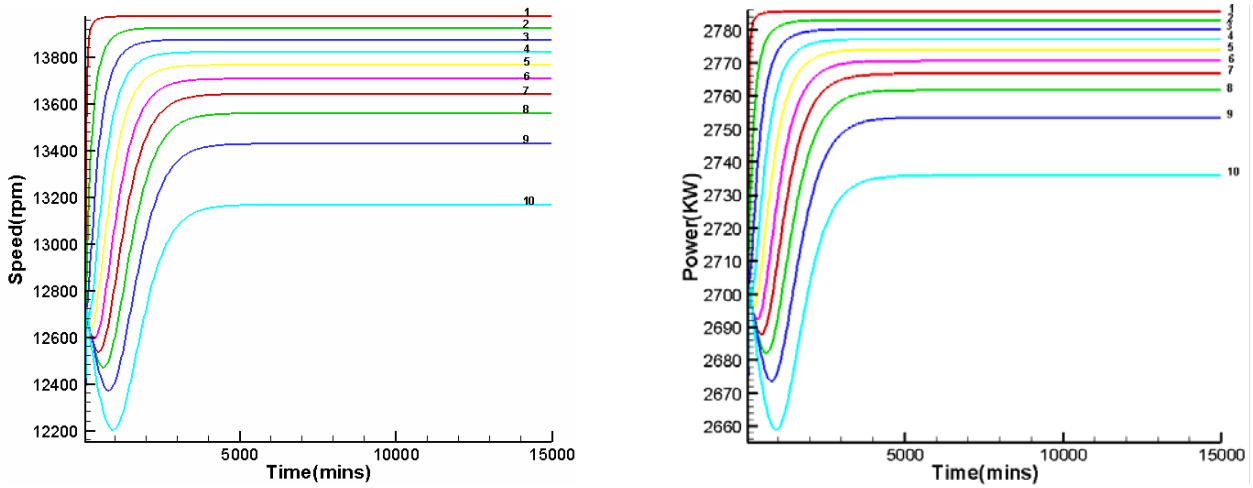

Fig. 3.5.23: Comparison of speed and power at each compressor station over time.

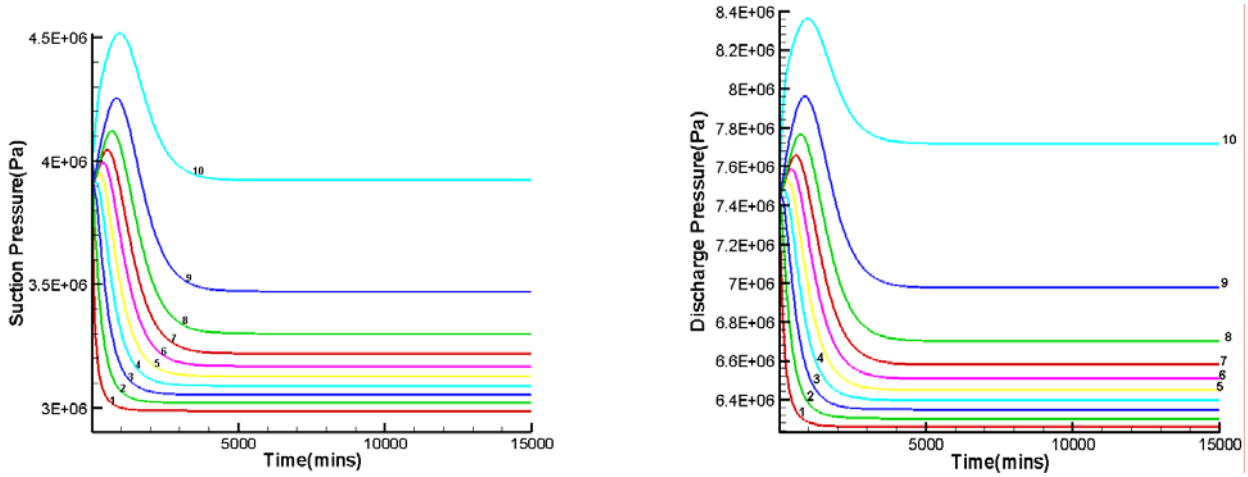

Fig. 3.5.24: Comparison of suction and discharge pressure at each compressor station over time.

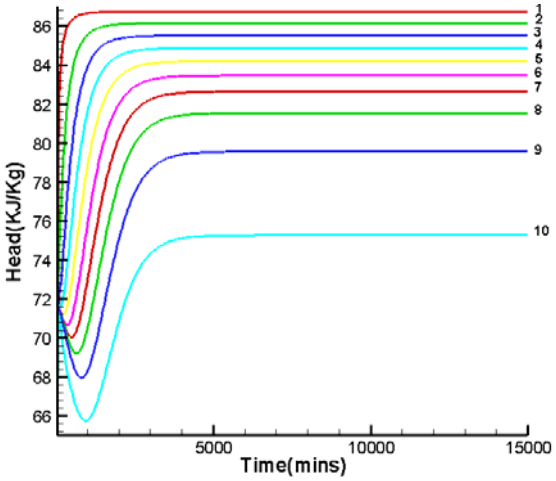

Fig. 3.5.25: Comparison of head at each compressor station over time.

As the compression unit in the first station works with a higher difference between the suction and discharge pressures, the temperature at discharge is higher in comparison to the same in the last station, as shown in Figure 3.5.26.

Fuel consumption depends on the head of the compression unit. Figure 3.5.27 shows that though the fuel consumption changes along the compressor stations, the difference is small.

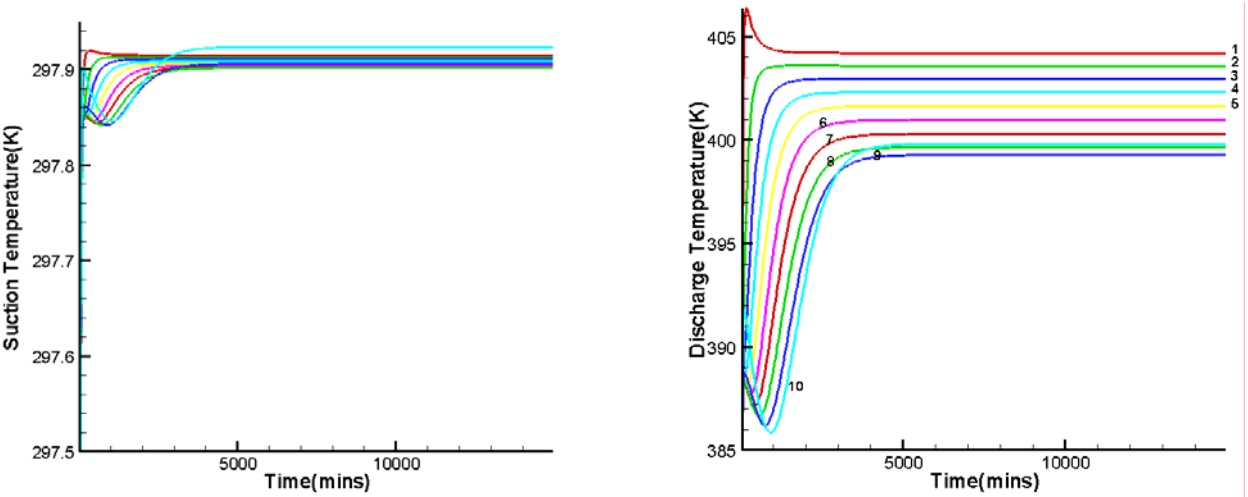

Fig. 3.5.26: Comparison of suction and discharge temperature at each compressor station over time.

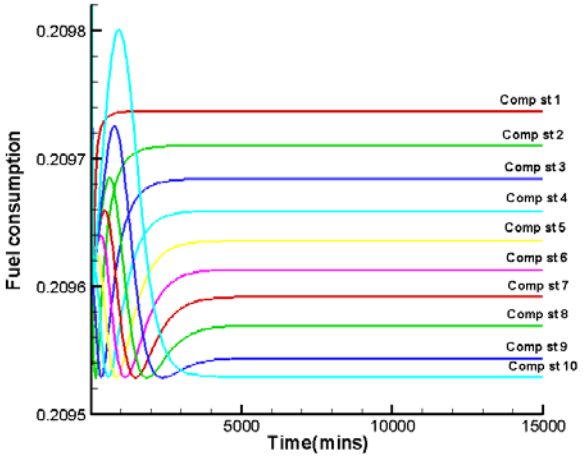

Fig.3.5.27: Comparison of fuel consumption at each compressor station over time.

The suction mass flow rate for a compression unit is greater than the discharge mass flow rate as a small percent of the gas is used by the gas turbine to drive the compressor. This can be seen in Figure 3.5.28.

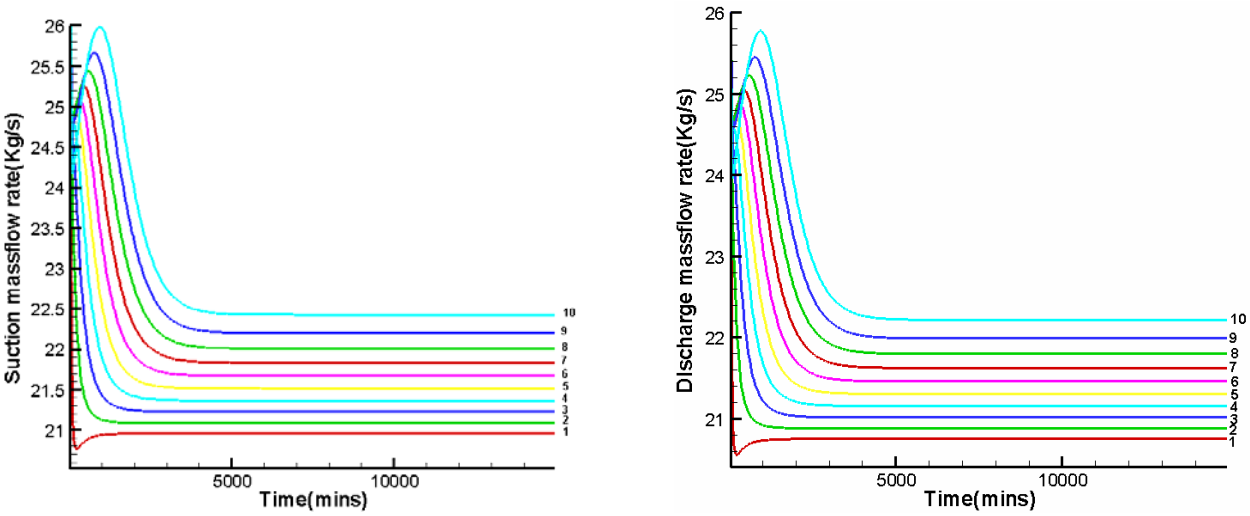

Fig. 3.5.28: Comparison of suction and discharge mass flow rates at each compressor station over time.

4.0 CONCLUSIONS

This study uses a fully implicit finite difference method to analyze transient, non-isothermal compressible gas flow through a gas pipeline system. The inertia term of the momentum equation is included in the analysis. The numerical results show that:

- **Optimization**

  Operational optimization using rigorous mathematical techniques is a viable tool for enhancing the efficiency of pipeline operations. Currently available commercial packages do not provide the capability for fully automated optimization of operational parameters; rather, these packages provide computational support for human decision making. In other words, the current generation of software in this area allows a human operator to simulate pipe flow in a network without detailed modeling of equipment such as compressors and drivers. Any decisions on how to optimize the operation of equipment must be made by the human operator based on simplified simulation of a few scenarios. Thus, the solutions are generally not truly optimal, and require considerable user involvement. This work advances the current state of pipeline simulations by using detailed equipment modeling and rigorous mathematical optimization that will automatically generate truly optimal solutions with practically no user involvement. This represents a significant advancement in the state-of-the-art in this field.

- **Solution Method**

  The fully implicit method has advantages, such as the guaranteed stability for large time step, which is very useful for simulating long-term transients in natural gas pipelines. The inertia term plays an important role in the gas flow analysis and cannot be neglected in the calculation. The effect of treating the gas in a non-isothermal manner is very necessary for pipeline flow calculation accuracies, and is extremely necessary for rapid transient processes. By using a computer simulation, the dynamic response of the compressor can be determined by changing boundary condition with respect to time. The current simulation lays a foundation on which to build a more detailed compressor station model with equipment such as scrubbers, coolers, etc. The penetrations of sudden

property changes along long length pipes are very small. The model was validated by comparing simulated results with those of others. The solution method was used to solve a large scale problem that included ten compressor stations, each with five compression units.

- **Implementation**

  The implementation of the simulation methods included the development of a graphical user interface called the Pipeline Editor. This editor is a feature-rich graphical user interface designed to provide pipeline designers with a graphical view of a pipeline systems and simulation data. The Pipeline Editor can be used to graphically build the pipeline system, manipulate an already built graph, simulate the model using parallel or sequential simulators, and display the results of such simulation graphically. The Pipeline Editor was developed using the Jgraph and Swing packages. The editor is an easy to use application that can be started from any computer using an Internet browser. Once started the Pipeline Editor connects to the Optimizer and the Sequential and Parallel Simulators. The application requires Java Web Start 1.2 and for execution.

5.0 REFERENCES

Ariel Corporation, 2001, "Ariel Application Method," http://12.2.241.6:9980/ariel/ext_data/application_manual/arieldb.htm.Beam, R.M., and Warming, R.F., 1975, "An Implicit Finite-Difference Algorithm for Hyperbolic Systems in Conservation-Law Form", *Journal of Computational Physics*, No.22, pp. 87-110.

Berard, G.P., and Eliason, B.G., 1978, "An Improved Gas Transmission System Simulator", *Society of Petroleum Engineers Journal*, Dec., pp. 389-398.

Botros, K.K., 1990, "Thermodynamic Aspects of Gas Recycling During Compressor Surge Control", *ASME Proceeding Pipeline Engineering Symposium*, New Orleans, Louisiana, pp. 57-65.

Botros, K.K., 1994, "Transient Phenomena in Compressor Stations during Surge", *Journal of Engineering for Gas Turbines and Power*, Vol. 116, Jan., pp.133-142.

Botros, K.K., Campbell, P.J., and Mah, D.B., 1989, "Dynamic Simulation of Compressor Station Installations Including Control Systems", *21st Annual Meeting Pipeline Simulation Interest Group (PSIG)*, Oct. 19-20, El Paso, Texas.

Botros, K.K., Campbell, P.J., and Mah, D.B., 1991, "Dynamic Simulation of Compressor Station Operation Including Centrifugal Compressor and Gas Turbine", *Transactions of the ASME*, Vol. 113, Apr., pp. 300-311.

Bryant, M., 1997, "Complex Compressor Station Modeling", *29th Annual Meeting Pipeline Simulation Interest Group (PSIG)*, Oct. 15-17, Tucson, Arizona.

Cameron, I., 1999, "Using An Excel-Based Model for Steady State and Transient Simulation", *31st Annual Meeting Pipeline Simulation Interest Group (PSIG)*, Oct. 20-22, St. Louis, Missouri.

Carter, R.G., 1996, "Compressor Station Optimization: Computational Accuracy and Speed", *28th Annual Meeting Pipeline Simulation Interest Group (PSIG)*, Oct. 23-25, San Francisco, California.

Chang, S., 2001, "A Program Development for Unsteady Gas Flow Analysis in Complex Pipe Networks", *33rd Annual Meeting Pipeline Simulation Interest Group (PSIG)*, Oct. 17-19, Salt Lake City, Utah.

Chapman, K.S., Abbaspour, M. and Keshavarz, A., 2003, "Development of a Virtual Pipeline System Testbed Using Non-Isothermal Transient Simulation", Gas Machinery Conference, Oct. 6-8, Salt Lake City, UT.

Chapman, K.S., and Keshavarz-Valian, A., 2003, "Development of Turbocharger-Reciprocating Engine Simulation (T-RECS)," Gas Research Institute, GRI-03/0005.

Costa, L.H, de Medeiros, J.L., and Pessoa, F.L.P, 1998, "Steady State Modeling and Simulation of Pipeline Networks for Compressible Fluids", *Brazilian Journal of Chemical Engineering*, Vol.15, No.4.

Deen, J.K., and Reintsema, S.R, 1983, "Modeling of High-Pressure Gas Transmission Lines", *Appl. Math. Modeling*, Vol.7, Aug. pp. 268-273.

Doonan, A.F., Fletcher, I. Cox, C.S., and Arden W.J.B., 1998, "Evaluation of A Remote Boundary Pressure Control Strategy Using SIMULINK™ ", *Proceeding from UKACC International Conference on Control' 98*, Sep. 1-4, No.455, pp.129-134.

Dranchuck, P.M., Purvis, R.A., and Robinson, D.B., 1974, "Computer Calculations of Natural Gas Compressibility Factors Using the Standing and Katz Correlation", *Institute of Petroleum Technical Series*, No. IP 74-008, pp.1-13.

Dupont, T., and Rachford, H.H., 1980, "The Effect of Thermal Changes Induced by Transients in Gas Flow", *12th Annual Meeting Pipeline Simulation Interest Group (PSIG)*, Oct. 16-17, Savannah, Georgia.

Fauer, D., 2002, "The Making of a Useful Pipeline Simulation Model", *34th Annual Meeting Pipeline Simulation Interest Group (PSIG)*, Oct. 23-25, Portland, Oregon.

Greyvenstein, G.P., and Laurie, D.P., 1994, "A Segregated CFD Approach to Pipe Network Analysis", *International Journal for Numerical Methods in Engineering*, Vol. 37, pp. 3685-3705.

Hartwick, W., 1968, "Efficiency Characteristics of Reciprocating Compressors," *American Society of Mechanical Engineers. Diesel and Gas Engine Power Division*, Dec. 1-5.

Hartwick, W., 1974, "Power Requirements and Associated Effects of Reciprocating Compressor Cylinder Ends Deactivated by Internal Bypassing," *American Society of Mechanical Engineers. Diesel and Gas Engine Power Division*, Dec. 17.

Hati, A., Verma, N., and Chhabra, R., 2001, "Transient Analysis of Gas Flow in a Straight Pipe", *Canadian Journal of Chemical Engineering*, Vol. 79, No. 1, Feb. pp. 18-27.

Heath, M.J., and Blunt, J.C., 1969, "Dynamic Simulation Applied to the Design and Control of a Pipeline Network", *J. Inst. Gas. Eng.*, Vol. 9, No. 4, pp. 261-279.

Hoeven, T.V., and Gasunie, N.V.N., 1992, "Some Mathematical Aspects of Gas Network Simulation", *24th Annual Meeting Pipeline Simulation Interest Group (PSIG)*, Oct. 22-23, Corpus Christi, Texas.

Ibraheem, S.O., and Adewumi, M.A., 1996, "Higher-Resolution Numerical Solution for 2-D Transient Natural Gas Pipeline Flows", *Society of Petroleum Engineers*, SPE 35626, pp. 473-482.

Issa, R.I., and Spalding, D.B., 1972, "Unsteady One-Dimensional Compressible Frictional Flow with Heat Transfer", *Journal Mechanical Engineering Science*, Vol. 14, No.6, pp. 365-369.

Jenicek, T., and Kralik, J., 1995," Optimized Control of Generalized Compressor Station", *27th Annual Meeting Pipeline Simulation Interest Group (PSIG)*, Oct. 18-20, Albuquerque, New Mexico

Kiuchi, T., 1994, "An Implicit Method for Transient Gas Flow in Pipe Networks", *Int. J. Heat and Fluid Flow*, Vol. 15, No. 5, pp. 378-383.

Letnowski, F.W., 1993, "Compressor Station Modeling in Networks", *25th Annual Meeting Pipeline Simulation Interest Group (PSIG)*, Oct. 14-15, Pittsburgh, Pennsylvania.

Lewandowski, A., 1994, "Object-oriented Modeling of the Natural Gas Pipeline Network", *26th Annual Meeting Pipeline Simulation Interest Group (PSIG)*, Oct. 13-14, San Diego, California.

Ludwig, E.E., 1983, "*Applied Process Design for Chemical and Petrochemical Plants*", Gulf Publishing Company, Houston, Texas.

Luongo, C.A., 1986, "An Efficient Program for Transient Flow Simulation in Natural Gas Pipelines", *15th Annual Meeting Pipeline Simulation Interest Group (PSIG)*, Oct. 30-31, New Orleans, Louisiana.

Maddox, R.N., and Zhou, P., 1983, "Use of Steady –State Equations for Transient Flow Calculations", *15th Annual Meeting Pipeline Simulation Interest Group (PSIG)*, Oct. 27-28, Detroit, Michigan .

Martinz-Romero, N., Osorio-Peralta, O., and Santamaria-Vite, I., 2002, "Natural Gas Network Optimization and Sensibility Analysis", *Proceedings of the SPE International Petroleum Conference and Exhibition of Mexico*, Feb. 10-12, pp. 357-370.

Mathews, H., 2000, "Compressor Performance Analysis," *Proceedings of the 2000 Gas Machinery Conference*, Oct. 4, Colorado Springs, Colorado.

McConnell, P., Smith, C., Maguire, P., and Turner, W.J., 1992, "Real-Time and Prediction Model of the Moomba-Sydney-Newcastle Natural Gas Pipeline", *24th Annual Meeting Pipeline Simulation Interest Group (PSIG)*, Oct. 22-23, Corpus Christi, Texas.

Metcalf, J.R., 2000, "Effects of Compressor Valves on Reciprocating Compressor Performance," *Proceedings of the 2000 Gas Machinery Conference*, Oct. 4, Colorado Springs, Colorado.

Modisette, J., 2002, "Pipeline Thermal Model", *34th Annual Meeting Pipeline Simulation Interest Group (PSIG)*, Oct. 23-25, Portland, Oregon

Mohitpour, M., Thompson, W., and Asante, B., 1996, "Importance of Dynamic Simulation on the Design and Optimization of Pipeline Transmission Systems", *Proceedings of the International Pipeline Conference*, American Society of Mechanical Engineers, Vol.2, pp. 1183-1188.

Murphy, H.G., 1989, "Compressor Performance Modeling to Improve Efficiency and the Quality of Optimization Decisions," *21st Annual Meeting Pipeline Simulation Interest Group (PSIG)*, Oct. 19-20, El Paso, Texas.

Odom, F.M., 1990, "Tutorial on Modeling of Gas Turbine Driven Centrifugal Compressors", *22nd Annual Meeting Pipeline Simulation Interest Group (PSIG)*, Oct. 18-19, Baltimore, Maryland.

Osiadacz, A.J., 1987, *Simulation and Analysis of Gas Networks*, Gulf Publishing Company, Houston, Texas.

Osiadacz, A.J., 1994, "Dynamic Optimization of High Pressure Gas Networks Using Hierarchical Systems Theory", *26th Annual Meeting Pipeline Simulation Interest Group (PSIG)*, Oct. 13-14, San Diego, California.

Osiadacz, A.J., 1996, "Deferent Transient Models- Limitations, Advantages and Disadvantages", *28th Annual Meeting Pipeline Simulation Interest Group (PSIG)*, Oct. 23-25, San Francisco, California.

Osiadacz, A.J., and Bell, D.J., 1995, "Dynamic Simulation of Gas Networks by Decomposition and Coordination", *Mathematical Engineering in Industry*,. Vol. 5, No. 3, pp. 235-254.

Osiadacz, A.J., and Chaczykowski, M., 1998, "Comparison of Isothermal and Non-Isothermal Transient Models", *30th Annual Meeting Pipeline Simulation Interest Group (PSIG)*, Oct. 28-30, Denver, Colorado.

Osiadacz, A.J., and Chaczykowski, M., 2001, "Simulation of Non-Isothermal Transient Gas Flow in a Pipeline", *Archives of Thermodynamics*, Vol. 22, No. 1-2, pp. 51-70.

Ouyang, L. and Aziz, K., 1996, "Steady-State Gas Flow in Pipes", *Journal of Petroleum Science and Engineering*, Vol.14, pp. 137-158.

Patankar, S. V., 1980, *Numerical Heat Transfer and Fluid Flow*, Hemisphere, Washington.

Phillippi, G, 2002, "Basic Compression Short Course", *Proceedings from the 2002 Gas Machinery Conference*, Oct 7-9, Nashville, TN.

Pierson, J. L., and Wilcox, K. D., 1984, "A Computer System for Analysis of Multi-Stage Reciprocating Compressors," *16th Annual Meeting Pipeline Simulation Interest Group (PSIG)*, Oct. 18-19, Chattanooga, Tennessee.

Price, G.R, McBrien, R.K., Rizopoulos, S.N., and Golshan, H., 1996, "Evaluating the Effective Friction Factor and Overall Heat Transfer Coefficient During Unsteady Pipeline Operation", *Proceedings of the International Pipeline Conference*, American Society of Mechanical Engineers, Vol.2, pp. 1175-1182.

Rachford, H.H., and Dupont, T.A., 1974, "A Fast Highly Accurate Means of modeling Transient Flow in Gas Pipelines by Variational Methods", *Society of Petroleum Engineers Journal*, pp. 356-362.

Rhoads, G.A., 1983, "Which Flow Equation - Does it Matter?" *15th Annual Meeting Pipeline Simulation Interest Group (PSIG)*, Oct. 27-28, Detroit, Michigan.

Rios-Mercado, R.Z., Suming, W., Ridgway, S., and Boyd, A., 2001, "A Reduction Technique for Natural Gas Transmission Network Optimization Problems", *Annals of Operation Research*, Vol. 117, pp. 217-234.

Santos, S.P., 1997, "Transient Analysis, A Must in Gas Pipeline Design", *29th Annual Meeting Pipeline Simulation Interest Group (PSIG)*, Oct. 15-17, Tucson, Arizona.

Schroeder, D.W., 2001, "A Tutorial on Pipe Flow Equations", *33rd Annual Meeting Pipeline Simulation Interest Group (PSIG)*, Oct. 17-19, Salt Lake City, Utah.

Schultz, J.M., 1962, "The Polytropic Analysis of Centrifugal Compressors", *Journal of Engineering for Power*, Jan., pp. 69-82.

Shapiro, A.H., 1953, *The Dynamics and Thermodynamics of Compressible Fluid Flow, Volume. 1*, John Wiley & Sons.

Stanley, R.A., and Bohannan, W.R., 1977, "Dynamic Simulation of Centrifugal Compressor Systems", *Proceedings of the Sixth Turbomachinery Symposium*, pp. 123-131.

Stoner, M.A., 1969, "Steady- State Analysis of Gas production Transmission and Distribution Systems", *Society of Petroleum Engineers of AIME*, SPE 2554.

Stoner, M.A., 1972, "Sensitivity Analysis Applied to a Steady-State Model of Natural Gas Transportation Systems", *Society of Petroleum Engineers Journal*, Apr., pp. 115-125.

Sung, W., Huh, D., Lee, J., and Kwon, O., 1998, "Optimization of Pipeline Networks with a Hybrid MCST-CD Networking Model", *SPE Production & Facilities*, August, Vol.13, No..3, pp. 213-219.

Tanaka, T., 1983, "A Computer Simulation of Unsteady-State Gas Flow in Pipeline", *J. Japan Petrol. Inst.* No. 26, pp.67-77.

Tao, W.Q., and Ti, H.C., 1998, "Transient Analysis of Gas Pipeline Network", *Chemical Engineering Journal*, No. 69, pp.47-52.

Thorley, A.R.D., and Tiley, C.H., 1987, "Unsteady and Transient Flow of Compressible Fluids in Pipelines - A Review of Theoretical and Some Experimental Studies", *Journal of Heat and Fluid Flow*, Vol.8, No.1, pp. 3-15.

Tian, S. and Adewumi, M.A., 1994, "Development of Analytical Design Equation for Gas Pipelines", *SPE Production & Facilities*, pp. 100-106.

Turner, W.J., and Simonson, M.J., 1984, "A Compressor Station Model for Transient Gas Pipeline Simulation", *16th Annual Meeting Pipeline Simulation Interest Group (PSIG)*, Oct. 18-19, Chattanooga, Tennessee.

Turner, W.J., and Simonson, M.J., 1985, "Compressor Station Transient Flow Modeled", *Oil & Gas Journal Technology*, May, pp. 79-83.

Wylie, E.B., Stoner, M.A., and Streeter, V.L., 1971, "Network System Transient Calculation by Implicit Methods", *Society of Petroleum Engineers Journal*, Dec., pp. 356-362.

Wylie, E.B., Streeter, V.L., and Stiner, M.A., 1974, "Unsteady State Natural-Gas Calculations in Complex Piping Systems", *Society of Petroleum Engineers Journal*, Feb., pp. 35-43.

Yow, W., 1971, "Analysis and Control of Transient Flow in Natural Gas Piping Systems", Ph.D. Thesis, *The University of Michigan*.

Zemansky, M.W., 1968, *Heat and Thermodynamics 5th Edition*, McGraw Hill.

Zhou, J. and Adewumi, M.A., 1995, "Simulation of Transient Flow in Natural Gas Pipelines", *27th Annual Meeting Pipeline Simulation Interest Group (PSIG)*, Oct. 18-20, Albuquerque, New Mexico.

APPENDIX A: FORMULATION OF GOVERNING PIPELINE SIMULATION EQUATIONS

This appendix includes all the details of the pipeline governing equations. While this level of detail is beyond the interest level of the typical reader, it was not found in any of the other literature, including text books. Hence, this information is included in this report to provide the pipeline simulation professional a concise development of the transient, non-isothermal compressible flow equations.

A.1 Governing Equations

The non-isothermal flow of natural gas in pipelines is governed by the time-dependent continuity, momentum, energy equations (Luongo 1986) and equation of state for homogeneous, geometrically one-dimensional flow. By simultaneously solving these equations, one can obtain the flow rate as well as the behavior of gas parameters along the pipe network.

A.1.1 Continuity Equation

The mass conservation concept illustrated for the control volume shown in Figure A.1.1 can be

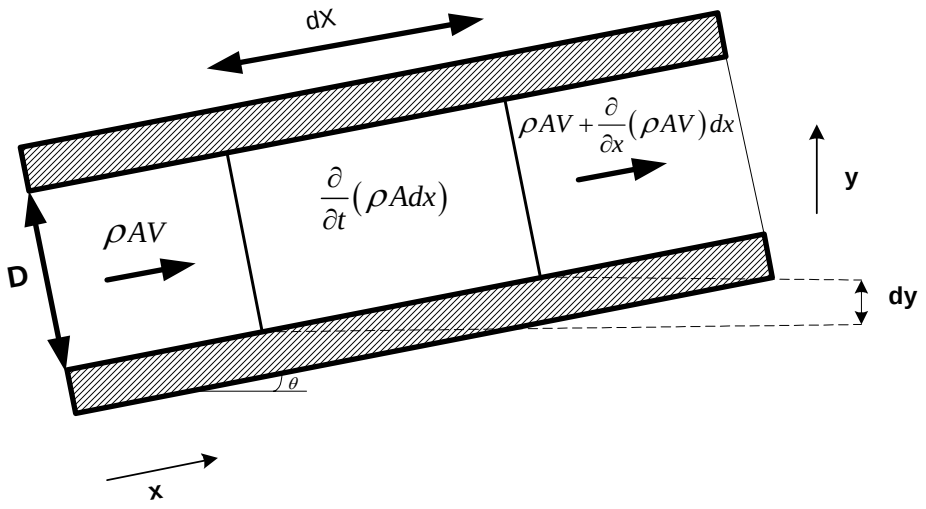

Fig. A.1.1: Control volume for the continuity equation.

written as:

$$\rho Av - \rho Av - \frac{\partial}{\partial x}(\rho Av)dx = \frac{\partial}{\partial t}(\rho Adx) \tag{A.1.1}$$

Then,

$$\frac{\partial}{\partial x}(\rho Av)dx + \frac{\partial}{\partial t}(\rho Adx) = 0 \tag{A.1.2}$$

Simplifying, the mass conservation equation reduces to:

$$\frac{\partial \rho}{\partial t} + \frac{\partial}{\partial x}(\rho v) = 0 \tag{A.1.3}$$

Where ρ is the density of the fluid $\left(kg/m^3\right)$ and v is the velocity of fluid directed along the axis of the pipe (m/s).

A.1.2 Momentum Equation

The momentum equation can be written for the control volume shown in Figure A.1.2 using the

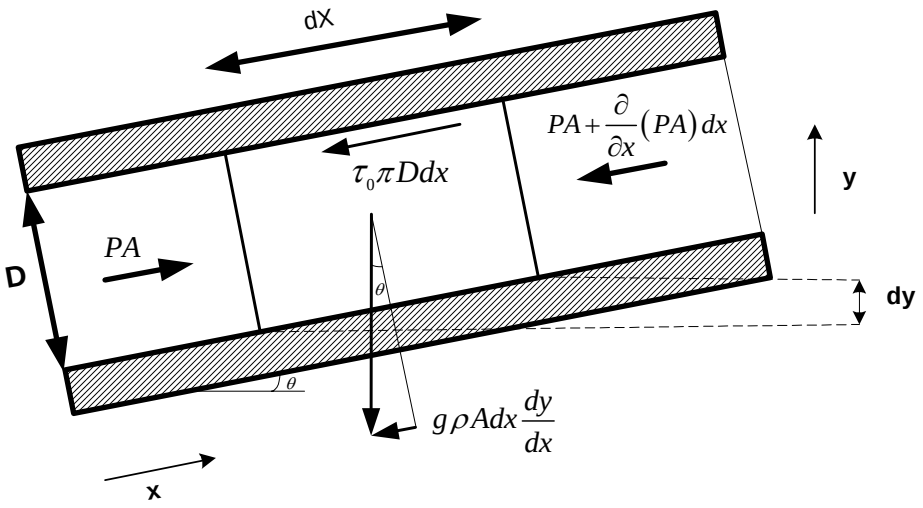

Fig. A.1.2: Control volume for the momentum equation.

following force component summation:

$$PA - PA - \frac{\partial}{\partial x}(PA)\,dx - \tau_0 \pi D dx - \rho g A dx\left(\frac{dy}{dx}\right) = (\rho A dx)\left(v\frac{\partial v}{\partial x} + \frac{\partial v}{\partial t}\right) \qquad \text{(A.1.4)}$$

Reducing and algebraically manipulating the momentum equation results in:

$$-A\frac{\partial P}{\partial x} - \tau_0 \pi D - \rho g A\left(\frac{dy}{dx}\right) = \rho A\left(v\frac{\partial v}{\partial x} + \frac{\partial v}{\partial t}\right) \qquad \text{(A.1.5)}$$

The parameter τ_0 is the shear stress between the fluid and the pipe wall and can be obtained by:

$$\tau_0 = \frac{f\rho v|v|}{8} \qquad \text{(A.1.6)}$$

The variable f is the Darcy friction factor. The absolute value of v is introduced to maintain the correct direction for negative velocities. Various researchers have used different relationships to define the friction factor by specifying a variety of functional relationships for *f*. Recognizing that $\frac{dy}{dx} = Sin\theta$, the momentum equation is reduced to:

$$-A\frac{\partial P}{\partial x} - \frac{f\rho v|v|}{8}\pi D - \rho g A Sin\theta = \rho A\left(v\frac{\partial v}{\partial x} + \frac{\partial v}{\partial t}\right) \qquad \text{(A.1.7)}$$

and,

$$w = \frac{f\rho v|v|}{8}\pi D \qquad \text{(A.1.8)}$$

Then,

$$\rho\frac{\partial v}{\partial t} + \rho v\frac{\partial v}{\partial x} + \frac{\partial P}{\partial x} = -\frac{w}{A} - \rho g Sin\theta \qquad \text{(A.1.9)}$$

A.1.3 Conservation of Energy

The basic form of the conservation of energy equation from the first law of thermodynamics (Shapiro 1953) is written for the control volume shown in Figure A.1.3 as:

$$Q = q\rho A dx = \frac{\partial}{\partial t}\left[\rho A dx\left(u + \frac{v^2}{2} + gy\right)\right] + \frac{\partial}{\partial x}\left[\rho v A\left(u + \frac{v^2}{2} + \frac{P}{\rho} + gy\right)\right]dx \qquad \text{(A.1.10)}$$

where q is the heat addition per unit mass per unit time and u is the internal energy.

Separating the second term results in:

$$q\rho A dx = \rho A dx\left[\frac{\partial}{\partial t}\left(u + \frac{v^2}{2} + gy\right) + v\frac{\partial}{\partial x}\left(u + \frac{v^2}{2} + gy\right)\right]$$

$$+\left[\left(u + \frac{v^2}{2} + gy\right)\left(\frac{\partial(\rho A)}{\partial t} + \frac{\partial(\rho v A)}{\partial x}\right)\right]dx \qquad \text{(A.1.11)}$$

$$+\left[\frac{P}{\rho}\frac{\partial(\rho v A)}{\partial x} + (\rho v A)\frac{\partial}{\partial x}\left(\frac{P}{\rho}\right)\right]dx$$

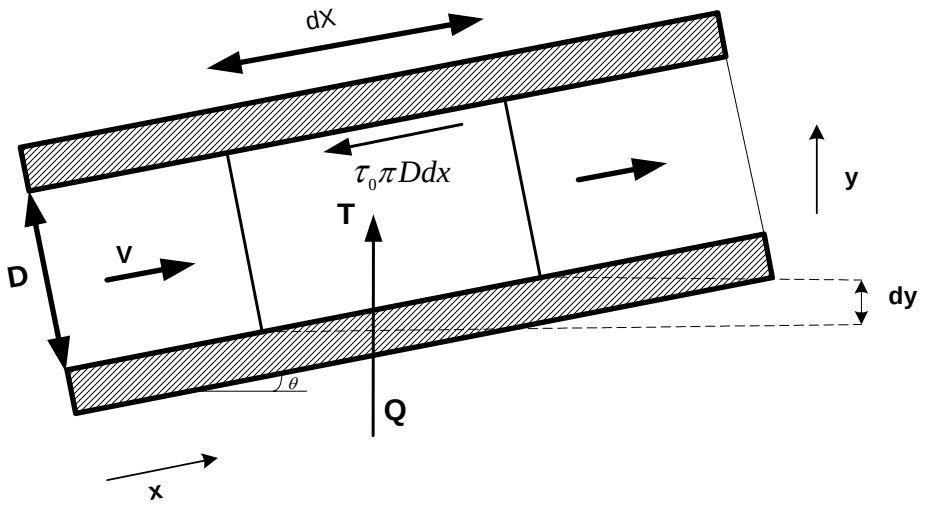

Fig. A.1.3: Control volume for the energy equation.

From the continuity equation the second term will be zero $\left(\frac{\partial(\rho A)}{\partial t}+\frac{\partial(\rho vA)}{\partial x}=0\right)$.

Dividing by $\rho A dx$, the energy equation reduces to:

$$q=\frac{D}{Dt}\left(u+\frac{v^2}{2}+gy\right)+\frac{v}{\rho}\frac{\partial P}{\partial x}+\frac{P}{\rho A}\frac{\partial(vA)}{\partial x} \tag{A.1.12}$$

Using the momentum equation and multiplying by v results in:

$$\frac{v}{\rho}\frac{\partial P}{\partial x}=-v\frac{Dv}{Dt}-\frac{wv}{\rho A}-vgSin\theta \tag{A.1.13}$$

So from continuity equation it can show that:

$$\frac{\partial}{\partial x}(vA)=-\frac{D\rho}{Dt}\frac{A}{\rho} \tag{A.1.14}$$

Then,

$$q=\frac{D}{Dt}\left(u+\frac{v^2}{2}+gy\right)-v\frac{Dv}{Dt}-\frac{wv}{\rho A}-vgSin\theta-\frac{P}{\rho^2}\frac{D\rho}{Dt} \tag{A.1.15}$$

On the other hand, considering the identity:

$$\frac{D}{Dt}(gy)=g\left(\frac{\partial y}{\partial t}+v\frac{\partial y}{\partial x}\right)=gvSin\theta \tag{A.1.16}$$

and,

$$\frac{D}{Dt}\left(\frac{v^2}{2}\right)=v\frac{Dv}{Dt} \tag{A.1.17}$$

results in:

$$q = \frac{Du}{Dt} - \frac{P}{\rho^2}\frac{D\rho}{Dt} - \frac{wv}{\rho A} \tag{A.1.18}$$

So that:

$$h \equiv u + \frac{P}{\rho} \tag{A.1.19}$$

and then:

$$\frac{Dh}{Dt} = \frac{Du}{Dt} + \frac{D}{Dt}\left(\frac{P}{\rho}\right) \tag{A.1.20}$$

Finally, this equation can be expanded to:

$$\frac{Dh}{Dt} = \frac{Du}{Dt} - \frac{P}{\rho^2}\frac{D\rho}{Dt} + \frac{1}{\rho}\frac{DP}{Dt} \tag{A.1.21}$$

and the energy equation reduces to:

$$q + \frac{wv}{\rho A} = \frac{Dh}{Dt} - \frac{1}{\rho}\frac{DP}{Dt} \tag{A.1.22}$$

Recognizing that $\Omega = q\rho A$ provides the final form of the conservation of energy equation:

$$\rho\frac{\partial h}{\partial t} + \rho v\frac{\partial h}{\partial x} - \frac{\partial P}{\partial x} - v\frac{\partial P}{\partial x} = \frac{\Omega + wv}{A} \tag{A.1.23}$$

where h is the specific enthalpy $\left(J/kg\right)$, Ω is the hHeat flow into the pipe per unit length of pipe per unit time $\left(J/(m.s)\right)$, and A is the cCross-sectional area of pipe $\left(\frac{\pi D^2}{4}\right)\left(m^2\right)$.

A.1.4 Equation of State

An equation of state for a gas relates the variables P, ρ and T. The type of equation, which is commonly used in gas industry, is:

$$\frac{P}{\rho} = ZRT \tag{A.1.24}$$

where Z is the compressibility factor which is a function of P and T, and R is the specific gas constant $\left(J/kg\right)$.

In their current form, equations (A.1.3), (A.1.9) and (A.1.18) are not convenient to solve. Therefore these equations need to be rewritten in terms of pressure, velocity and temperature as the dependent variables by using the equation of state. To obtain ρ in terms of P, Z, and T from the equation of state:

$$\rho = \frac{P}{ZRT} \tag{A.1.25}$$

Therefore:

$$\ln\left(\rho\right) = \ln\left(P\right) - \ln\left(R\right) - \ln\left(T\right) - \ln\left(Z\right) \tag{A.1.26}$$

Differentiating this equation with respect of time:

$$\frac{1}{\rho}\frac{D\rho}{Dt} = \frac{1}{P}\frac{DP}{Dt} - \frac{1}{R}\frac{DR}{Dt} - \frac{1}{T}\frac{DT}{Dt} - \frac{1}{Z}\frac{DZ}{Dt} \tag{A.1.27}$$

The term $\frac{1}{R}\frac{DR}{Dt}$ is zero, so the compressibility factor is a function of P and T such that:

$$dZ = \left(\frac{\partial Z}{\partial P}\right)_T dP + \left(\frac{\partial Z}{\partial T}\right)_P dT \tag{A.1.28}$$

$$\frac{DZ}{Dt} = \left(\frac{\partial Z}{\partial P}\right)_T \frac{DP}{Dt} + \left(\frac{\partial Z}{\partial T}\right)_P \frac{DT}{Dt} \tag{A.1.29}$$

therefore:

$$\frac{1}{\rho}\frac{D\rho}{Dt} = \left\{\frac{1}{P} - \frac{1}{Z}\left(\frac{\partial Z}{\partial P}\right)_T\right\}\frac{DP}{Dt} - \left\{\frac{1}{T} + \frac{1}{Z}\left(\frac{\partial Z}{\partial T}\right)_P\right\}\frac{DT}{Dt} \tag{A.1.30}$$

Substituting this into equation (A.1.3):

$$\left\{\frac{1}{P} - \frac{1}{Z}\left(\frac{\partial Z}{\partial P}\right)_T\right\}\frac{DP}{Dt} - \left\{\frac{1}{T} + \frac{1}{Z}\left(\frac{\partial Z}{\partial T}\right)_P\right\}\frac{DT}{Dt} + \frac{\partial v}{\partial x} = 0 \tag{A.1.31}$$

To obtain h in terms of P, Z, and T, Zemansky (1968) described the thermodynamic identity for enthalpy as:

$$dh = CpdT + \left\{\frac{T}{\rho}\left(\frac{\partial \rho}{\partial T}\right)_P + 1\right\}\frac{dP}{\rho} \tag{A.1.32}$$

and then:

$$\frac{Dh}{Dt} = Cp\frac{DT}{Dt} + \left\{\frac{T}{\rho}\left(\frac{\partial \rho}{\partial T}\right)_P + 1\right\}\frac{1}{\rho}\frac{DP}{Dt} \tag{A.1.33}$$

Substituting this relationship into equation (A.1.25):

$$\rho Cp\frac{DT}{Dt} + \left\{\frac{T}{\rho}\left(\frac{\partial \rho}{\partial T}\right)_P\right\}\frac{DP}{Dt} = \frac{\Omega + wv}{A} \tag{A.1.34}$$

Finding $\frac{DP}{Dt}$ and $\frac{DT}{Dt}$ from equations (A.1.31) and (A.1.34) such that:

$$\rho Cp\left[\frac{1}{P}-\frac{1}{Z}\left(\frac{\partial Z}{\partial P}\right)_T\right]\frac{DP}{Dt}+\left[\frac{1}{T}+\frac{1}{Z}\left(\frac{\partial Z}{\partial T}\right)_P\right]\frac{T}{\rho}\left(\frac{\partial \rho}{\partial T}\right)_P\frac{DP}{Dt}$$
$$=-\rho Cp\frac{\partial v}{\partial x}+\left[\frac{1}{T}+\frac{1}{Z}\left(\frac{\partial Z}{\partial T}\right)_P\right]\frac{\Omega+wv}{A} \quad \text{(A.1.35)}$$

From the equation of state and considering constant pressure, it can be found that:

$$\frac{1}{\rho}\left(\frac{\partial \rho}{\partial T}\right)_P=-\frac{1}{T}\left\{1+\frac{T}{Z}\left(\frac{\partial Z}{\partial T}\right)_P\right\} \quad \text{(A.1.36)}$$

Substituting this into equation (A.1.35) and dividing by Cp gives:

$$\frac{\rho}{P}\left\{\left[1-\frac{P}{Z}\left(\frac{\partial Z}{\partial P}\right)_T\right]-\frac{P}{\rho CpT}\left[1+\frac{T}{Z}\left(\frac{\partial Z}{\partial T}\right)_P\right]^2\right\}\frac{DP}{Dt}+\rho\frac{\partial v}{\partial x}$$
$$=\frac{1}{CpT}\left[1+\frac{T}{Z}\left(\frac{\partial Z}{\partial T}\right)_P\right]\frac{\Omega+wv}{A} \quad \text{(A.1.37)}$$

Now equations (A.1.34) and (A.1.35) are used to determine an expression for $\frac{DT}{Dt}$:

$$\rho Cp\left[\frac{1}{P}-\frac{1}{Z}\left(\frac{\partial Z}{\partial P}\right)_T\right]\frac{DT}{Dt}+\left[\frac{1}{T}+\frac{1}{Z}\left(\frac{\partial Z}{\partial T}\right)_P\right]\frac{T}{\rho}\left(\frac{\partial \rho}{\partial T}\right)_P\frac{DT}{Dt}$$
$$=\frac{T}{\rho}\left(\frac{\partial \rho}{\partial T}\right)_P\frac{\partial v}{\partial x}+\left[\frac{1}{P}-\frac{1}{Z}\left(\frac{\partial Z}{\partial P}\right)_T\right]\frac{\Omega+wv}{A} \quad \text{(A.1.38)}$$

Dividing this expression by Cp and substituting for $\frac{1}{\rho}\left(\frac{\partial \rho}{\partial T}\right)_P$ from the equation of state as before gives:

$$\frac{\rho}{P}\left\{\left[1-\frac{P}{Z}\left(\frac{\partial Z}{\partial P}\right)_T\right]-\frac{P}{\rho CpT}\left[1+\frac{T}{Z}\left(\frac{\partial Z}{\partial T}\right)_P\right]^2\right\}+\frac{1}{Cp}\left[1+\frac{T}{Z}\left(\frac{\partial Z}{\partial T}\right)_P\frac{\partial v}{\partial x}\right]$$

$$=\frac{1}{CpT}\left[1-\frac{P}{Z}\left(\frac{\partial Z}{\partial P}\right)_T\right]\frac{\Omega+wv}{A} \tag{A.1.39}$$

A.1.5 Wave Speed (Throley 1987)

Treating the entropy s as a function of pressure and density:

$$s = s(P, \rho) \tag{A.1.40}$$

Then:

$$ds=\left(\frac{\partial s}{\partial P}\right)_\rho dP+\left(\frac{\partial s}{\partial \rho}\right)_P d\rho \tag{A.1.41}$$

For an isentropic process:

$$0=\left(\frac{\partial s}{\partial P}\right)_\rho\left(\frac{\partial P}{\partial \rho}\right)_s+\left(\frac{\partial s}{\partial \rho}\right)_P \tag{A.1.42}$$

Therefore:

$$\left(\frac{\partial P}{\partial \rho}\right)_s=-\frac{\left(\frac{\partial s}{\partial T}\right)_P\left(\frac{\partial T}{\partial \rho}\right)_P}{\left(\frac{\partial s}{\partial T}\right)_\rho\left(\frac{\partial T}{\partial P}\right)_\rho} \tag{A.1.43}$$

In a similar manner, the temperature T is written as a function of pressure and density $T = T(P, \rho)$, such that:

$$dT=\left(\frac{\partial T}{\partial P}\right)_\rho dP+\left(\frac{\partial T}{\partial \rho}\right)_P d\rho \tag{A.1.44}$$

For constant temperature equal to zero, then:

$$\frac{\left(\frac{\partial T}{\partial \rho}\right)_P}{\left(\frac{\partial T}{\partial P}\right)_\rho} = -\frac{1}{\left(\frac{\partial \rho}{\partial P}\right)_T} \tag{A.1.45}$$

Thus:

$$\left(\frac{\partial P}{\partial \rho}\right)_s = \left[\frac{\left(\frac{\partial s}{\partial T}\right)_P}{\left(\frac{\partial s}{\partial T}\right)_\rho}\right]\left[\frac{1}{\left(\frac{\partial \rho}{\partial P}\right)_T}\right] \tag{A.1.46}$$

But from Zemansky (1968):

$$\left(\frac{\partial s}{\partial T}\right)_P = \frac{Cp}{T} \tag{A.1.47}$$

and:

$$\left(\frac{\partial s}{\partial T}\right)_\rho = \frac{Cv}{T} = \frac{Cp}{T} - \left(\frac{\partial v}{\partial T}\right)_P \left(\frac{\partial P}{\partial T}\right)_v \tag{A.1.48}$$

So:

$$\left(\frac{\partial P}{\partial T}\right)_v = -\frac{\left(\frac{\partial v}{\partial T}\right)_P}{\left(\frac{\partial v}{\partial P}\right)_T} \tag{A.1.49}$$

Therefore:

$$\left(\frac{\partial s}{\partial T}\right)_{\rho} = \frac{Cp}{T} - \frac{1}{\rho^2}\left[\frac{\left(\frac{\partial \rho}{\partial T}\right)_P^2}{\left(\frac{\partial \rho}{\partial P}\right)_T}\right] \tag{A.1.50}$$

and,

$$\left(\frac{\partial s}{\partial T}\right)_{\rho}\left(\frac{\partial \rho}{\partial P}\right)_T = \frac{Cp}{T}\left(\frac{\partial \rho}{\partial P}\right)_T - \frac{1}{\rho^2}\left(\frac{\partial \rho}{\partial T}\right)_P^2 \tag{A.1.51}$$

From the equation of state it has already been proved that:

$$\left(\frac{\partial \rho}{\partial T}\right)_P = -\frac{\rho}{T}\left[1 + \frac{T}{Z}\left(\frac{\partial Z}{\partial T}\right)_P\right] \tag{A.1.52}$$

and also:

$$\left(\frac{\partial \rho}{\partial P}\right)_T = \frac{\rho}{P}\left[1 - \frac{P}{Z}\left(\frac{\partial Z}{\partial P}\right)_T\right] \tag{A.1.53}$$

Substituting these identities into equation (A.1.39) gives:

$$\left(\frac{\partial P}{\partial \rho}\right)_s = \frac{Cp}{T}\left[\frac{Cp}{T}\left\{\frac{\rho}{P}\left[1 - \frac{P}{Z}\left(\frac{\partial Z}{\partial P}\right)_T\right] - \frac{1}{CpT}\left[1 + \frac{T}{Z}\left(\frac{\partial Z}{\partial T}\right)_P\right]^2\right\}\right]^{-1} \tag{A.1.54}$$

And it follows that:

$$\left(\frac{\partial P}{\partial \rho}\right)_s = \frac{1}{\left[\frac{\rho}{P}\left\{1 - \frac{P}{Z}\left(\frac{\partial Z}{\partial P}\right)_T - \frac{P}{\rho CpT}\left[1 + \frac{T}{Z}\left(\frac{\partial Z}{\partial T}\right)_P\right]^2\right\}\right]} \tag{A.1.55}$$

where the term $\left(\frac{\partial P}{\partial \rho}\right)_s^{\frac{1}{2}}$ can be defined as the isentropic wave speed V_w. Using the equation of state $\frac{P}{\rho} = ZRT$, the isentropic wave speed is expressed as:

$$V_w = \sqrt{\frac{ZRT}{\left\{1 - \frac{P}{Z}\left(\frac{\partial Z}{\partial P}\right)_T - \frac{P}{\rho CpT}\left[1 + \frac{T}{Z}\left(\frac{\partial Z}{\partial T}\right)_P\right]^2\right\}}} \tag{A.1.56}$$

Substituting this equation (A.1.56) into equations (A.1.37) and (A.1.38) and using the momentum equation (A.1.9), the final equation set will be:

$$\left(\frac{\partial P}{\partial t}\right) + v\left(\frac{\partial P}{\partial x}\right) + \rho V_w^{\,2}\left(\frac{\partial v}{\partial x}\right) = \frac{V_w^{\,2}}{CpT}\left[1 + \frac{T}{Z}\left(\frac{\partial Z}{\partial T}\right)_P\right]\frac{\Omega + wv}{A} \tag{A.1.57}$$

$$\left(\frac{\partial v}{\partial t}\right) + v\left(\frac{\partial v}{\partial x}\right) + \frac{1}{\rho}\left(\frac{\partial P}{\partial x}\right) = -\frac{w}{A\rho} - gSin\theta \tag{A.1.58}$$

$$\left(\frac{\partial T}{\partial t}\right) + v\left(\frac{\partial T}{\partial x}\right) + \frac{V_w^{\,2}}{Cp}\left[1 + \frac{T}{Z}\left(\frac{\partial Z}{\partial T}\right)_P\right]\left(\frac{\partial v}{\partial x}\right) = \frac{V_w^{\,2}}{CpP}\left[1 - \frac{P}{Z}\left(\frac{\partial Z}{\partial P}\right)_T\right]\frac{\Omega + wv}{A} \tag{A.1.59}$$

As a matter of convenience, these equations can be changed to mass flow rate, $\dot{m}$. This is desirables as the mass flow rate is of interest as opposed to the gas velocity at each point in the pipeline system. To accomplish this, the velocity is defined in terms of the mass flow rate:

$$v = \frac{\dot{m}}{\rho A} = \frac{\dot{m}ZRT}{PA} \tag{A.1.60}$$

Then:

$$\frac{\partial v}{\partial x} = \frac{\partial}{\partial x}\left(\frac{\dot{m}ZRT}{PA}\right) = \frac{R}{A}\frac{\partial}{\partial x}\left(\frac{\dot{m}ZT}{P}\right)$$

$$= \frac{R}{AP^2}\left(P\left(ZT\frac{\partial \dot{m}}{\partial x} + \dot{m}T\frac{\partial Z}{\partial x} + \dot{m}Z\frac{\partial T}{\partial x}\right) - \dot{m}ZT\frac{\partial P}{\partial x}\right) \quad \text{(A.1.61)}$$

and:

$$\frac{\partial v}{\partial t} = \frac{R}{AP^2}\left(P\left(ZT\frac{\partial \dot{m}}{\partial t} + \dot{m}T\frac{\partial Z}{\partial t} + \dot{m}Z\frac{\partial T}{\partial t}\right) - \dot{m}ZT\frac{\partial P}{\partial t}\right) \quad \text{(A.1.62)}$$

Also,

$$\frac{\partial Z}{\partial x} = \left(\frac{\partial Z}{\partial P}\right)_T \frac{\partial P}{\partial x} + \left(\frac{\partial Z}{\partial T}\right)_P \frac{\partial T}{\partial x} \quad \text{(A.1.63)}$$

$$\frac{\partial Z}{\partial t} = \left(\frac{\partial Z}{\partial P}\right)_T \frac{\partial P}{\partial t} + \left(\frac{\partial Z}{\partial T}\right)_P \frac{\partial T}{\partial t} \quad \text{(A.1.64)}$$

Substituting these equations into equations (A.1.61) and (A.1.62) gives:

$$\frac{\partial v}{\partial x} = \frac{ZRT}{AP^2}\left[P\frac{\partial \dot{m}}{\partial x} - \dot{m}\left(1 - \frac{P}{Z}\left(\frac{\partial Z}{\partial P}\right)_T\right)\frac{\partial P}{\partial x} + \frac{P\dot{m}}{T}\left(1 + \frac{T}{Z}\left(\frac{\partial Z}{\partial T}\right)_P\right)\frac{\partial T}{\partial x}\right] \quad \text{(A.1.65)}$$

$$\frac{\partial v}{\partial t} = \frac{ZRT}{AP^2}\left[P\frac{\partial \dot{m}}{\partial t} - \dot{m}\left(1 - \frac{P}{Z}\left(\frac{\partial Z}{\partial P}\right)_T\right)\frac{\partial P}{\partial t} + \frac{P\dot{m}}{T}\left(1 + \frac{T}{Z}\left(\frac{\partial Z}{\partial T}\right)_P\right)\frac{\partial T}{\partial t}\right] \quad \text{(A.1.66)}$$

Substituting these equations into equations (A.1.57), (A.1.58) and (A.1.59) gives:

$$\frac{\partial P}{\partial t} + \frac{\dot{m}ZRT}{PA}\left[1 - \frac{V_w^{\,2}}{ZRT}\left(1 - \frac{P}{Z}\left(\frac{\partial Z}{\partial P}\right)_T\right)\right]\frac{\partial P}{\partial x} + \dot{m}V_w^{\,2}\left(\frac{1}{\dot{m}}\frac{\partial \dot{m}}{\partial x} + \frac{1}{T}\left(1 + \frac{T}{Z}\left(\frac{\partial Z}{\partial T}\right)_P\right)\frac{\partial T}{\partial x}\right)$$

$$= \frac{V_w^{\,2}}{CpT}\left\{1 + \frac{T}{Z}\left(\frac{\partial Z}{\partial T}\right)_P\right\}\left(\frac{\Omega}{A} + \frac{\dot{m}ZRT}{PA^2}w\right) \quad \text{(A.1.67)}$$

$$\frac{ZRT}{AP^2}\left\{P\left(\frac{\partial \dot{m}}{\partial t}+\frac{\dot{m}ZRT}{PA}\frac{\partial \dot{m}}{\partial x}\right)-\dot{m}\left(1-\frac{P}{Z}\left(\frac{\partial Z}{\partial P}\right)_T\right)\times\left(\frac{\partial P}{\partial t}+\frac{\dot{m}ZRT}{PA}\frac{\partial P}{\partial x}\right)+\frac{P\dot{m}}{T}\left(1+\frac{T}{Z}\left(\frac{\partial Z}{\partial T}\right)_P\right)\right.$$

$$\left.\times\left(\frac{\partial T}{\partial t}+\frac{\dot{m}ZRT}{PA}\frac{\partial T}{\partial x}\right)\right\}+\frac{ZRT}{P}\frac{\partial P}{\partial x}=-\frac{wZRT}{PA}-g\sin\theta \tag{A.1.68}$$

$$\frac{\partial T}{\partial t}+\frac{V_w^{\,2}}{Cp}\left(1+\frac{T}{Z}\left(\frac{\partial Z}{\partial T}\right)_P\right)\frac{ZRT}{AP^2}\left[P\frac{\partial \dot{m}}{\partial x}-\dot{m}\left(1-\frac{P}{Z}\left(\frac{\partial Z}{\partial P}\right)_T\right)\frac{\partial P}{\partial x}\right]+\frac{\dot{m}ZRT}{PA}$$

$$\times\left(1+\frac{V_w^{\,2}}{CpT}\left(1+\frac{T}{Z}\left(\frac{\partial Z}{\partial T}\right)_P\right)^2\right)\frac{\partial T}{\partial x}=\frac{V_w^{\,2}}{CpP}\left\{1-\frac{P}{Z}\left(\frac{\partial Z}{\partial P}\right)_T\right\}\left(\frac{\Omega}{A}+\frac{\dot{m}ZRT}{PA^2}w\right) \tag{A.1.69}$$

A.2 Initial Values for Governing Equations

The momentum balance equation for natural gas flow under isothermal conditions in pipes has the following differential form from equation (A.1.9):

$$\frac{\partial v}{\partial t}+\frac{1}{\rho}\frac{\partial P}{\partial x}+g\frac{dy}{dx}+v\frac{\partial v}{\partial x}+2\frac{fv^2}{D}=0 \tag{A.2.1}$$

Initial values for the partial differential equations are obtained at time t=0 from a steady state solution. The steady state solution can be easily obtained from the foregoing equation set by setting $\frac{\partial v}{\partial t}$ equal to zero in equation (A.2.1), forcing P and v to be only functions of x:

$$\frac{1}{\rho}\frac{dP}{dx}+g\frac{dy}{dx}+v\frac{dv}{dx}+2\frac{fv^2}{D}=0 \tag{A.2.2}$$

where P is pressure (Pa), ρ is gas density $\left(\text{kg/m}^3\right)$, g is acceleration due to gravity (m/s^2), y is elevation (m), v is gas velocity (m/s), f is the Fanning friction factor, and D is the pipe diameter (m). The coefficient α is introduced to represent the variation in the velocity profile over the pipe cross-section:

$$\frac{dP}{\rho} + gdy + \frac{vdv}{\alpha} + 2\frac{fv^2}{D}dx = 0 \tag{A.2.3}$$

There are four terms appearing in equation (A.2.3), the pressure drop term, the elevation term, the kinetic energy term, and the frictional pressure drop term.

For real gases, $PV = nZ\bar{R}T$ where Z is the compressibility factor, $\bar{R}$ is the universal gas constant $\left(\text{J.Kgmol}^{-1}.\text{K}^{-1}\right)$, V is the volume of gas $\left(\text{m}^3\right)$, and n is the moles of gas. Or, this can be represented as:

$$\rho = \frac{PM}{Z\bar{R}T} = \frac{28.97\gamma_g}{Z\bar{R}T}P = BP \tag{A.2.4}$$

Where M is the gas molecular weight and γ_g is the specific gravity of the gas.

If q_G is the volumetric flow rate at standard condition, then the local gas velocity is:

$$v = q_G Z\left(\frac{T}{T_{sc}}\right)\left(\frac{P_{sc}}{P}\right)\left(\frac{\pi}{4}D^2\right)^{-1} \tag{A.2.5}$$

where P_{sc} is the gas pressure at standard condition $\left(\text{Pa}\right)$ and T_{sc} is the gas temperature at standard condition $\left(\text{K}\right)$.

Often, the compressibility factor Z does not vary greatly over the range of pressures and temperatures existing in pipelines so that it can be assumed constant, thus yielding:

$$dv = -q_G Z\left(\frac{T}{T_{sc}}\right)\left(\frac{P_{sc}}{P}\right)\left(\frac{\pi}{4}D^2\right)^{-1}dP = -v\frac{dP}{P} \tag{A.2.6}$$

Substituting equations (A.2.4), (A.2.5) and (A.2.6) into equation (A.2.3):

$$2PdP - \frac{2B_1C_1}{\alpha}\frac{dP}{P} + \left(Gp^2 + A_1\right)dx = 0 \tag{A.2.7}$$

where $A_1 = \frac{4 f B_1 C_1}{D}$, $B_1 = \frac{28.97 \gamma_g}{Z \bar{R} T}$, $C_1 = \left(q_G Z \frac{4 T P_{sc}}{\pi D^2 T_{sc}} \right)^2$, and $G = 2 B_1 g \sin\theta$.

For convenience, equation (A.2.7) can be rewritten as:

$$\frac{P^2 - \left(B_1 C_1 / \alpha \right)}{P^2 \left(G P^2 + A_1 \right)} dP^2 = -dx \tag{A.2.8}$$

This equation can be integrated analytically assuming that A_1, B_1 and C_1 are constant:

$$L - \frac{D}{2\alpha f} \ln \frac{P_j}{P_i} = \left(\frac{1}{G} + \frac{D}{4\alpha f} \right) \ln \frac{A_1 + G P_i^2}{A_1 + G P_j^2} \tag{A.2.9}$$

where L is the length of pipe.

With:

$$G_k = \frac{L - \frac{D}{2\alpha f} \ln \frac{P_j}{P_i}}{\frac{1}{G} + \frac{D}{4\alpha f}} = \frac{G \left[L - \frac{D}{2\alpha f} \ln \frac{P_j}{P_i} \right]}{1 + \left(\frac{D}{4\alpha f} \right) G} \tag{A.2.10}$$

and $G' = GL$, then equation (A.2.9) can be rearranged to solve for the flow rate:

$$q_G = \left(\frac{\pi}{8} \right) \left(\frac{T_{sc}}{P_{sc}} \right) \left(\frac{\bar{R}}{28.97} \right)^{0.5} \frac{D^{2.5}}{\sqrt{f Z T \gamma_g}} \left(\frac{P_i^2 - e^{G_k} P_j^2}{L} \frac{G'}{e^{G_k} - 1} \right)^{0.5} \tag{A.2.11}$$

This equation is the most general integrated flow equation published in the literature. It accounts for the effects of elevation, friction, and kinetic energy change. Note that for horizontal flow $G = 0 \Rightarrow G' = 0$ and $G_k = 0$. This makes the last term in equation (A.2.11) singular. The singularity can be removed with the application of L'Hopital's rule or by directly substituting $G = 0$ into equation (A.2.8) or (A.2.9). In either case the result is:

$$q_G = \left(\frac{\pi}{8}\right)\left(\frac{T_{sc}}{P_{sc}}\right)\left(\frac{\overline{R}}{28.97}\right)^{0.5} \frac{D^{2.5}}{\sqrt{fZT\gamma_g L}}\left(P_i^2 - P_j^2\right)^{0.5} E_k \tag{A.2.12}$$

Where E_k is the correction factor for the kinetic energy change and it is defined by:

$$E_k = \left(1 - \frac{D}{2\alpha fL}\ln\frac{P_j}{P_i}\right)^{0.5} \tag{A.2.13}$$

Another approach can be neglecting the kinetic energy term as follows:

$$2PdP + \left(GP_{av}^2 + A_1\right)dx = 0 \tag{A.2.14}$$

The resulting equation is the well-known AGA equation (Institute of Gas Technology):

$$q_G = \left(\frac{\pi}{8}\right)\left(\frac{T_{sc}}{P_{sc}}\right)\left(\frac{\overline{R}}{28.97}\right)^{0.5} \frac{D^{2.5}}{\sqrt{fZT\gamma_g L}}\left[\left(P_i^2 - P_j^2\right) - \frac{57.69\gamma_g P_{av}^2 g}{\overline{R}ZT}\Delta Z\right]^{0.5} \tag{A.2.15}$$

For horizontal pipes, with $G' = 0$ and ΔZ =0, both equations (A.2.12) and (A.2.15) reduce to:

$$q_G = \left(\frac{\pi}{8}\right)\left(\frac{T_{sc}}{P_{sc}}\right)\left(\frac{\overline{R}}{28.97}\right)^{0.5} \frac{D^{2.5}}{\sqrt{fZT\gamma_g L}}\left(P_i^2 - P_j^2\right)^{0.5} \tag{A.2.16}$$

The general friction factor equation for smooth pipes is:

$$f = r\,\mathrm{Re}^{-s} \tag{A.2.17}$$

where:

$$\mathrm{Re} = b\left(\frac{P_{sc}}{T_{sc}}\right)\frac{\gamma_g q_G}{D\mu_g} \tag{A.2.18}$$

and the values of *r* and *s* are listed in Table A.2.1. The constant $b = \dfrac{115.88}{\pi\overline{R}}$ is 4.4364×10^{-3}.

Table A.2.1 Constants *r* and *s* (Ouyang and Aziz, 1996). Using the Fanning friction factor for smooth pipes in equation (A.2.16) and then solving the equation for flow rate, the flow equation is:

$$q_G = a_1 E_p \left(\frac{T_{sc}}{P_{sc}}\right)^{a_2} \left[\frac{\left(P_i^2 - P_j^2\right) - \frac{c\gamma_g P_{av}^2 g}{ZT}\Delta Z}{TZL}\right]^{a_3} \left(\frac{1}{\gamma_g}\right)^{a_4} D^{a_5} \qquad \text{(A.2.19)}$$

The parameter E_p is the pipe efficiency that accounts for the effect of pipe roughness. The constant *c* is 0.00697. If the elevation term is neglected, the flow equation reduces to:

$$q_G = a_1 E_p \left(\frac{T_{sc}}{P_{sc}}\right)^{a_2} \left[\frac{\left(P_i^2 - P_j^2\right)}{TZL}\right]^{a_3} \left(\frac{1}{\gamma_g}\right)^{a_4} D^{a_5} \qquad \text{(A.2.20)}$$

The values of a_1 to a_5 are constant and are provided in Table A.2.2.

Table A.2.1: Constants *r* and *s* (Ouyang and Aziz, 1996).

Eqn	Blasius	1/7th	1/8th	1/9th	Mod.1/9th	1/10th	Panhandle	Mod. Panhandle	IGT
r	0.0763	0.0763	0.0563	0.0437	0.046	0.03475	0.02118	0.003678	0.04675
s	0.25	0.25	0.222	0.20	0.20	0.182	0.1461	0.03922	0.20

Equation (A.2.11) can be used with a variety of correlations by simply replacing the Fanning

Table A.2.2: Constant coefficients in equation (A.2.20) (Ouyang and Aziz, 1996).

Equations	a_1 **(SI units)**	a_1 **(Field units)**	a_2	a_3	a_4	a_5
Panhandle	157.92	435.73	1.0788	0.5394	0.4604	2.6182
Mod. Panhandle	157.92	737.50	1.0200	0.5100	0.4900	2.5300
IGT	169.09	343.28	1.1110	0.5560	0.4444	2.6667
Weymouth	137.19	433.50	1.0000	0.5000	0.5000	2.6667

friction factor with the appropriate correlation. The resulting equation is:

$$q = a_1 E \left(\frac{T_{sc}}{P_{sc}}\right)\left(\frac{(P_i^2 - e^{G'}P_j^2)}{TZL}\frac{G'}{e^{G'}-1}\right)^{a_2}\left(\frac{1}{\gamma_g}\right)^{a_3}\left(\frac{D^{a_4}}{\mu_g^{a_5}}\right) \quad \text{(A.2.21)}$$

When the elevation term is neglected, the simplified flow equation for horizontal pipes is obtained from equation (A.2.21):

$$q = a_1 E \left(\frac{T_{sc}}{P_{sc}}\right)\left[\frac{\left(P_i^2 - P_j^2\right)}{TZL}\right]^{a_2}\left(\frac{1}{\gamma_g}\right)^{a3}\left(\frac{D^{a_4}}{\mu_g^{a_5}}\right) \quad \text{(A.2.22)}$$

The values of a_1 to a_5 are constant and provided in Table A.2.3.

For this work, equation (A.2.20) was employed with the coefficients for the Panhandle equation.

Table A.2.3: Constant coefficients in equation (A.2.22) (Ouyang and Aziz, 1996).

Equations	a_1 **(SI units)**	a_1 **(Field units)**	a_2	a_3	a_4	a_5
Blasius	17.1541	265.5812	0.5714	0.4286	2.7143	0.1429
1/7th power law	17.4983	270.9114	0.5714	0.4286	2.7143	0.1429
1/8th power law	21.6136	295.8711	0.5624	0.4376	2.6873	0.1249
1/9th power law	25.6034	319.0366	0.5556	0.4444	2.6667	0.1111
Modified 1/9th power law	24.8841	310.0735	0.5556	0.4444	2.6667	0.1111
1/10th power law	29.6754	342.9768	0.5501	0.4499	2.6502	0.1001
Panhandle	40.3120	402.7467	0.5394	0.4606	2.6182	0.0788
Modified Panhandle	108.1291	722.5812	0.5100	0.4900	2.5300	0.0200
IGT	24.6615	307.3000	0.5556	0.4444	2.6667	0.1111
Weymouth	137.1902	433.5065	0.5000	0.5000	2.6667	0.0000

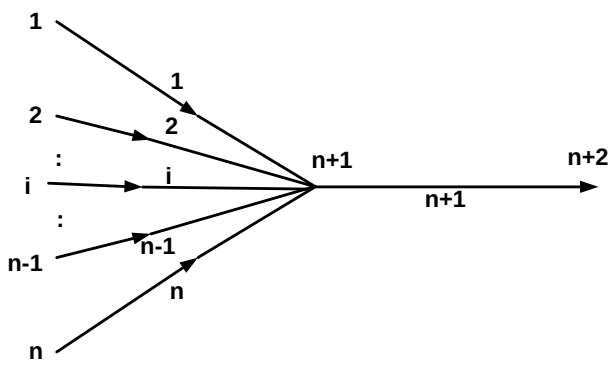

Fig. A.3.1: Combining junction.

A.3 Combining Junctions

Figure A.3.1 shows the common combining junction. The combining junction is used to bring one or more pipes into a single pipe.

Conservation of mass for point (n+1) is:

$$q_G(1) + q_G(2) + \ldots + q_G(i) + \ldots + q_G(n) = q_G(n+1) \tag{A.3.1}$$

Then using equation (A.2.20) with constant temperature and compressibility factor (*Z*) becomes:

$$a_1 E_p \left(\frac{T_{sc}}{P_{sc}}\right)^{a_2} \left[\frac{\left(P_1^2 - P_{n+1}^2\right)}{TZL(1)}\right]^{a_3} \left(\frac{1}{\gamma_g}\right)^{a_4} D(1)^{a_5} +$$

$$a_1 E_p \left(\frac{T_{sc}}{P_{sc}}\right)^{a_2} \left[\frac{\left(P_2^2 - P_{n+1}^2\right)}{TZL(2)}\right]^{a_3} \left(\frac{1}{\gamma_g}\right)^{a_4} D(2)^{a_5} + \ldots +$$

$$a_1 E_p \left(\frac{T_{sc}}{P_{sc}}\right)^{a_2} \left[\frac{\left(P_i^2 - P_{n+1}^2\right)}{TZL(i)}\right]^{a_3} \left(\frac{1}{\gamma_g}\right)^{a_4} D(i)^{a_5} + \ldots +$$

$$a_1 E_p \left(\frac{T_{sc}}{P_{sc}}\right)^{a_2} \left[\frac{\left(P_n^2 - P_{n+1}^2\right)}{TZL(n)}\right]^{a_3} \left(\frac{1}{\gamma_g}\right)^{a_4} D(n)^{a_5} =$$

$$a_1 E_p \left(\frac{T_{sc}}{P_{sc}}\right)^{a_2} \left[\frac{\left(P_{n+1}^2 - P_{n+2}^2\right)}{TZL(n+1)}\right]^{a_3} \left(\frac{1}{\gamma_g}\right)^{a_4} D(n+1)^{a_5} \tag{A.3.2}$$

In equation (A.3.2) the P_{n+1} is unknown. Once the pressure is known, the flow for each pipe can then be determined. Equation (A.3.2) is then reformulated to:

$$\left[\frac{\left(P_1^2-P_{n+1}^2\right)}{L(1)}\right]^{a_3} D(1)^{a_5} + \left[\frac{\left(P_2^2-P_{n+1}^2\right)}{L(2)}\right]^{a_3} D(2)^{a_5} +\ldots+ \left[\frac{\left(P_i^2-P_{n+1}^2\right)}{L(i)}\right]^{a_3} D(i)^{a_5} +\ldots+$$

$$\left[\frac{\left(P_n^2-P_{n+1}^2\right)}{L(n)}\right]^{a_3} D(n)^{a_5} = \left[\frac{\left(P_{n+1}^2-P_{n+2}^2\right)}{L(n+1)}\right]^{a_3} D(n+1)^{a_5} \quad \text{(A.3.3)}$$

Finally, P_{n+1} will be:

$$P_{n+1} = \left[P_{n+2}^2 + \left(\sum_{j=1}^{n}\left(\frac{\left(P_j^2-P_{n+1}^2\right)L_{n+1}}{L_j}\right)^{a_3}\left(\frac{D_j}{D_{n+1}}\right)^{a_5}\right)^{1/a_3}\right]^{0.5} \quad \text{(A.3.4)}$$

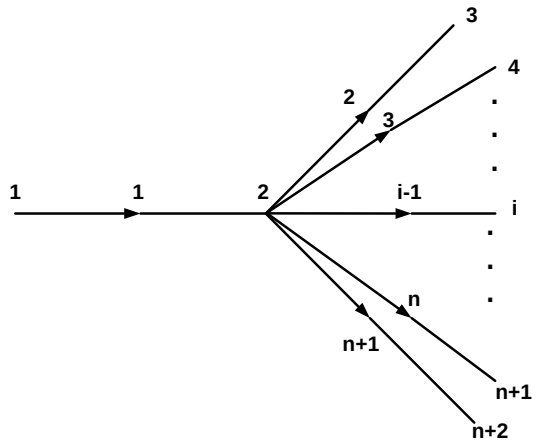

Fig. A.4.1: Dividing junction.

Now the flow through each pipe in the junction can be determined by equation (A.2.20).

A.4 Dividing Junctions

Figure A.4.1 shows the dividing junction. This is a common arrangement where gas flows from one pipe into two or more pipes, for example, at the outlet of a compressor station.

Conservation of mass for point (2) is:

$$q_G(1) = q_G(2) + q_G(3) + \ldots + q_G(i) + \ldots + q_G(n) + q_G(n+1) \quad \text{(A.4.1)}$$

The pressure at point 2 (P_2) is unknown. Once determined, then the flow for each line can be calculated. Reformulating equation (A.4.1) in a similar manner as with the splitting junction:

$$\left[\frac{\left(P_1^2-P_2^2\right)}{L(1)}\right]^{a_3} D(1)^{a_5}=\left[\frac{\left(P_2^2-P_3^2\right)}{L(2)}\right]^{a_3} D(2)^{a_5}+\left[\frac{\left(P_2^2-P_4^2\right)}{L(3)}\right]^{a_3} D(3)^{a_5}+\ldots+$$

$$\left[\frac{\left(P_2^2-P_i^2\right)}{L(i-1)}\right]^{a_3} D(i-1)^{a_5}+\ldots+\left[\frac{\left(P_2^2-P_{n+1}^2\right)}{L(n)}\right]^{a_3} D(n)^{a_5}+\left[\frac{\left(P_2^2-P_{n+2}^2\right)}{L(n+1)}\right]^{a_3} D(n+1)^{a_5} \quad \text{(A.4.2)}$$

Finally P_2 will be:

$$P_2=\left[P_1^2-\left(\sum_{j=3}^{n+2}\left(\frac{\left(P_2^2-P_j^2\right)L_1}{L_{j-1}}\right)^{a_3}\left(\frac{D_{j-1}}{D_1}\right)^{a_5}\right)^{1/a_3}\right]^{0.5} \quad \text{(A.4.3)}$$

A.5 Branches

Figure A.5.1 shows a kind of branch that can be used to simulate gas pipeline systems.

Conservation of mass is:

$$q_G(1)+q_G(2)+\ldots+q_G(i)+\ldots+q_G(n)=q_G \quad \text{(A.5.1)}$$

The variable q_G is the flow between points *i* and *j*. An additional relationship shows that:

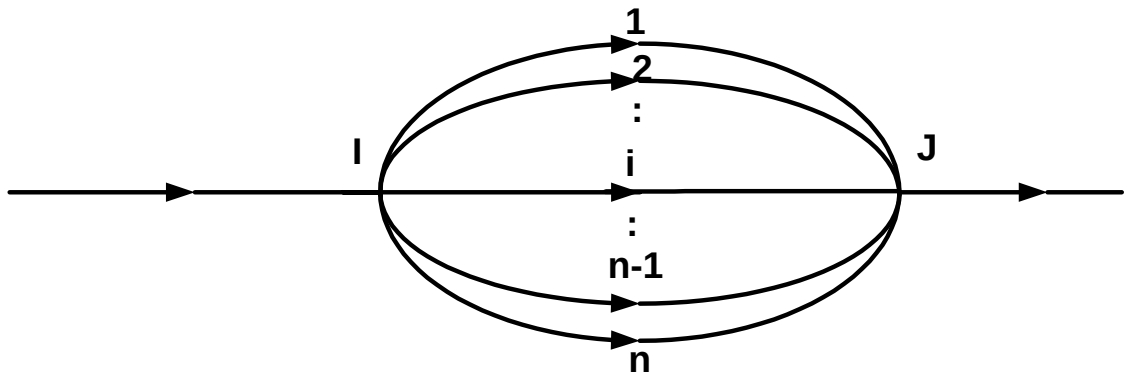

Fig. A.5.1: Branches.

$$\frac{q_G(1)}{q_G(i)} = \left(\frac{L(i)}{L(1)}\right)^{a_3}\left(\frac{D(1)}{D(i)}\right)^{a_5}$$

$$\frac{q_G(2)}{q_G(i)} = \left(\frac{L(i)}{L(2)}\right)^{a_3}\left(\frac{D(2)}{D(i)}\right)^{a_5}$$

$$\vdots$$

$$\frac{q_G(n)}{q_G(i)} = \left(\frac{L(i)}{L(n)}\right)^{a_3}\left(\frac{D(n)}{D(i)}\right)^{a_5}$$

Substituting this set of equations into equation (A.5.1):

$$q_G = q_G(i)\left(1+\left(\frac{L(i)}{L(1)}\right)^{a_3}\left(\frac{D(1)}{D(i)}\right)^{a_5}+\left(\frac{L(i)}{L(2)}\right)^{a_3}\left(\frac{D(2)}{D(i)}\right)^{a_5}+\ldots+\left(\frac{L(i)}{L(n)}\right)^{a_3}\left(\frac{D(n)}{D(i)}\right)^{a_5}\right) \quad \text{(A.5.2)}$$

Finally:

$$q_G(i) = \frac{q_G}{1+\frac{L(i)^{a_3}}{D(i)^{a_5}}\left(\left(\sum_{j=1}^{n}\frac{D(j)^{a_3}}{L(j)^{a_5}}\right)-\frac{D(i)^{a_3}}{L(i)^{a_5}}\right)} \quad \text{(A.5.3)}$$

A.6 Finding Pressure for Each Node in the Pipe

Figure A.6.1 shows a pipe divided into *N*-1 segment.

Considering constant flow into the pipe, the flow between node 1 and i is:

$$q_G = a_1 E_p\left(\frac{T_{sc}}{P_{sc}}\right)^{a_2}\left[\frac{\left(P_1^2-P_i^2\right)}{TZ\Delta x(i-1)}\right]^{a_3}\left(\frac{1}{\gamma_g}\right)^{a_4} D^{a_5} \quad \text{(A.6.1)}$$

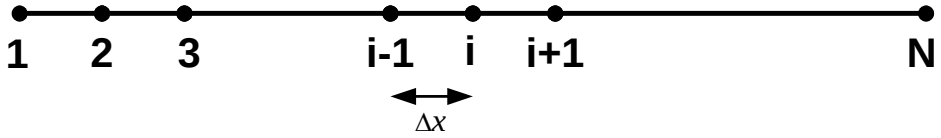

Fig. A.6.1: Pipe mesh.

Then, it is possible to obtain P_i:

$$P_i = \sqrt{P_1^2 - (i-1)\sqrt[a_3]{C_1}} \tag{A.6.2}$$

where $C_1 = \dfrac{q_G (TZ\Delta x)^{a_3}}{a_1 E_p \left(\dfrac{T_{sc}}{P_{sc}}\right)^{a_2} \left[\dfrac{1}{\gamma_g}\right]^{a_4} D^{a_5}}$.

APPENDIX B: PIPELINE AND COMPRESSOR STATION SIMULATION MEETING

Date: August 28, 2002

Location: Kansas State University, Manhattan, Kansas

Attendees:

Mohammad Abbaspour, Graduate Research Assistant, NGML

Greg Beshouri, President, Advanced Engine Technology Corporation

James Cadero, El Paso Corporation

Kirby Chapman, Director and Principal Investigator, NGML

Gary Choquette, Northern Natural Gas Company

Sam Clowney, Consultant, El Paso Corporation

Michael Goodman, El Paso Corporation/Registration Chair, Pipeline Simulation Interest Group (PSIG)

Anders Johnson, El Paso Corporation (via conference call)

Tan Lui, Graduate Research Assistant, Computer & Information Sciences

Robert Nelson, El Paso Corporation

Jacque Shultz, Laboratory Operations Manager, NGML

Virg Wallentine, Professor and Head, Computer & Information Sciences

Michael Whelan, PRCI

Charlie Zheng, Assistant Professor, Mechanical & Nuclear Engineering

Meeting opened by Kirby Chapman with introductions and a review of the expected meeting outcomes. These outcomes were:

1. Identify positives and negatives of existing pipeline simulation software;

2. Determine features and models that need to be developed to make existing software more useable and accurate; and

3. Determine specific outcomes from the current DOE project that will be most useful to the gas transmission industry.

Chapman reviewed the original scope and intent of the existing U.S. Department of Energy-sponsored research project. Chapman re-iterated that the goal is to develop a modeling tool that can be used by the industry to create a sophisticated understanding of how the various pipeline system components interact with each other.

A general roundtable discussion began that basically discussed the use, and the shortcomings and best parts of the primary three commercially-available pipeline simulation software packages:

1. Advantica/Stoner

2. Gregg Engineering

3. Energy Solutions, International

Uses

- Assess the impact of storage systems on the dynamic availability of natural gas. One example cited was that during the course of a day, storage can be depleted to meet demands, but then recharged later in the day since the demand is not there.

- One user company indicated that the compressor curves that are used for the simulations are generally developed once, and then considered valid forever. The thought here is that something needs to be implemented to update, or validate, existing compressor and/or engine curves that are used in the simulations.

- A company named Adaptive Trade was contracted by one end user to attempt to use the existing simulation codes for optimization studies.

- A second company, ProStrategic, developed optimization processes for the airline industry. The end-users are attempting to use this same strategy to determine how much

capacity is available in the pipeline, and then how to price the last few cubic feet of capacity; similar to pricing airline seats.

- Many end-users use the simulation packages to determine the quantity of extra horsepower available in a system. Some let the simulation packages select the equipment in the compressor stations to meet the existing power requirements. However the program-selected equipment may not match reality.

- Simulations are used for operations and design. In operations mode, the simulations are used to determine the setpoints for a particular system. These setpoints are then sent to "gas control." A new set of information is then acquired from the pipeline and used to update the simulation. There may be a bandwidth issue on just how much information can be transferred from the pipeline compressor stations to the facilities planning group (facilities planning is the group that determines how much gas will be sent to various points, and is effectively responsible for ensuring that there is a plan for getting the gas through the pipeline system).

- Planning groups determine the incremental horsepower that is necessary to overcome a constraint (bottleneck) in the pipeline system

- Online models are used to interface with SCADA systems to try and save fuel and, hopefully, determine where and when maintenance is necessary.

- The consensus of the group was that these three simulation systems adequately handle the calculations that determine the flow rate and pressure drop between compressor stations.

Potential Uses Not Currently Available

- Determine the impact of "upset" conditions. For example, if a GMWC 330 is not balanced, then how does that impact the flow of gas through the compressor station?

- An expert system that will look at detailed information from systems such as El Paso's COMET database. The expert system would then analyze this data to determine if the system is operating at peak capacity and to issue maintenance flags.

- Diagnose problems on a particular unit in a compressor station.
- Standardize engine/compressor performance calculations. Currently there are several methods to determine engine and compressor performance calculations. The possibility that the current DOE project could be used to standardize these calculations was considered by the group as a definite positive outcome. The specific use would be to determine the potential hp available during planning phase. Individual data points that would be used are:
    i. Speed
    ii. Compressor pocket position
    iii. Compressor geometry
    iv. May be able to treat the driver and compressor as one unit
- Determine individual compressor flow rate
- Remotely map compressor to update compressor curves
- Ambient de-rates and up-rates
    i. This is currently built in on gas turbine control systems
    ii. Is not built in on reciprocating engine controls
    iii. This may present a problem on permitting.
    iv. One company actually uses two operating permits – one for the summer and one for the winter. These permitting constraints are used in the simulation software.
    v. Another operating company has interpreted legal documents by stating that you cannot guarantee a supply unless the ambient de-rate/up-rate strategies are included in the automatic control systems.

- One of the largest and newest complications in the planning phases are distributed power plants. Currently, these plants purchase interruptible supplies since they are low cost. These plants typically only operate 12 hours per day, and will therefore create a reliance on the accuracy of transient modeling.

- One major drawback in transient modeling is the inability to effectively model engine startup and shutdown. The simulation programs start and stop equipment instantaneously.

- The primary benefit of a new initiative is the significantly enhanced ability to model the components within the compressor station yard. This would include the engines and compressors, yard valves, gas coolers and scrubbers, and yard piping. The group felt this was not currently available in the existing simulation programs.

Prioritizing the Discussions and Needs

Following the roundtable discussions, the group developed a list of deficiencies in the current three programs. The general consensus is that the group would like the DOE project to focus on components within the compressor station yard. The most optimum output would be the ability of the end user to develop a sophisticated compressor station model, and then have the ability to incorporate that compressor station model into one or more of the existing commercial packages. Hence, the group recommended that the focus be changed to dynamically modeling the components within the compressor, including everything between the side valves. The compressor station can be a conventional station, storage injection, etc. This needs to be established as a standard. The group will propose an interface to the K-State model to the three different vendors, describing how they can interface with the K-State model. The vendor pipeline software and the add-on we developed would have to operate on the same platform.

This will be initiated by first submitting a co-signed letter to DOE explaining the outcome of this meeting. After DOE concurrence is received, a second set of co-signed letters will be submitted to the vendor companies, i.e., Gregg Engineering, Advantica/Stoner, and Energy Solutions, International, explaining the outcome of the meeting and requesting a conference call between them, K-State, and at least two industry end users. Key vendor contact points are:

- Thomas Rey, Gregg Engineering, contact point. We would like to receive a donated license to develop an add-on module, (713) 988-6900. Note: Thomas expressed concern that DOE and K-State are developing a free version of their software. Goodman will visit with Thomas to assure him that this not the case, and that instead we plan to develop enhancement software that can be included in their product. **(Since the meeting, Mike talked to Thomas and explained to him that this has evolved into the development of a standardized compressor simulation utility. He responded favorably and would be interested in discussing this further with the research team)**

- Jason Modisett, ESI, Houston, 13831, Northwest Freeway, Suite 235, Houston, Texas 77040, United States, Tel: (713) 782-7500, Fax: (713) 895-8383

- Advantica/Stoner, Don Schroeder, Carlisle, PA, PSIG Board Member

- Simulutions, Kevin Hemple, Calgary

Gary Choquette and Mike Goodman agreed to co-sign letters and represent the end-user community (assuming there would not be a problem with the operating companies).

Mike Goodman agreed to request a 10 minute slot at the upcoming Pipeline Simulation Interest Group meeting. K-State would use this slot to mention what we are doing and to encourage vendors and end users to become involved. **(Since the meeting, Mike completed this task. Kirby and Mohammad will attend the PSIG meeting in late October.)**

List of Deficiencies in Existing Simulations

- Engine Modeling
    i. Ensure a proposed operating point falls within the realm of the equipment
    ii. Can have a situation where reciprocating engines drive centrifugal compressors (this might be similar to electrical compression) – hence, need to have the ability to match engines and compressors
    iii. Modeling startup – needs to mimic unit controls
    iv. Controls

v. Operating envelope

vi. Performance curve fits

vii. Ambient up-rating and de-rating

- Compressor modeling
  i. Establish pockets that are open
  ii. Geometry
  iii. Pulsation effects and valve design
  iv. Integrate compressor constraints into simulation tools
  v. Limited by ability to gather and use data from compressor performance maps (Note: NNG has abandoned performance map curve fits in favor of lookup tables)
  vi. Not a comprehensive set of rules on how to do this – need to have this as standardized as possible
- Station yard piping
  i. Currently available by treating station piping as equivalent length of pipe
  ii. The loss is significant enough that it does need to be treated, but maybe not that much
  iii. May be able to save 5% fuel costs by re-routing pipe in the yard
  iv. Yard valve, coupled to engine coming on line
  v. Gas compressibility effect
  vi. Heat transfer
  vii. Joule-Thompson

- Can actually get below ground temperature depending on gas velocity
- Sometimes the gas does not even get to ground temperature

viii. The simulation systems do not seem to adjust the particular models over ranges of operation

ix. Is the wholesale replacement of yard plug valves with full open valves economical?

- Gas composition – this is not done well currently
- Scrubbers and filters
  i. Remove heavy condensates, methane hydrates, etc.
  ii. Can be oil from compressors
  iii. Pressure drop can be high
- Gas cooling
  i. If a cooler is designed for summer operation, then you can achieve much higher throughputs in the winter by running the coolers.
  ii. Gregg Engineering uses simple discharge temperature settings
  iii. One comment was that adding coolers could be construed as “de-bottlenecking,” and would trigger a new source review from the EPA.
  iv. Anders feels this is an area with a lot of potential for improvement
- Expert system
  i. The simulation systems do not seem to adjust the particular models over ranges of operation
  ii. Expert system could review the output
  iii. Looks at reasonableness of total model

iv. Capture expertise

v. Compare model results to actual SCADA data, and diagnose the problem. This would be inside the fence. Need to distinguish between intuition and facts.

- Verify accuracy of data
- If throughput hp is less than engine bhp, then
  - Engine mechanical problem
  - Compressor valve problems
  - Etc.
  - Send up a maintenance flag on the chosen system

- Ease of use

i. May need to change modeling parameters

ii. The simulation systems do not seem to adjust the particular models over ranges of operation

- Optimization methods

i. Minimum pressure at delivery points

ii. Determine which delivery point is the critical point, and then back calculate how the pipe needs to operate

iii. Need to be able to put constraints on pipe, and then have the simulation deal with the consequences – a line pack management system tied into the simulation

iv. Linepack position has more influence on fuel efficiency that the efficiency of the particular engine/compressor selections

v. May want to have this look at O&M costs – determine maintenance costs based on equipment type

vi. Criteria to define which units to start and stop

- Operating costs
- Operating envelope
- First on/First off – this will depend on the scenario and conditions -- expert system?
- Come up with a list of prioritized units that are brought on line based on operating costs, mcf of fuel consumed, output results to "global" simulation so that the entire system can be optimized

vii. Electrical compression costs

- How does this impact the overall cost of delivering a parcel of gas?
- Variation in costs of electricity

viii. Reliability – this is nearly 100%, so this is not really an issue

ix. You can move 80% of product with 50% of the horsepower. The last 20% moves into the exponential increase in power

x. So as we increase capacity, the cost per cubic foot based on physics. We can loop line, add mid-station compression, etc.

xi. Some pipelines do not have a fuel tracker and others do. Fuel optimization is much more valuable to those that do not.

- Failure analysis
- Data quality – how to recognize when a data point is not valid – what can be done to fix this

i. All vendors have some sort of technique to deal with this

ii. Check to see if curves still match the operating points

iii. Band tolerances, etc.

iv. Instrument drift – orifice plates, for example

v. Can change the pipe roughness in the models to adjust for instrument drift, etc.

- Transient operation
  i. Models assume equipment is either on or off
  ii. Do not consider the ramp-up of the equipment
  iii. Stoner does allow the user to enter a ramp up time (three minutes, etc.)
  iv. Block hp mode – just generic hp at the compressor station. States so many hp per MMCF
  v. Involves substantially more information than the steady state model
- Fairly large difference between the two models on high pressure systems (2,200 psi) – error could be 10%
  i. Compressibility
  ii. Heat transfer
  iii. Joule-Thompson
    - Can actually get below ground temperature depending on gas velocity
    - Sometimes the gas doesn't even get to ground temperature
  iv. The simulation systems do not seem to adjust the particular models over ranges of operation
- Commercialized software has its drawbacks
  i. We have a pretty good idea of what is in the commercialized packages, but then again, maybe not
  ii. Upgrades to software may not be readily implemented
  iii. There are undocumented features in the programs – what modeling techniques are used?

iv. How are the defaults established? The heat transfer coefficient seems to be a big deal

v. If you find a major hole in the computation method, at least GE is fairly responsive to fixing these errors. If it is more of a minor thing, then they are not responsive

vi. A third vendor: Energy Solutions, International (Pipeline Studio)

vii. GE seems to be leading the GUI

viii. There isn't a common platform

ix. GE has a data transport tool. Stoner uses an Access database

x. PSIG set up a voluntary committee to try and establish a standard language. The farthest they got was to determine that it would be XML

- Interface seems to be the driving force behind which system is selected
- TGP tries to stay snugged up to maximum allowable operating pressure (MAOP). The question becomes how much pressure drop is there between the compressor discharge and the inlet to the pipeline.